Identification and Functional Characterization of the Novel Mineralocorticoid Receptor Target Gene Cnksr3

vorgelegt von
Diplom-Ingenieur
Tim Ziera

Von der Fakultät III - Prozesswissenschaften
der Technischen Universität Berlin
zur Erlangung des akademischen Grades
Doktor der Ingenieurwissenschaften
- Dr.-Ing. -

genehmigte Dissertation

Promotionsausschuss:

Vorsitzender: Prof. Dr. U. Stahl
Berichter: Prof. Dr. R. Lauster
Berichter: PD. Dr. K. Prelle
Berichter: Prof. Dr. L.-A. Garbe

Tag der wissenschaftlichen Aussprache: 23.10.2009

Berlin 2009

D83

Keywords

Aldosterone, Epithelial Na^+ Channel, Chromatin Immunoprecipitation (ChIP), Microarray, Reporter Gene Assay, Ussing Chamber, Site-Directed Mutagenesis

Abstract

The mineralocorticoid receptor (MR) is a ligand-dependent transcription factor mainly expressed in epithelial cells at the distal nephron and distal colon where it regulates salt and water homeostasis. MR expression and function is also found in several non-epithelial tissues particularly in the cardiovascular system. Dysregulation of aldosterone-MR signaling is frequently involved in hypertension and cardiac failure.

While therapeutic benefits of MR antagonists in the above noted diseases are undisputed, the molecular mechanisms of action remain to be fully elucidated. Activated by aldosterone the MR elicits most of its physiological actions by altering gene expression of target genes including genes that modulate the activity of the epithelial sodium channel (ENaC) in the kidney. In the recent years a number of gene expression studies have been carried out to identify primary MR target genes. The search for MR target genes is yet hampered by the ubiquitously expressed glucocorticoid receptor (GR). Both MR and GR can be activated by aldosterone and cortisol, albeit at different concentrations. Hence, the current knowledge of MR target genes is likely to be mixed with actual GR target genes.

In order to identify MR target genes involved in aldosterone signaling cell culture models were established that allow a clear separation of MR- versus GR-mediated effects on gene regulation and transepithelial sodium transport as physiological readout. Microarray gene expression profiling in human embryonic kidney cells (HEK293) stably expressing MR led to the identification of 36 aldosterone regulated genes. Chromatin Immunoprecipitation (ChIP) in combination with reporter gene assays confirmed that at least 12 out of these 36 candidate genes were directly regulated by MR. This approach led to the identification of the novel MR target gene cnksr3. Expression analysis in different nephron segments, microdissected from mice kidneys, confirmed that cnksr3 was highly expressed in the renal cortical collecting duct (CCD), the prime target segment of aldosterone-regulated sodium retention in the kidney. Mouse CCD-derived cells (M1) that either stably overexpressing or silencing CNKSR3 were electrophysiologically analyzed and showed that CNKSR3 expression correlated with, and was required for, ENaC-mediated transepithelial sodium transport. Moreover, CNKSR3 expression inhibited the RAS-RAF-MEK-ERK signaling cascade, a pathway involved in the modulation of ENaC cell surface expression.

In conclusion, CNKSR3 a member of a family of scaffold proteins involved in RAS-RAF-MEK-ERK pathway regulation is a direct MR target gene and is crucial for the maintenance of transepithelial sodium transport in the kidney.

Zusammenfassung

Der Mineralocorticoid-Rezeptor (MR) ist ein liganden-abhäniger Transkriptionsfaktor, der vorwiegend in den Epithelzellen des distalen Nephrons und des distalen Kolons exprimiert wird, wo er die Salz- und Wasserhomeostase reguliert. Die MR-Expression und -Funktion ist ebenso in nicht-epithelialen Geweben zu finden, insbesondere dem Herz-Kreislauf-System. Eine Dysregulation des Aldosteron-MR-Systems ist oftmals bei der Entstehung von Bluthochdruck und bei kardialen Störungen beteiligt.

Der therapeutische Nutzten von MR-Antagonisten zur Behandlung oben genannter Erkrankungen ist unumstritten, dennoch sind die molekularen Mechanismen dieser Prozesse nur unvollständig verstanden. Der MR übt seine physiologische Funktion Aldosteron-abhängig durch die Änderung der Expression von Target-Genen aus, unter anderem von Genen, die die Aktivität des epithelialen Natriumkanals (ENaC) in der Niere regulieren. In der Vergangenheit wurden verschiedene Genexpressions-Studien zur Identifizierung direkt MR-regulierter Gene durchgeführt. Diese Suche nach MR-regulierten Genen ist jedoch durch den ubiquitär exprimierten Glucocorticoid Rezeptor (GR) erschwert. Obwohl MR und GR durch unterschiedliche Konzentrationen von Aldosteron und Cortisol aktiviert werden, ist die Wahrscheinlichkeit hoch, dass unter den derzeitig als MR-reguliert bekannten Genen auch solche sind, die tatsächlich über den GR reguliert sind.

Zur Identifizierung von direkt MR-regulierten Genen wurden neue Zellkulturmodelle etabliert, die eine Trennung MR- bzw. GR- vermittelter Effekte auf Ebene der Genexpression erlauben, sowie den transepithelialen Natriumtransport als physiologischen Parameter messbar machen. Über eine Microarray-Genexpressionsanalyse in stabil MR-exprimierenden humanen embryonalen Nierenzellen (HEK293) wurden 36 Aldosteron-regulierte Gene identifiziert. Durch Kombination von Chromatin-Immunopräzipitation (ChIP) und Reportergen-Assays wurde bestätigt, dass mindestens 12 der 36 identifizierten Gene direkt über den MR reguliert sind. Dieser experimentelle Ansatz führte zur Identifizierung des noch nicht als MR-reguliert beschriebenen Gens cnksr3. Die Expressionsanalyse in verschiedenen Nephronsegmenten bestätigte, dass cnksr3 stark im kortikalen Sammelrohr [*engl.* Cortical Collecting Duct (CCD)] in der Niere exprimiert wird, welches das Hauptsegment der Aldosteron-regulierten Natriumrückresorption ist. Elektrophysiologische Messungen in Maus CCD Zellen (M1), die entweder cnksr3 überexprimieren oder reprimieren, zeigten, dass der ENaC-vermittelte transepitheliale Natriumtransport mit der cnksr3-Expression korrelierte bzw. von dessen Expression abhängig war. Ferner blockierte die Expression von cnksr3 die RAS-RAF-MEK-ERK Signalkaskade, ein Signalweg, der in die Regulation des Membraneinbaus der ENaC-Ionenkanalproteine involviert ist.

Zusammengefasst wurde gezeigt, dass cnksr3, ein Mitglied einer Familie von Gerüst-Proteinen, die an der RAS-RAF-MEK-ERK Signaltransduktion beteiligt sind, ein direkt MR-reguliertes Gen ist. CNKSR3 spielt eine zentrale Rolle bei der Aufrechterhaltung des transepithelialen Natriumtransports in der Niere.

1. Introduction

All creatures face the challenge to maintain a stable intracellular milieu by adapting dynamically to ever-changing environmental conditions. This maintenance is referred to as "homeostasis" and is achieved by regulatory circuits that require sensory mechanisms, set points and feedback loops. Salt and water homeostasis is critical for the survival of terrestrial organisms in a in that respect largely hostile environment. The salt and water homeostasis is closely associated with the tight regulation of the components of extracellular liquid, a corresponding volume of interstitial fluid and blood plasma. The main effectors are located in epithelial tissues e.g. of the kidney and the colon where salt and water are either excreted or reabsorbed under the control of a hormonal system, the renin-angiotensin-aldosterone system.

1.1. The renin-angiotensin-aldosterone system

The renin-angiotensin-aldosterone system (RAAS) is a hormonal system which plays an important role in the regulation of salt and water homeostasis and blood pressure. Specialized cells in the renal cortex detect decreases in sodium (Na^+) concentration (macula densa) and blood pressure (juxtaglomerular cells) and stimulate the secretion of the enzyme renin by juxtaglomerular cells. In the circulating blood renin cleaves liver-derived inactive angiotensinogen and thus converts it into angiotensin I. Angiotensin I is then converted to angiotensin II by angiotensin-converting enzyme (ACE), which is located at the luminal side of the pulmonary and renal endothelium. Angiotensin II is a potent vasoconstrictor of renal arterioles and further stimulates the secretion of aldosterone (1). Also an increase of extracellular potassium is a potent stimulator of aldosterone biosynthesis (2). The steroid hormone aldosterone is synthesized by the outer section (zona glomerulosa) of the adrenal cortex in the adrenal gland. Increased circulating level of aldosterone results in sodium reabsorption and water retention particularly in the kidney. Aldosterone exerts its actions through the mineralocorticoid receptor (MR), a ligand-dependent transcription factor belonging to the nuclear receptor superfamily. The pivotal role of MR in the RAAS feedback loop was clearly demonstrated by MR knockout mice, who died during the first two weeks of life (3). Although these mice can be rescued by exogenous NaCl administration, they exhibit a persistently activated RAAS and suffer from volume depletion (4).

1.2. The mineralocorticoid receptor

The nuclear receptor superfamily is divided into several subfamilies. The mineralocorticoid receptor (MR) belongs to the type I (steroid hormone) receptor subfamily that includes the glucocorticoid receptor (GR), progestin receptor (PR), androgen receptor (AR) and estrogen receptors (ER). Although these receptors are all ligand-activated transcription factors with common structural features, divergence is achieved by their distinct cognate ligands and molecular mechanisms of action, which regulate a wide variety of physiological processes ranging from organ development to stress response and mood control (5). MR, in particular, is required for the maintenance of electrolyte and water homeostasis and blood pressure (6).

The NR3C2 gene encoding human MR (hMR) is localized on chromosome 4 in the q31.1 region, spans 450 kb and is composed of ten exons. The first two exons, referred to as 1α and 1β, are untranslated but generate different mRNA isoforms, which differ in their relative abundance in a tissue specific manner (7). The molecular function of these distinct hMR mRNA transcripts remains to be determined but is assumed to be involved in the regulation of transcript stability and/or translational efficacy. Exons 2 to 9 code for the 107 kDa hMR protein (8). The schematic representation of the NR3C2 gene coding for MR is shown in Figure 1.1.

As all members of this receptor family MR contains four characteristic domains: an N-terminal domain (NTD or A/B domain), followed by a central DNA-binding domain (DBD or C domain), a hinge region (D domain), and a C-terminal E-domain containing the ligand-binding domain (LBD). The NTD contains smaller regions responsible for hormone-independent regulation of transcription, named activation function (AF) regions. These regions are termed AF1a and AF1b to distinguish them from the AF2 region at the C-terminus of the LBD. The DBD contains two zinc finger structures. One of which, termed the P box, recognizes the hormone response elements (HRE) in the promoters of MR target genes and mediates base-specific contacts within the major groove of the DNA. A second zinc finger motif, the D box, is oriented alongside the axis of the DNA and facilitates receptor homo-dimerization (5). The DBD further contains a nuclear export signal (NES) located between the two zinc fingers (9). The hinge region, located between the DBD and the LBD, is flexible in order to enable the receptor to twist and alter conformation. The C-terminal E domain mediates the ligand-dependent activation of the receptor. It contains the LBD, a nuclear localization signal (NLS), and a trans-activating function (AF-2). In the absence of ligand the LBD is associated with a multi-protein complex of chaperones including Hsp90/ Hsp70 and

immunophilins, which stabilize the receptor in an inactive but ligand-affine conformation. Upon ligand binding the LBD adopts a more compact structure, resulting in a release of associated chaperones and a translocation of the receptor into the nucleus. Once in the nucleus MR modulates the expression of its target genes as described in further detail in section 1.5 below.

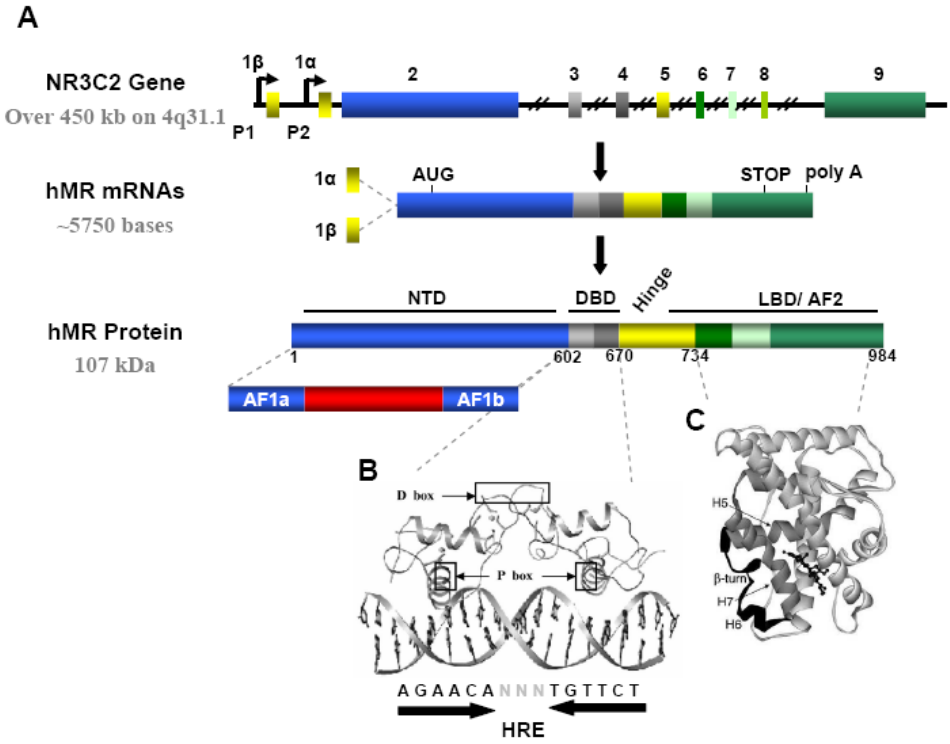

Fig. 1.1: Schematic representation of the NR3C2 gene (adapted from Pascual-Le Tallec, 2005) **A**: The human NR3C2 gene encodes for two alternative mRNA isoforms and one mineralocorticoid receptor (MR) protein. As a member of the steroid receptor superfamily MR harbours distinct functional domains able to modulate transcription upon ligand activation. **B**: The DNA binding domain (DBD) recognizes resonse elements of DNA by its two zinc finger structures. **C**: The predicted crystal structure of the MR ligand binding domain (LBD) with aldosterone in the ligand binding pocket based on crystal structure of the PR (10).

In summary MR is a ligand-operated transcription factor mainly located in the cytoplasm of cells. Upon ligand binding, the receptor undergoes a conformational change and translocates to the nucleus, where it binds as a homodimer to inverted repeat DNA half sites in the promoter of target genes, activating or repressing their transcriptional activity.

1.3. The role of MR in pathophysiology

MR is expressed in polarized epithelial tissues, such as the distal part of the nephron, the distal colon, and the salivary glands (7). These tissues are considered the classical aldosterone target tissues, where MR regulates ion and water homeostasis (11, 12). As mentioned above, the importance of MR is reflected by the phenotype of MR knockout mice, who develop

symptoms of pseudohypoaldosteronism (PHA) in the first week of life and die in the second week after birth from dehydration by renal sodium and water loss. These mice exhibit a strongly impaired amiloride-sensitive, and thus ENaC-mediated, transepithelial sodium transport in the kidney and colon (3).

In man there is only one MR mutation associated with a distinct phenotype described. A missence mutation in the MR LBD (S810L) causes an autosomal dominant form of hypertension exacerbated by pregnancy (13). Ligands, e.g. progesterone and cortisone that normally do not activate wt MR become agonists for the MR S810L mutant, which causes a constitutive MR activation (13, 14).

MR is also expressed in non-epithelial tissues which are clearly not primarily involved in sodium transport e.g. the hippocampus, the heart, blood vessels, adipocytes and macrophages (15-18). The role of MR in physiology and pathophysiology in non-classical aldosterone target tissues has attracted considerable attention. The clinical relevance of MR in the pathogenesis of cardiac dysfunction was demonstrated by two large clinical trials, the Randomized Aldoactone Evaluation Study (RALES) and Eplerenone Post-Acute Myocardial Infarction Heart Failure Efficacy and Survival Study (EPHESUS). Patients with heart failure or post-acute myocardial infarction who received in addition to their usual treatment regimen low doses of MR antagonists showed a 30% reduction in morbidity and mortality (19, 20). Recent studies demonstrated that macrophage MR null mice were resistant against mineralocorticoid-mediated cardiac fibrosis, despite normal macrophage recruitment (21). Another example that MR plays a role in extra-renal physiology was demonstrated by mice with a forebrain-specific MR knockout. These animals showed impaired spatial learning linked to behavioral stereotype (22).

These studies clearly indicate that the MR is involved in many physiological processes and that dysregulation of MR signaling is linked to intensively studied human diseases, such as hypertension and cardiac failure.

1.4. MR selectivity

All cells expressing MR also express GR (11, 23, 24). MR and GR are closely related members of the nuclear hormone receptor family. Both receptors exhibit a 15% homology for the NTD, 94% for the DBD, and 57% for the LBD (25). This high homology is clearly reflected in the overlapping DNA binding specificities and cross-reactivity with their cognate ligands. Both receptors appear to recognize common DNA sequences (11, 12) and exhibit a broad overlap of target genes. MR and GR have equivalent affinity for cortisol (26). In

contrast, MR binds aldosterone with much higher affinity than GR does (27). However, GR can also be activated at supraphysiological concentrations of aldosterone (28-30). Given the circulating cortisol levels are at least 100-fold higher than those of aldosterone, occupancy of MR by aldosterone should be precluded. This raises the question of mechanisms that confer to mineralocorticoid specificity.

1.4.1. The pre-receptor level

At the pre-receptor level MR is protected against permanent glucocorticoid occupancy by the enzyme 11β-hydroxysteroid dehydrogenase type 2 (11β-HSD2), which converts cortisol into its MR-inactive 11-keto congener cortisone (16, 31) (Fig. 1.2). This metabolite has negligible affinity for MR. The importance of 11β-HSD2 becomes clear by the syndrome of apparent mineralocorticoid excess (AME) caused by a loss of function mutation in the 11β-HSD2 gene. In the absence of 11β-HSD2 cortisol activates MR resulting in severe hypertension mediated by increased ENaC activity (31-33). In the classical aldosterone target organs such as kidney and colon 11β-HSD2 is co-expressed with MR (34). However, other aldosterone-sensitive tissues such as heart or hippocampus lack 11β-HSD2 expression (35), indicating that mineralocorticoid specificity is not exclusively ensured by 11β-HSD2.

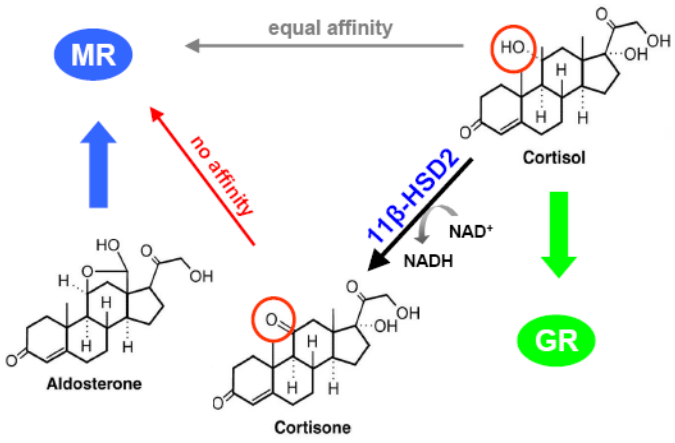

Fig. 1.2: Inactivation of cortisol by the 11β-HSD2
In epithelial tissues the enzyme 11β-hydroxysteroid dehydrogenase type 2 (11β-HSD2) confers to aldosterone specificity through converting cortisol into its MR-inactive metabolite cortisone.

1.4.2. The receptor level

At the receptor level two mechanisms are thought to contribute to mineralocorticoid selectivity:

1) Ligand-dependent receptor conformation

Even though the affinity of cortisol and aldosterone for MR is in the same order of magnitude, cortisol dissociates more rapidly from MR than aldosterone does (36). Additionally, *in vitro* transactivation assays revealed that MR is more sensitive to aldosterone than to cortisol (25, 37). This indicates that the aldosterone-activated MR complexes are more stable. This hypothesis has been reinforced by a study of Peter Fuller and colleagues, demonstrating that intra-molecular contacts between the N and C-terminus of MR are stronger in presence of aldosterone than of cortisol (38).

2) DNA-specific receptor conformation

Upon ligand binding MR binds to specific hormone response elements (HREs), typically imperfect palindromic, hexameric half sites separated by 3 base pair (bp) spacers in the promoters of target genes. It is widely accepted that MR and GR recognize common response elements, but evidence is increasing that these elements comprise capabilities that confer to the receptors activity. Recent studies from the Yamamoto laboratory reported that GREs linked to target genes are highly conserved across species, but vary substantially around a consensus (39). They further demonstrated that consensus sequences differing in a single bp, differentially affect GR conformation and regulatory activity (40). Therefore it is likely that common DNA consensus sequences differentially modulate MR vs. GR conformation and thereby activity. It can be speculated, whether consensus sequences further tighten ligand-dependent receptor conformation, important for specific co-regulator recruitment, and thus target gene regulation. The recruitment of co-regulator proteins is considered as the post-receptor level that confers to nuclear receptor-mediated transcriptional specificity.

1.4.3. The post-receptor level

Co-regulator molecules are recruited by steroid receptors to enhance or repress transcription and are thus divided into co-activators and co-repressors respectively. To date more than 285 co-regulator proteins have been described. Some of them appear to be general modulators, pleiotropic in their action, and cellular expression, whereas others seem to be receptor specific or limited in their tissue distribution (41). For a detailed review on this topic see references (42, 43).

About a dozen of co-regulators have been described that modulate MR activity. The MR dependent co-regulator recruitment is schematically depicted in figure 1.3. Among the most important co-activators were CBP/p300 (44), SRC-1 (45, 46), PGC-1α (46), TIF-1 and RIP-140 (45) involved in chromatin remodeling and acetylation and the RNA helicase RHA (47).

Co-repressors e.g. PIAS1 (48) and DAXX (49) have been demonstrated *in vitro* to bind MR and to repress its transcriptional function. The first example for a MR selective co-activator is the Pol II elongation factor ELL (eleven-nineteen lysine-rich leukemia). It was demonstrated that the co-activating properties of ELL are restricted to MR, because it strongly represses transactivation of GR and had no effect on PR and AR (50). A comprehensive study comparing the interaction of a panel of cofactor binding peptides with LBD from MR, GR, PR and AR demonstrated that the number of cofactors binding to MR was much less than for GR and PR and not dissimilar from AR (51). This provides further support for MR and GR functional diversity of action.

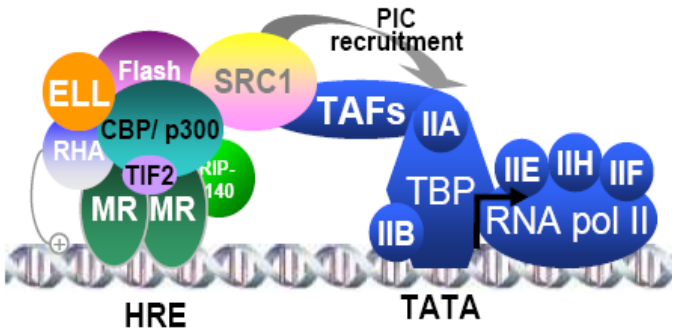

Fig. 1.3: Co-regulator recruitment by MR
MR binds to hormone responsive elements (HREs) in the promoter of target genes and recruits a series of co-activator or co-repressor complexes that control initiation of transcription by interaction with the preinitiation complex (PIC); The PIC comprises TBP and TAFs at the proximal promoter (TATA-box) and is associated with the RNA pol II.

Taken together, MR has equal affinity to aldosterone and cortisol, the natural ligand of the GR, and the ubiquitously expressed GR is activated by supraphysiological concentrations of aldosterone. To date several mechanisms have been identified that confer to MR specificity. Nevertheless, this cross-reactivity makes it experimentally difficult to attribute observed effects to either MR or GR. To investigate the mechanisms by which the aldosterone-activated MR exerts its function requires experimental systems that largely eliminate interference with GR.

1.5. Molecular mechanisms of action

Aldosterone-activated MR exerts its physiological action through modulation of gene expression, which occurs after a lag period of 0.5-1 h. In contrast, there is increasing evidence of rapid (within minutes after aldosterone exposure) so called non-genomic effects that involve second messenger signaling pathways. To date it is not clear whether these rapid non-genomic actions are mediated by MR or by a putative novel transmembrane receptor.

The best-known effect of aldosterone-activated MR is the increase of sodium reabsorption across target epithelium in the aldosterone-sensitive distal nephron (ASDN) (52),

which is the principle site for sodium retention in the body. This vectorial electrogenic transport is mediated by the apically localized epithelial sodium channel (ENaC, SCNN1) and catalyzed by the basolateral sodium potassium adenosinetriphosphatase Na-K-ATPase (ATP1A1). The activity and surface expression of ENaC is hereby the rate limiting step and consequently the prime target of the regulative impact of aldosterone-activated MR in the kidney. In the recent years a number of gene products that are induced by aldosterone have been identified, that have led to a much better understanding of the MR and its molecular mechanism of action. The following chapter will focus on MR target genes that have been shown to be crucial for the aldosterone-controlled transepithelial sodium transport.

MR functions as a ligand-dependent transcription factor (see section 1.2) by modulating the transcription of target genes (41, 53). The mode by which MR alters the expression of its target genes can be divided into an early and a late phase. Early responsive genes are considered as direct MR target genes and respond to short time aldosterone exposure. These genes code for regulatory factors that mediate acute effects through modulating channel trafficking and possibly the open probability of already synthesized channels (54). As aldosterone exposure continues late responsive genes are regulated. This regulation does not exclude direct regulatory mechanisms but probably requires factors induced in the early phase. Late responsive genes code, among others, for the transporters themselves. The long-term regulation occurs probably via the number of functional channels expressed.

1.5.1. Channels and transporters involved MR-regulated transepithelial sodium transport

ENaC is composed of three distinct but similar subunits (α, β and γ) and located in the apical membrane of epithelial cells. Each subunit consists of two transmembrane domains and a large (50 kDa) extra-cellular region, whereas the amino and the carboxy-termini of all subunits (~8-10 kDa) are cytosolic. The importance of all three ENaC subunits in the mechanism of salt homeostasis has been demonstrated by different knockout mouse models. Targeted disruption of α-ENaC (55), β-ENaC (56) and γ-ENaC (57) led to severe salt wasting phenotypes in neonates, who died within 2 days after birth probably from hyperkaliemia. The expression of all three ENaC subunits is stimulated by aldosterone in a tissue specific manner. In the kidney the α-ENaC subunit is responsive to aldosterone (58), whereas in the colon only β and γ-ENaC subunits are induced by aldosterone (59, 60). Interestingly, under normal conditions in the kidney, when the rate of sodium transport is low, α-ENaC is transcribed to a lesser extent than β- and γ-ENaC (61).

The Na-K-ATPase is present in all cells to ensure basic cellular ion homeostasis but it also contributes to specialized tissue functions (62). In epithelial cells involved in sodium transport the expression of the Na-K-ATPase is restricted to the basolateral membrane where it catalyses, dependently on ATP hydrolysis, the transport of 3 Na^+ ions out of the cell in exchange for 2 K^+ ions into the cell (63). Its primary role is to maintain high intracellular K^+ and low intracellular sodium concentrations. Thus the Na-K-ATPase becomes the driving force for sodium reabsorption in epithelia which can develop high lumen-to-blood concentration gradients. The Na-K-ATPase is composed of 2 subunits: a large catalytic α-subunit (113 kDa), which transports the cations and hydrolyzes ATP, and a smaller β-subunit (35 kDa), which has been proposed to be involved in the structural assembly of the enzyme (64). mRNA level coding for the α- and β-Na-K-ATPase subunits were increased upon aldosterone treatment in rat kidney epithelial cells (65) and HEK293 cells (66).

1.5.2. Early MR-responsive genes modulating sodium retention

The majority of rapid MR-responsive genes directly or indirectly modulate ENaC in its surface expression or activity. ENaC is a protein complex with rapid turnover due to an ubiquitinylation pathway that exerts a tonic inhibition on ENaC surface expression (54, 67).

A central player in the group of proteins which influence the surface expression of ENaC by interfering with this ubiquitinylation pathway is the serine/threonine kinase SGK1 (68-70), whose regulation by aldosterone has been shown in the ASDN and the distal colon. In cell culture experiments it has been shown that activation of SGK1 is dependent on the insulin-induced phosphatidylinositol 3-kinase (PI3K) signaling cascade. In contrast to aldosterone-mediated signaling, which requires gene expression, insulin rapidly (within minutes) stimulates PI3K activity through a multiple step transduction pathway (12). The detailed mechanisms by which aldosterone induces PI3K activity remain to be elucidated. It is assumed that this activation might be mediated by the aldosterone-induced K-RAS2 (71), which has been shown to interact with PI3K (72). Thus SGK1 consolidates two extracellular signals (aldosterone and insulin) to regulate sodium transport. Activated SGK1 phosphorylates the E3 ubiquitin ligase Nedd4-2 and thereby induces its interaction with specific 14-3-3 protein isoforms (73-75). This impairs the interaction of Nedd4-2 and ENaC, which causes channels to remain in the apical membrane that are otherwise targeted for proteasome degradation (41).

In addition to the ubiquitinylation route of regulating ENaC surface expression the RAS-RAF-MEK-ERK pathway has emerged as an ENaC regulatory pathway. ERK seems to be constitutively activated in collecting duct cells and has a potent inhibitory effect on ENaC (reviewed in Bhalla et al. and references therein (54)). ERK appears to act via ENaC phosphorylation, which stimulates interaction with Nedd4 ubiquitin ligases (76). However, the expression of the core pathway proteins RAS, RAF, MEK and ERK seems not to be regulated by aldosterone. On the other hand, several proteins which specifically regulate the activity of that pathway have been reported to be aldosterone-regulated MR target genes including K-RAS2 (71, 77), NDRG2 (78, 79), and GILZ1 (80, 81). Recent studies demonstrated that GILZ1 stimulates ENaC-mediated sodium transport in *Xenopus leavis* oocytes and kidney epithelial cells by inhibiting RAF (82). Further studies revealed that GILZ1 directly interacts with the α- and β-ENaC subunits and is assembled with an ENaC regulatory complex containing RAF-1 and Nedd4-2 (83). This supports the hypothesis that aldosterone exerts its sodium stimulatory effect through triggering the formation of an inhibitory complex that protects ENaC from tonic degradation by Nedd4-2.

Apart from ENaC the basolateral localized Na-K-ATPase might also be a target to fine-tune sodium reabsorption. However, the only aldosterone-induced protein identified so far that directly regulates the Na-K-ATPase activity is the corticoid hormone-induced factor (CHIF) (84). CHIF is a member of the FXYD protein family, which is expressed in epithelia of the nephron and the distal colon (85, 86), while its regulation by corticoids seems to be restricted to the colon (85, 87).

A schematic overview how these early aldosterone-induced genes modulate ENaC-mediated transepithelial sodium transport is shown in Figure 1.4. However, this picture is still incomplete. There are several lines of evidence that there are yet unidentified genes involved that also regulate ENaC activity or mediate crosstalk of already known regulatory processes.

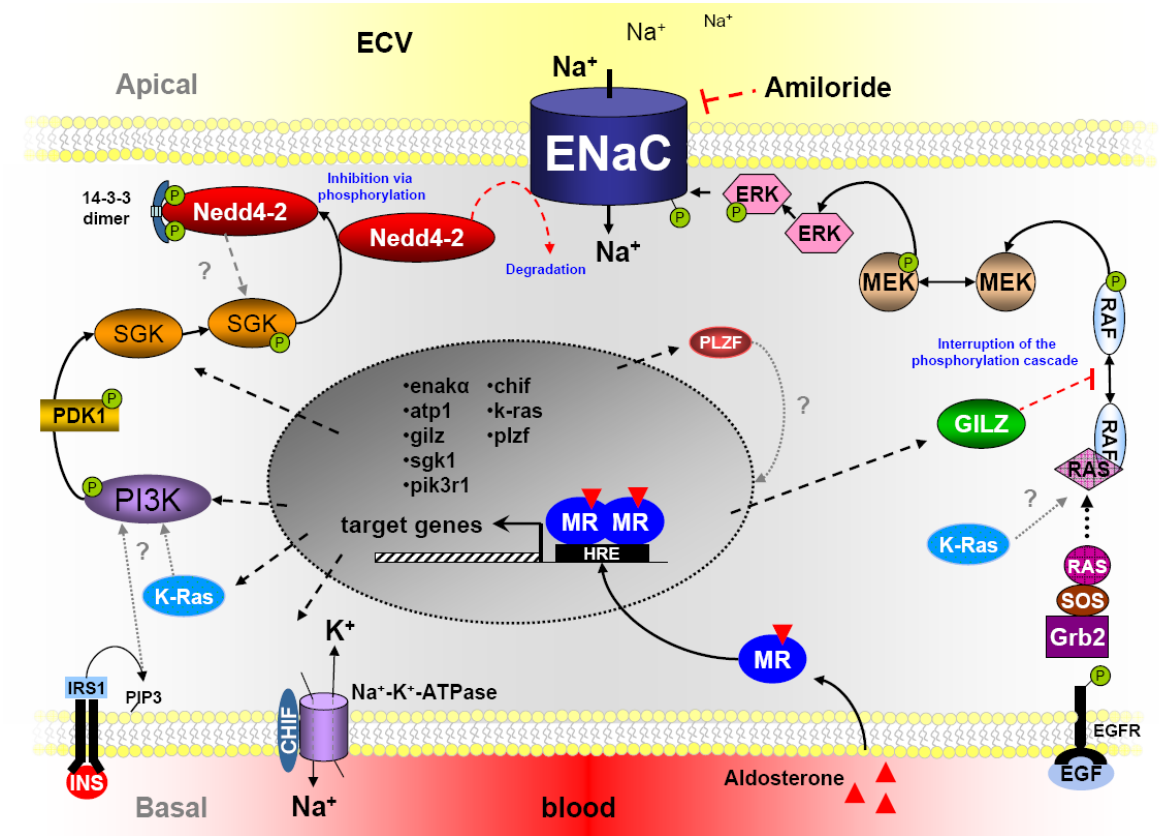

Fig. 1.4: Schematic depiction of aldosterone-regulated ENaC activity in an epithelial cell
Aldosterone-activated MR translocate into the nucleus and bind as homodimers to hormone response elements (HREs) in the promoter of target genes, activating or repressing their transcriptional activity. Aldosterone-induced proteins negatively regulate the activity of Nedd4-2, which decreases ENaC cell surface expression. P, phosphate; ECV, extracellular volume; EGF, epidermal growth factor; INS, insulin. See text for definitions of other abbreviations.

1.6. Aim of study

The mineralocorticoid receptor (MR) plays a pivotal role in salt and water homeostasis and thus blood pressure. Dysregulation of MR signaling is involved in hypertension and cardiac failure, two diseases with an enormous medical and economic burden for western societies. Pharmacological blockade of MR can lower blood pressure and improve prognosis in patients with severe heart failure, as convincingly demonstrated in clinical trials.

The detailed molecular mechanisms by which the MR exerts its effects are still not well understood and lag far behind the knowledge of other steroid hormone receptors. That might be in part due to the lack of appropriate *in vitro* models and the cross-reactivity with the ubiquitously expressed glucocorticoid receptor (GR).

The present study aimed at the generation of appropriate *in vitro* models that allow a clear separation of MR- versus GR-mediated effects in order to identify direct MR target genes and to study their involvement in aldosterone-mediated physiological processes. Gaining new insights into the molecular mechanisms of MR may provide the basis for the

development of novel pharmaceuticals. Furthermore these studies should provide the basis for novel *in vitro* test systems for the characterization of newly synthezised antimineralocorticoid compounds. In the recent years it became increasingly evident that antimineralocorticoid drugs, either given alone or on top of standard therapy, are beneficial in the treatment of cardiovascular diseases. Also, the antimineralocorticoid activity of Drospirenone, a progestin used in contraception and hormone therapy, has led to additional health benefits in women.

2. Materials and Methods

2.1. Material

2.1.1. Plastic ware

All plastic ware required for cell culture maintenance was purchased from BD (Heidelberg, Germany) or Corning® distributed by Sigma-Aldrich (Schnelldorf, Germany). Cell culture dishes and multi-well plates were purchased from NUNC™ distributed by Thermo Fisher Scientific (Langenselbold, Germany). Plasticware for molecular biology was purchased from Biozym (Oldendorf, Germany) or Eppendorf AG (Hamburg, Germany).

2.1.2. Chemicals

If not stated otherwise, all chemicals were purchased from Sigma (Fulka) (Steinheim, Germany) or Merck (Darmstadt, Germany) in p.a. (pro analysi) grade. Except for RU-compounds (Sigma-Aldrich) hormones were synthesized in-house (Medicinal Chemistry department of BSP).

2.1.3. Water

Water was purified utilizing the Milli-Q Gradient (Millipore, Schwalbach, Germany). For PCR and restriction analysis nuclease-free ultra pure water (Ambion, Foster City, CA, USA) was used.

2.1.4. Buffers

- DNA annealing buffer: 100 mM Tris-HCl, 1 M NaCl, 10 mM EDTA
- Chromatin sonication buffer: 10 mM Tris-HCl pH 8.0, 100 mM NaCl, 1 mM EDTA, 0.5 mM EGTA, 0.1% Lauroylsarcosin, 0.1% Na-deoxycholate
- DNA loading buffer: 50% (w/v) Glycerin, 10 nM Tris, 10 mg/ml Orange G, pH = 7.5
- Lysis buffer for Western blot analysis: complete Lysis-M, EDTA free (Roche, Basel, Swiss)
- RIPA buffer: 10 mM Tris-HCl pH 8.0, 1% Triton X-100, 1% Na-deoxycholate

- Transfer buffer: $NaHCO_3$ (10 mM), Na_2CO_3 (3 mM), SDS (0.05%), Methanol (20%)
- 20x MOPS SDS running buffer: NuPAGE (Invitrogen, La Jolla; CA, USA)
- 1x PBS: 137 mM NaCl, 2.7 M kcl, 8.2 mM Na_2HPO_4, 1.5 mM KH_2PO_4
- 50x TAE (tris acetate EDTA) buffer: 2 M Tris/HCl, 1 M acetic acid, 0.1 M EDTA
- 10x TBE buffer: 0.89 M Tris/HCl, 0.89 M boric acid, 20 mM EDTA
- 10x TBS buffer: 500 mM Tris.HCl, 1500 mM NaCl pH 7.4
- TBST: 1x TBS, Tween (0.05%)

2.1.5. Media

For bacterial culture the following media were used: LB medium: 1% (w/v) bacto trypton, 0.5% (w/v) bacto yeast extract, 1% (w/v) NaCl; LB agar: LB medium with 1.5% (w/v) bacto agar. Media for cell culture were purchased from Gibco® (Invitrogen). PBS for cell culture and trypsin was purchased from PAA (Biochrom AG, Berlin, Germany).

2.1.6. Size standards

DNA size markers: TrackIt™ 1 kb Plus DNA Ladder, TrackIt™ 100 bp DNA Ladder (Invitrogen). Protein size marker: Precision Plus Dual Color (Bio-Rad, Hercules, CA, USA)

2.1.7. Oligonucleotides

Oligonucleotides were designed using the computer software Vector NTI (Invitrogen), SeqMan and PrimerSelect (DNASTAR, Madison, WI, USA) and purchased form Metabion, (Munich, Germany).

Table 2.1: Oligonucleotides

Sequence 5' - 3'	Primer Name	used for
CTCCGCCCAGTTCCGCCCATTC	SV40 For2	Genotyping
ACGCCGAGTTAACGCCATCAAAAA	LacZeo Rev1	Genotyping
CCGCCCAGTTCCGCCCATTCTC	SV40 For1	Genotyping
GGGCAGTTCGGTTTCAGGCAGGTCTT	Hygro Rev3	Genotyping
CTCACGGGGATTTCCAAGTCTC	CMV For1	Genotyping
TGGAATAGCACCGGAAACACAG	hMR Rev1	Genotyping
CCTCCCCCGTGCCTTCCTTGACC	BGH For1	Genotyping
AACCATCGGCGCAGCTATTTACCC	Hygro Rev2	Genotyping
ATGCCTGCTGATGGGAACTGGAT	CNKSR3 human For	qPCR
CCGCTCGGTCGTGGGTCTG	CNKSR3 human Rev	qPCR
ATGTGAGTGGGCCCAACGACCTAC	SGK human For	qPCR
GCTTCCTTGACGCTGGCTGTGAC	SGK human Rev	qPCR

Sequence 5' – 3'	Primer Name	used for
GGGCCTAACCAGCCTTGGGAGTAT	TSC22D3 human For	qPCR
CCGTGGCCGCATTCAGAGG	TSC22D3 human Rev	qPCR
GAAGTTGGCCGCATGAAGA	Cyclophilin human F1	qPCR
GCCTAAAGTTCTCGGCCGT	Cyclophilin human R1	qPCR
CTGACCGAGCGTGGCTACA	beta-Actin human F1	qPCR
GCCATCTCCTGCTCGAAGTC	beta-Actin human R1	qPCR
GGATGCGGTGAGGGAGTGGTA	SCNN1A human For	qPCR
AAGCGGCAGGCGAAGATGAA	SCNN1A human Rev	qPCR
CTGGAAGGCCGCTGTGGTG	FKBP5 human For	qPCR
TGTTCTTCCCGCTGCATTTTCTC	FKBP5 human Rev	qPCR
GGCAACAGTTGAACACCAGGAAAATC	PDK4 human For	qPCR
AGGCGTTGGTGCAGTGGAGTATGTAT	PDK4 human Rev	qPCR
AGCGCAGCGACGGGTTGTT	PHLDA1 human For	qPCR
CAGCTGCTTGGGCGGGATAA	PHLDA1 human Rev	qPCR
AGCGCTCCCGGGACTACTCG	ZBTB16 human For 3	qPCR
GTGGCCCTTCATGTGCTTCTGC	ZBTB16 human Rev 3	qPCR
CAGCCGGCTCGGTGTCCTC	MAFB human For	qPCR
AGCGCCTCGGGGTTCATCTG	MAFB human Rev	qPCR
GGGGGACACCTGGAAGGATTACTG	KLF9 human For	qPCR
CACGGAGGGGGTCTGGATGG	KLF9 human Rev	qPCR
CGCGGTGGGCAAGACGAG	RHOU human For	qPCR
GCCGCCCATCCACAGACAC	RHOU human Rev	qPCR
CAAAATTCGGCGTGGACAGTTCT	TRIB1 human For	qPCR
AGTAGGATCTCGGGGGCAGTGA	TRIB1 human Rev	qPCR
ACGTGGACCGGCTGGAGGAG	ARL4C human For	qPCR
ATAGGTGGTGGCCGGGATAAGC	ARL4C human Rev	qPCR
CCGGCCGACTTTGGAGGTGT	BCL6 human For	qPCR
TGAGGGGGCAGCAGGTTTGAG	BCL6 human Rev	qPCR
CATCATCACGCTGGTGGTCCTCTT	EFNB2 human For	qPCR
CGCTGCGCTTGGGTGTGG	EFNB2 human Rev	qPCR
CCAACGGCGAGGATCACTTCAG	ETV1 human For	qPCR
CCAACGGCGAGGATCACTTCAG	ETV1 human Rev	qPCR
CCGGCGCTTCAGGCACTACA	F3 human For	qPCR
ACTTGATTGACGGGTTTGGGTTCC	F3 human Rev	qPCR
CCGGGCAAGGGCAACTACTG	FOXG1 human For	qPCR
GCGCGGTCCATGAAGGTGA	FOXG1 human Rev	qPCR
ATTCCGCCTAACCCCGTATGTGAC	Per1 human For	qPCR
TGTGCCGCGTAGTGAAAATCCTCT	Per1 human Rev	qPCR
ACCCACCAGCACTGCCTCCTAAA	PI3KR1 human For	qPCR
TCCCCAGTACCATTCAGCATCTTG	PI3KR1 human Rev	qPCR
CGTGGGGCAGCACAAAGGTCT	RASGEF1B human For	qPCR
GGGAAGGCGGTTGGCACAA	RASGEF1B human Rev	qPCR
TCGCCCAGGCTTCTTCTCCAG	TBX3 human For	qPCR
CCTCGGCGTCGCTCTCACC	TBX3 human Rev	qPCR
TCGCCTGTTGGCTGCCTTACTACAT	CXCR4 human For	qPCR
TAGGGCCTCGGTGATGGAAATCC	CXCR4 human Rev	qPCR
ACCCCGCACCTCCACTCCATC	NFKB1A human For	qPCR
GAAGGGCAGTCCGGCCATTACA	NFKB1A human Rev	qPCR
AGGTCAGTACTTGGGACTGTGTCAGG	PKP2 human/ rat/ mouse For	qPCR
CGTGGGTGATCCCAGTGTGAAA	PKP2 human/ rat/ mouse Rev	qPCR
CCCCATGCGAGCTCATCAAGGGAAAGAC	CDC42EP3 human For	qPCR

Sequence 5' – 3'	Primer Name	used for
AGGGCCCAAGATCAAGCTGCAGGGAGAG	CDC42EP3 human Rev	qPCR
ACCCGCACCTCATTCCTACATCAAT	NRP1 human For	qPCR
TCGCCTTGCGTTTGCTGTCAT	NRP1 human Rev	qPCR
GAGTATGCGGCTGTTGGGATTCT	MBLN1 ChIP For	ChIP
CTATGACTTGTGCCTGTGCTGGTG	MBLN1 ChIP Rev	ChIP
TAACACCCAGGGTCATTCTGTCAAA	MGC21644 ChIP For	ChIP
TCCTTGCTGAATGAATGAATGAACTG	MGC21644 ChIP rev	ChIP
TCAGGTGGGACAGCGGGAGAG	SGK1 ChIP For	ChIP
GTAACAAGCGAAGGGAGGGGTAGC	SGK1 ChIP Rev	ChIP
CCGGGCTTGTAAGATGTGAGAATG	SCNN1A ChIP For	ChIP
TCCTTAGGAAGCTGCCGTGTGC	SCNN1A ChIP Rev	ChIP
TGTTGCTCACAGCGAGACAGAGTG	CNKSR3 Prom. ChIP For	ChIP
CGGGCCCCGCTTTCCTT	CNKSR3 Prom. ChIP Rev	ChIP
CTCGATAGGGGGTACAAAAAGT	CNKSR3 ChIP For	ChIP
ATAGATGAGGCAGTACCCACAAA	CNKSR3 ChIP Rev	ChIP
CAAGGCGCAAGTAATTCTAACACAGG	CXCR4 ChIP For	ChIP
TGGAGACAGAAGGATTTAGGGAAGGA	CXCR4 ChIP Rev	ChIP
AACGCACTGGAGTGTGGAAATCAA	RHOB ChIP For	ChIP
ATCCAGAGGGGAACAGAACATCCA	RHOB ChIP Rev	ChIP
TTGAGGGGCTGCCCAGATACATTTA	PDK4 ChIP For	ChIP
GATCACCGCAAAAGGTAAGGCAAACT	PDK4 ChIP Rev	ChIP
CCCGGCCAAGGGGTTAGGAA	KLF9 ChIP For	ChIP
CTGGGCTGGGGCTGGATTGAT	KLF9 ChIP Rev	ChIP
ATGCCGTTCTCAGCCATCTACTCTG	PIK3R1 ChIP For	ChIP
TTGATGGAGGAAATGTGAAA	PIK3R1 ChIP Rev	ChIP
TGGGTTCCACCACATATACAACAGTTTG	GILZ ChIP For	ChIP
TAAGAGGCCCCAGTACTTTTCCAATAGC	GILZ ChIP Rev	ChIP
ATGAAGGGGAACAAGCGTGAGG	SCNN1A ChIP control For	ChIP
GCCGTGGATGGTGGTGTTGTT	SCNN1A ChIP control For	ChIP
GCATCTCGAGCACCGGCATCGCTGTTCTGC	pGL4.23 SGK1 rep500bp For XhoI	Reporter
GCATAAGCTTAGGGGGCGGAAATAAAAGTCGTCT	pGL4.23 SGK1 rep500bp Rev HindIII	Reporter
ACATCTCGAGAACATTGGGTTCCACCACATA	pGL4.23 GILZ rep626bp For XhoI	Reporter
ACATAAGCTTCAGGGAATTCTGATACCAGTTA	pGL4.23 GILZ rep626bp Rev HindIII	Reporter
GCTATGAGCTCAGGCGGGAGAATCGCTGGAACCTG	pGL4.10 CNKSR3 Prom. For SacI	Reporter
GCTATCTCGAGCGCGCTCGGGTTGCAAAGTTTCA	pGL4.10 CNKSR3 Prom. Rev XhoI	Reporter
GCTATCTCGAGCTGCCTCACTTATTCAAATTCTTCTGAT	pGL4.23 CNKSR3 4kb up For XhoI	Reporter
GCTATGAGCTCTCACCGAGTCTGAAACTCTTGGTATTAT	pGL4.23 CNKSR3 4kb up Rev SacI	Reporter
GCATCTCGAGGACAACTGAAATGCGAAGTAGAGTA	pGL4.23 PIK3R1 For XhoI	Reporter
GCATAAGCTTTGATGGAGGAAATGTGAAATGTAAG	pGL4.23 PIK3R1 Rev HindIII	Reporter
GCTATGAGCTCGCTTGTGCCAGACATTTGAGGGTAGA	pGL4.10 PDK4 For SacI	Reporter
GCTATCTCGAGTGGGACGGGGCTCCGAGTC	pGL4.10 PDK4 Rev XhoI	Reporter
ACATCTCGAGGAGGAGAGGGCTCAAAGAAGAAGCAGACTT	pGL4.23 FKBP5 For XhoI	Reporter
ACATGAGCTCAGCCACGTTTTCTCCTTACCCATCCTTCT	pGL4.23 FKBP5 Rev SacI	Reporter
ACATAAGCTTTTTCCGCGAGGTTATTATGAGCTGAGTGTT	pGL4.23 NFKBIA For HindIII	Reporter
ACATGAGCTCGAAAGACGAGGAGTACGAGCAGATGGTCAAG	pGL4.23 NFKBIA Rev SacI	Reporter
ACATAAGCTTATCTCCCCTAACCCAGGCAGTCCTTGAT	pGL4.23 PER1 For HindIII	Reporter
ACATGAGCTCGTCTTTGGTACCAGGCCAGCAGATGTGT	pGL4.23 PER1 Rev SacI	Reporter
ACATGAGCTCCTGGTTACTAGGGAATTCCGCACAAGTTC	pGL4.23 CALM1 For SacI	Reporter
ACATAAGCTTTCTGGGAATAAGAAAGGGAAATGCTGCTA	pGL4.23 CALM1 Rev HindIII	Reporter
GCTATGAGCTCGTGGAGCCGCAGTTGGTTGAAT	pGL4.23_MBLN1 For SacI	Reporter
GCTATCTCGAGGCTGCAGAGGGCTCGAAAGTCTAA	pGL4.23_MBLN1 Rev XhoI	Reporter

Sequence 5' - 3'	Primer Name	used for
GCTATCTCGAGCTAAATGGAAATAGCCCTTCATAAATCC	pGL4.23 MGC21644 For XhoI	Reporter
GCTATGAGCTCCAAAGTTGCATAGATGAATGTAGCAGTG	pGL4.23 MGC21644 Rev SacI	Reporter
GCTATCTCGAGAAATGAGGCGGAAGCCACATCTGACT	pGL4.23 SCNN1A For XhoI	Reporter
GCTATGAGCTCAATCTTTATGGGTGTGGGTGTGAGTGTG	pGL4.23 SCNN1A Rev SacI	Reporter
GCTATGAGCTCGCTGGCCCCTCTCCTGTCTCTAAAA	pGL4.23 CXCR4 For SacI	Reporter
GCTATCTCGAGGAGTAAAAATGGCTCTCCCCCAAAAA	pGL4.23 CXCR4 Rev XhoI	Reporter
GCTATGAGCTCTGGTCTTGGGCAGTGGCTCCTA	pGL4.23 RHOB For SacI	Reporter
GCTATCTCGAGGGGGGATCTCACCTGCTGAAAATAATAC	pGL4.23 RHOB Rev XhoI	Reporter
ACATCTCGAGGCATGGGGGCCGTACAGAAGGGGGAACT	pGL4.23 KLF9 For XhoI	Reporter
ACATAAGCTTCGGCCAGGCTGTGCGGGAGGAGATG	pGL4.23 KLF9 Rev HindIII	Reporter
ACATGCTAGCCCAGTTCTTTTGTGGGTACTGCCTC	GRE1 mut Rev NheI	Mutation
ACATGCTAGCTTGCCCTGAAGTGCAGAAGCTACTAA	GRE1 mut For NheI	Mutation
ACATCCCGGGACCCCCTATCGAGTTGCAGATTATCCA	GRE2 mut Rev ApaI	Mutation
ACATCCCGGGAGTAATAAAAATCCACAGGAAAAAATGCAG	GRE2 mut For ApaI	Mutation
ACATGAATTCGCTGGTGTAAATGGCATTCTGTTCT	GRE3 mut Rev EcoRI	Mutation
ACATGAATTCTACAGTTCCAATTTAACTTTATGGGACTC	GRE3 mut For EcoRI	Mutation
ACATCTTAAGTTTTGGATAATCTGCAACTCGATAG	GRE4 mut Rev AflII	Mutation
ACATCTTAAGGAATGCCATTTACACCAGCTGTTCT	GRE4 mut For AflII	Mutation
CTCCCCGGGATGAGAATGTGAG	CNKSR3 mus musculus For	qPCR
CGGGCAGCTGATCGGAATCT	CNKSR3 mus musculus Rev	qPCR
GTGCGCGACCCCTGCTACCT	TSC22D3 mus musculus For	qPCR
CACTGGCTCCGGAGGCACTGT	TSC22D3 mus musculus Rev	qPCR
CGGCCTGCCCCCGTTTTAT	SGK1 mus musculus For	qPCR
TTGGCACCCAGCCTCTTGGTC	SGK1 mus musculus Rev	qPCR
GCAGCCAGTGGAGCCTGTGGT	SCNN1A mus musculus For	qPCR
CTGGCCCCTCGTCCTGGAGA	SCNN1A mus musculus Rev	qPCR
ACCGCCCACTGTGGCTGAGC	SCNN1B mus musculus For	qPCR
CCCCGGGATGGGCAGAGTCT	SCNN1B mus musculus Rev	qPCR
ACTGGATTTCCCCGCTGTCACTATCT	SCNN1G mus musculus For	qPCR
CCCGGCGTTTCCGAGGTG	SCNN1G mus musculus Rev	qPCR
CTGGCCGGGACCTGACAGACTAC	beta-Actin mus musculus For	qPCR
CACGCACGATTTCCCTCTCAGC	beta-Actin mus musculus Rev	qPCR
CACCATGGAAACCAAAGGCTACCACAGTCTCCCTGAAGGCCTA	CDS rattus MR For	Expression
TCACTTTCTGTGAAAGTAAAGGGGTTTGGCATTCCCAGACT	CDS rattus MR Rev	Expression
CACCATGGAACCCGTGACCAAGTGGAG	CDS hCNKSR3 For	Expression
TCAGTGAGTCAACAGTTTGAGGCGCGTAAA	CDS hCNKSR3 Rev + STOP	Expression
GTGAGTCAACAGTTTGAGGCGCGTAAAC	CDS hCNKSR3 Rev - STOP	Expression
CACCATGGAGCCCGTGACCAAGTGGAGC	CDS mCNKSR3 For	Expression
TCAGTGAGTCAACAGCTTGAGGCG	CDS mCNKSR3 Rev + STOP	Expression
GTGAGTCAACAGCTTGAGGCG	CDS mCNKSR3 Rev - STOP	Expression

*blue highlighted bases are overhangs required for cleavage close to ends; red highlighted bases are restriction sites

2.1.8. Vectors and plasmids

- pcDNA3.1/V5His®TOPO® vector (Invitrogen)
- pcDNA5/FRT (Invitrogen)
- pGL4.10 [luc2] (Promega, Madison, WI, USA)

- pGL4.23 [luc2/ minP] (Promega)
- pENTR2B (Invitrogen)
- pENTR/U6 (Invitrogen)
- pGT4 Lentiviral backbone (provided by Dr. Dr. Florian Prinz)
- pGT3 Lentiviral backbone (provided by Dr. Dr. Florian Prinz)
- pGT4-JRed Lentivirus (provided by Dr. Dr. Florian Prinz)

2.1.9. Antibodies

Table 2.2: Primary antibodies

MR antibody 6G1*	mouse monoclonal	provided by Dr. C. Gomez-Sanchez
CNKSR3	mouse polyclonal	Abnova #H00154043-A01
Beta-Actin	mouse monoclonal	Sigma-Aldrich #A3854
Pan-Cadherin	rabbit polyclonal	Abcam #ab16505
RNA polymerase II	mouse monoclonal	Abcam #ab24758
V5 epitope	mouse monoclonal	Invitrogen #R960-25
GR antibody	mouse monoclonal	Novocastra #NCL-GCR
Myc antibody	goat polyclonal	Abcam #ab9132
MEK1/2	rabbit polyclonal	Cell Signaling #9122
phospho-MEK1/2 (Ser217/221)	rabbit monoclonal	Cell Signaling #2338
phospho-MAPK (Thr202/Tyr204)	rabbit monoclonal	Cell Signaling #4377

*the generation and epitope specificity for this antibody is described in Gomez-Sanchez et al., 2006 (88).

Table 2.3: HRP-labeled secondary antibodies

Goat anti rabbit HRP-conjugated	Pierce #1858415
Goat anti mouse HRP-conjugated	Pierce #1858413

2.2. Methods

2.2.1. Molecular biology

2.2.1.1. Restriction digest

Restriction endonucleases including corresponding buffers were purchased from New England BioLabs (NEB) (Ipswich, MA, USA). Restriction digest from 250 ng up to 3 µg plasmid DNA was performed according to manufacturers' recommendations.

2.2.1.2. Fill-in of cohesive ends

To generate blunt ends restriction digest was followed by fill-in of 5´ overhangs. To this end purified DNA fragments were incubated with 1 mM dNTPs and 1U Klenow enzyme (NEB) in NEBuffer2 at 37°C for 30 min. Inactivation of the enzyme was achieved by incubating the reaction mixture at 75°C for 20 min. If different buffer conditions for subsequent enzymatic reactions were required, DNA was phenol/chloroform extracted and resolved in water.

2.2.1.3. Purification of DNA fragments

Purification of PCR products was performed using the QIAquick PCR purification kit (Qiagen, Hilden, Germany) according to manufacturers' recommendations. DNA fragments obtained by restriction analysis were separated by agarose gel electrophoresis. Bands of interest were excised and DNA was extracted using the QIAquick Gel Extraction Kit (Qiagen) according to manufacturers' instructions. DNA was eluted in 30-50 µl nuclease-free water (Ambion).

2.2.1.4. Ligation of DNA fragments

DNA ligation was performed using a T4 DNA Quick-Ligase (NEB) and the 2x ligation buffer supplied with the enzyme. 25-50 ng vector DNA was incubated with a 5-fold molar excess of the insert fragment. The following equation was used to calculate the amount of insert DNA: m_{Insert} (ng) = 5 x m_{Vector} (ng) x $length_{Insert}$ (bp)/$length_{Vector}$ (bp).

2.2.1.5. Transformation of E. coli and bacterial cultures

Transformation of *E. coli* cells was performed using a heat shock transformation procedure according to manufacturers' recommendations. *E. coli* TOP10 cells (Invitrogen) were thawed on ice. After application of vector DNA cells were incubated for 30 sec at 42°C and mixed with S.O.C. medium. Cells were incubated for 1 h at 37°C in a shaker rotating at 200 rpm and then plated on LB agar containing selection marker. The same protocol was used for transformation of *E. coli* Stbl3™ cells (Invitrogen) with Lentiviral constructs. Positive transformants were identified either by PCR or restriction digest analysis.

Bacterial cultures for DNA mini preparations were grown overnight in 4 ml LB medium containing either 100 µg/ml ampicillin or 50 µg/ml kanamycin as selection marker at 37°C in a shaker rotating at 200 rpm. For DNA maxi preparation starter cultures were grown under the conditions described above for 5 h and were then transferred to 200 ml LB medium containing an appropriate selection marker. Cultures were grown overnight at 37°C in a shaker rotating at 200 rpm.

2.2.1.6. Preparation of plasmid and genomic DNA

The following kits were used for plasmid DNA preparation according to manufacturers' instructions: QIAprep Spin Miniprep kit and QIAfilter Plasmid Maxi kit (Qiagen). DNA was eluted in nuclease-free water (Ambion).

Genomic DNA was prepared from HEK293 cells by using the NucleoSpin® Tissue kit (Macherey-Nagel, Düren, Germany) according to manufacturers' recommendations. Purified DNA was directly used as a template for restriction or PCR analysis.

2.2.1.7. Agarose gel electrophoreses

1% (w/v) agarose was melted in TAE buffer using a microwave oven and allowed to cool down to 70-60°C before 0.5 µg/ml ethidium bromide was added. DNA samples were mixed with loading buffer [50% glycerol (w/v), 10 mM Tris-EDTA, pH 7.5] [6:1, (v/v)] containing Orange G dye (10 mg/ml) to track DNA migration. To assess the length of DNA fragments appropriate size standards were loaded in one lane. DNA was visualized using the Versadoc 3000 Imaging System.

2.2.1.8. RNA preparation and cDNA synthesis

Total RNA was isolated using QIAshredder and RNeasy Mini Kits (Qiagen) according to manufacturers' recommendations. To prevent genomic DNA contamination an on-column DNase digestion step was included. The RNA integrity number (RIN), a measure of the RNA degradation grade, was determined using RNA LabChips and the Agilent Bioanalyzer 2100 (Agilent Technologies Inc., Santa Clara, CA, USA). RNA concentrations were determined on the Peqlab NanoDrop (Peqlab Biotechnology, Erlangen, Germany). Copy DNA (cDNA) was synthesized from 1-3 µg of total RNA using the Superscript™ III reverse transcriptase (Invitrogen) according to the manufacturers' instructions. In order to enrich for mRNA transcripts oligo(dT) primers were applied.

2.2.1.9. Polymerase chain reaction (PCR)

DNA amplification was performed using PfuUltra^{TM} II Fusion HS DNA Polymerase (Stratagene, La Jolla, CA, USA). In case of non-specific PCR products or a smear, a touchdown PCR (TD-PCR) protocol was applied in order to enrich for specific PCR product during the first cycles. In brief: during the first cycling steps the annealing temperature followed a gradient, starting 2°C above predicted primer T_m. In decremental steps of 1°C per cycle the annealing temperature was decreased until reaching a temperature 2°C below calculated optimal primer annealing temperature, followed by a set of 25 amplification cycles.

2.2.1.10. Quantitative real time PCR analysis

Quantitative real time PCR (qPCR) was performed using a 7500 fast real-time PCR-System (Applied Biosystems Inc, Foster City, CA, USA) to determine relative mRNA expression. MR-expressing M1 and HEK293 cell clones and the non MR-expressing parental cell lines were starved in culture medium containing 3% charcoal-treated FBS (see section 2.2.2.2) for 24 h before addition of indicated concentrations of aldosterone. Appropriate amounts of DMSO were used as a vehicle control. RNA was isolated followed by reverse transcription for cDNA synthesis (see section 2.2.1.8). PCR analyses were performed in triplicates using QuantiFast SYBR Green mix (Qiagen) with 200 nm of each primer and 25 ng of cDNA in a final reaction volume of 20 µl. An initial denaturation step at 95°C for 5 min was necessary to activate the DNA polymerase. The program consisted of 40 cycles of a two-step cycling protocol, including a denaturation step at 95°C for 10 sec and a combined annealing/ extension step at 60°C for 30 sec. In order to check specificity of PCR products a

melting curve analysis was performed subsequently to PCR analysis. Data were analyzed using the $2^{-\Delta\Delta CT}$ method (89) and normalized to the expression of beta-actin gene (referred as reference gene) [relative expression (fold induction) = $2^{-\Delta\Delta CT}$; $\Delta\Delta CT = (CT_{target} - CT_{ref}{}^{(treatment)}) - (CT_{target} - CT_{ref}{}^{(control)})$].

The qPCR on microdissected nephron samples (see section 2.2.3) was carried out on an iCycler (Biorad Laboratories, Marnes La Coquette, France) using gene-specific primers to quantify the relative abundance of each gene with SYBR Green I as the fluorescent molecule. Relative expression of the mRNA was quantified using the equation described by M.W. Pfaffl (90) (ratio = $(E_{target})^{\Delta CT}{}_{target}{}^{(control-sample)}/(E_{ref})^{\Delta CT}{}_{ref}{}^{(control-sample)}$). Values of mRNA levels were normalized for HPRT1 mRNA in mice (91).

2.2.1.11. Cloning of expression and reporter constructs

The coding sequence (CDS) for human wt MR was subcloned from a pcDNA3.1-hMR expression plasmid (provided by Dr. Steffen Borden) into a pcDNA5/FRT vector (Invitrogen) via XhoI and HindIII. The CDS for rat MR was amplified by RT-PCR from rat kidney total mRNA and cloned into pcDNA3.1/V5His®TOPO® vector (Invitrogen). The CDS for human wt CNKSR3 was amplified by RT-PCR from HEK293 total mRNA. In order to fuse the CDS of CNKSR3 in frame to a V5 epitope tag on its C-terminus, a second primer-set was used, which contained a reverse PCR primer lacking the stop codon (see Table 2.1). Both sequences were inserted into pcDNA3.1 directional TOPO vector. Analogue to this, two plasmids encoding for the wt and a C-terminal V5 tagged version of mouse CNKSR3 (CDS was amplified from total mouse kidney mRNA) were generated accordingly. In order to generate lentiviral expression constructs the CDS encoding the mouse wt CNKSR3 was subcloned into pENTR2B vector and recombined by Gateway® cloning (92) according to manufacturers' recommendations (93) into a pLenti6 (Invitrogen) derived destination vector, pGT4. shRNA cassettes were subcloned into pENTR/U6 (see section 2.2.1.12) and selected pENTR/U6 shRNA constructs were recombined by Gateway® cloning into a modified pLenti-6 destination vector (pGT3).

For reporter assays, plasmids pGL4.10 and pGL4.23 (Promega) were used. Both plasmids contain the firefly *luc2* reporter gene. pGL4.23 contains an additional minimal promoter upstream of *luc2*. MR binding regions identified by ChIP experiments were amplified by PCR from human genomic DNA (Promega #G3041) with appropriate primer-sets (see Table 2.1) containing restriction sites for inserting ~500 bp PCR fragments upstream of the reporter gene. Plasmid pGL4.10 was used for fragments less than 600 bp distant from

the transcription start site (TSS) of a gene (these included PDK4 and the proximal CNKSR3 promoter fragment). Plasmid pGL4.23 was used for fragments more than 600 bp distant from the TSS of a gene (these included an upstream sequence of CNKSR3-4 kb up, GILZ, KLF9, NFKBIA, FKBP5, PI3KR1, PER1, an intronic region of SCNN1A, RHOB, CALM1, MGC21644, CXCR4 and MBNL1). Several pGL4.23-CNKSR3 derived reporter plasmids were generated by PCR-based site-directed mutagenesis using primer-sets (see Table 2.1) carrying the desired mutations. All constructs generated were confirmed by DNA sequencing. The pcDNA5/FRT N-terminal 9-fold myc-tagged human MR expression plasmid was kindly provided by Dr. Horst Irlbacher.

2.2.1.12. Constructs for RNA interference

Complementary synthetic DNA oligonucleotides for RNA interference (RNAi) were designed using Invitrogens RNAi Designer online platform (94). Constructs for shRNA expression were cloned according to the BLOCK-iT user manual (95). In brief: oligonucleotides (Table 2.4) were hybridized with their respective complementary sequences in order to generate double strand (ds) oligos. To this end, 200 µM of top and bottom strand oligos were incubated in annealing buffer at 95°C for 5 min and cooled down to RT for 10 min. Annealed oligos were analyzed in comparison to single strand oligos by gel electrophoresis on a 3% agarose gel. 10 nM ds oligos and 1 ng of pENTR/U6 vector (Invitrogen) were mixed for the ligation reaction. 10 µl of ligation mixture were used for transformation of *E. coli* TOP10 chemically competent cells. As a control a non-target oligonucleotide (Qiagen) was used.

Table 2.4 shRNAs targeting CNKSR3

CACCGGATTGCCTCATAGCAGAAATTTCAAGAGAATTTCTGCTATGAGGCAATCC	shRNA1 top CNKSR3
AAAAGGATTGCCTCATAGCAGAAATTCTCTTGAAATTTCTGCTATGAGGCAATCC	shRNA1 bottom CNKSR3
CACCGCCTGGGCATGTACATCAAGTTTCAAGAGAACTTGATGTACATGCCCAGGC	shRNA2 top CNKSR3
AAAAGCCTGGGCATGTACATCAAGTTCTCTTGAAACTTGATGTACATGCCCAGGC	shRNA2 bottom CNKSR3
CACCGCTACAGAGGACACAGTAAGATTCAAGAGATCTTACTGTGTCCTCTGTAGC	shRNA3 top CNKSR3
AAAAGCTACAGAGGACACAGTAAGATCTCTTGAATCTTACTGTGTCCTCTGTAGC	shRNA3 bottom CNKSR3
CACCGGAGCAGGTGCTACATCAACTTTCAAGAGAAGTTGATGTAGCACCTGCTCC	shRNA4 top CNKSR3
AAAAGGAGCAGGTGCTACATCAACTTCTCTTGAAAGTTGATGTAGCACCTGCTCC	shRNA4 bottom CNKSR3
CACCTTCTCCGAACGTGTCACGTTTCAAGAGAACGTGACACGTTCGGAGAA	shRNA non-target control top
AAAATTCTCCGAACGTGTCACGTTCTCTTGAAACGTGACACGTTCGGAGAA	shRNA non-target control bottom

*blue highlighted bases represent the linker for directional integration into the pENTR/U6 vector, red highlighted bases represent the loop sequence, black nucleotides represent the sense or antisense sequence

2.2.1.13. Western blot analysis

Equal amounts (20-40 µg) of protein were resolved by PAGE electrophoresis in SDS 12% gradient gels (Invitrogen) and transferred onto nitrocellulose membranes (Amersham Biosciences, Freiburg, Germany) using a semi-dry blotting technique. Membranes were blocked with Tris-buffered saline (TBST) containing 0.05% Tween20 and 5% dry milk (Carnation purchased from Nestlé) for 1 h at room temperature. Primary antibodies (see Table 2.2) were incubated overnight in TBST containing 2% dry milk or 5% BSA at 4°C. Membranes were washed 3 times with TBS and then incubated for 1 h at room temperature with an appropriate HRP-conjugated secondary antibody (see Table 2.3) in TBST containing 5% dry milk. Finally, membranes were washed 3 times with PBS and incubated in West Dura Substrate (Pierce, Rockford, IL, USA) and exposed to chemiluminescence films (Amersham Bioscience).

2.2.1.14. Chromatin immunoprecipitation

Chromatin immunoprecipitation (ChIP) experiments were carried out as described in reference (96) with the following modifications: for each ChIP sample 9 x 10^6 HEK293-hMR-myc cells seeded in 14 cm cell culture plates were treated with 10 nM aldosterone or 0.001% DMSO as a vehicle control for 60 min. Cross-linking was performed using 1% formaldehyde for 9 min at room temperature. Chromatin was sonicated in 1 ml sonication buffer using a Bioruptor (Diagenode, Liège, Belgium) to an average chromatin size of 200–500 bp. Sonicated chromatin of aldosterone or vehicle-treated cells was incubated with 3 µg anti-myc antibody (see Table 2.2) and 30 µl magnetic protein A beads (Dynal, Invitrogen) and incubated on a rotating platform overnight at 4°C. Beads were washed in RIPA buffer containing increasing salt concentrations (140 mM NaCl to 500 mM NaCl). Finally, beads were washed in a LiCl detergent solution containing 10 mM Tris-HCl pH 8.0, 250 mM LiCl, 1 mM EDTA and 0.5% Na-deoxycholate. Elution of antibody captured chromatin off the magnetic beads was carried out with 10% Chelex100 for 10 min at 95°C as described. Processed eluate was used as a template for qPCR analysis. As a reference negative control, a sequence located in the second exon of the scnn1a gene was used, which is not bound by the MR. “Fold enrichment” of myc-MR was calculated by the ΔΔCT method as described in section 2.2.1.10. The ratio of sequence enriched in the aldosterone vs. vehicle group was normalized for input DNA [fold enrichment = $(\Delta CT_{\text{Aldo IP}} - \Delta CT_{\text{Aldo Input}})/ (\Delta CT_{\text{Vehicle IP}} - \Delta CT_{\text{Vehicle Input}})$].

2.2.1.15. Affymetrix microarray experiments

In order to determine aldosterone-regulated genes in HEK293-hMR$^+$ cells on a genome-wide level Affymetrix gene profiling experiments were carried out. The Affymetrix microarray technology is based on a hybridization technique. In brief: for each covering RefSeq sequence these arrays provide multiple independent oligonucleotides (25 mers), so-called probe sets which consists of 11 probe pairs. Every probe pair contains a perfect match (PM) oligonucleotide and a corresponding mismatch (MM) oligonucleotide. The average differences between PM and MM provide data to quantify and control cross-hybridisation. The HG-U133Plus2.0 arrays used in this study contains 54,120 probe sets covering 47,401 transcripts of 38,572 genes. Biotinylated cRNAs synthesized from total RNAs obtained from different treatment groups were hybridized on arrays. The arrays were washed, stained with phycoerythrin-coupled streptavidin and scanned for hybridisation signals. After data collection, data adjustment, and statistical analysis an alteration of the gene regulation pattern was extracted.

Microarray experiments were carried out by the Microarray Core Facility at Bayer Schering Pharma AG. Statistical analyses were carried out by Dr. Florian Sohler.

Total RNA was isolated from aldosterone or vehicle treated HEK293-hMR$^+$ cells and checked for integrity as described in section 2.2.1.8. 2 µg of total RNA were used to prepare biotinylated and fragmented cRNA following the instructions of the Affymetrix One-Cycle Target Labeling protocol (Affymetrix, Santa Clara, CA, USA). Biotin-labeled cRNA quality and quantity was determined by means of Agilent bioanalyzer RNA LabChips (expected fragment size: 1000-2000 nucleotides) and by Nanodrop analysis respectively. A total of 15 µg fragmented cRNA from each sample was hybridized on an Affymetrix GeneChip HG-U133Plus2.0 array at 45°C for 16 h under constant agitation. Arrays were scanned using a GeneChip Scanner 3000 7G (Affymetrix), and scanned images were extracted utilizing the Affymetrix GCOS Software. The generated data files (CEL format) containing probe level expression data were refined and condensed by using GeneData Expressionist Refiner (GeneData AG, Basel, Swiss) software with the implemented MAS5.0 statistical algorithm. For background/noise adjustment a locally weighted linear regression analysis (LOWESS) was carried out using all experiments as a reference. To identify differentially expressed genes the following statistical analyses were applied: a 2-Way analysis of variance (ANOVA) was performed with the factors time and treatment. The “fold change” was computed separately for each time point. Probe sets with a fold change of 1.5-fold or higher at any time

point and a p-value from the treatment effect in the 2-Way ANOVA > 10^{-5} [corresponding to a false discovery rate of 0.018 according to the method of Benjamini and Hochberg (97)] were considered as aldosterone-regulated.

2.2.1.16. Determination of MR copy number

The MR copy number per cell was determined by ^{3}H-aldosterone binding assays as described in (98). In brief: in Scatchard analysis the saturable binding concentration was determined using increasing concentrations (0.1-10 nM) ^{3}H-aldosterone (Perkin Elmer, specific radioactivity 73.9 Ci/mmol). To determine the number of MR/cell 1.5 x 10^{5} living cells per sample were incubated for 1 h at RT under constant agitation with 5 nM ^{3}H-aldosterone in the absence (total binding) and presence of a 2000-fold excess of unlabeled aldosterone (non-specific binding). Specific binding of aldosterone was calculated as the difference between total and displaceable radioactivity measured. Experiments were also carried out in presence of a 2000-fold excess of the GR antagonist RU486, to exclude binding of aldosterone to the GR. The number of MR molecules expressed per cell was calculated by the radioactivity determined for specific aldosterone binding to the MR, the specific activity of ^{3}H-aldosterone (cpm/fmol), and the number of cells applied [Δcpm (^{3}H-aldosterone in presence of RU486 – aldosterone$_{cold}$)/specific activity (cpm/fmol) x 6.022 x 10^{8} = Value X/cell number]. The specific activity (cpm/fmol) was determined by the ^{3}H-aldosterone (Ci/mmol) considering the counter efficiency (TopCount NXT, Perkin Elmer), scintillation fluid and the disintegrations per minute [(dpm), a Curie (Ci) equals 2.22 x 10^{12} dpm].

2.2.2. Cell biology

2.2.2.1. Cell culture

HEK293 cells were maintained in DMEM high glucose supplemented with 100 U/ml penicillin, 100 mg/ml streptomycin (PS), and 10% fetal bovine serum (FBS) (Gibco®). M1 cells were grown in Ham's F12/DMEM supplemented with PS, 5% FBS and 1 µM dexamethasone. MDCK cells were maintained in MEM with Earle's Salts supplemented with PS and 10% FBS. Cells were incubated in a humidified atmosphere at 37°C and 5% CO_2. For the maintenance of different cell clones (see section 2.2.2.5**)** derived from parental cell lines, appropriate antibiotics were added to culture media to keep selective pressure.

2.2.2.2. Charcoal treatment of serum

In order to deprive serum from hormones and growth factors, heat-inactivated FBS (56°C for 30 min) was incubated with 10 mg/ml activated charcoal in an over-head-shaker for 4 h at room temperature. Charcoal was allowed to settle over night at 4°C. To remove residual charcoal supernatant was centrifuged at 9,000 rpm for 1 h. Charcoal-treated FBS was sterile filtered and stored in aliquots at -20°C.

2.2.2.3. Lentivirus production

Lentivirus production and infection of cells were carried out as described in (99). In brief: 6 x 10^6 HEK 293FT cells were seeded in 75 cm^2 flasks. Cells were transfected with lentiviral vectors using Lipofectamine 2000 (Invitrogen) according to manufacturers' recommendations. After transfection cells were incubated in 10 ml culture medium. Every 24 h medium was replaced and supernatants containing viruses were collected, centrifuged (3,000 rpm for 5 min at 4°C), and stored at 4°C. In order to remove residual cellular debris, viral supernatants were filtered through a low protein binding filter (Millipore, Ø 0.45 µm), condensed by centrifugation at 18,000 rpm for 2 h at 4°C, and resuspended in 500 µl of residual medium. Viral stocks were stored in 100 µl aliquots at -80°C. To determine viral titer a HIV-1 P24 ELISA was performed according to manufacturers' recommendations (Perkin Elmer, Inc., Waltham, MA, USA). Titers ranged from 1-5 x 10^5 (for unconcentrated virus) up to 2 x 10^7 (for concentrated virus) transducing units (TU)/ml.

2.2.2.4. Lentiviral transduction of mammalian cells

Cells were grown in 12-well plates until they reached 70% confluence. For lentiviral transduction culture medium was replaced with medium containing supernatants from lentivirus production (see section 2.2.2.3). The total volume of virus-containing medium was kept as low as possible to maximize transduction efficiency. Cells were transduced with a multiplicity of infection (MOI) of ~1. Cells were incubated at 37°C for 2 h. Then virus-containing medium was removed and replaced by fresh antibiotic-free medium. Cell were incubated overnight and seeded in 25 cm^2 cell culture flasks. After 48 h medium was replaced with medium containing appropriate antibiotics for selection of recombinants as described in section 2.2.2.5.

2.2.2.5. Generation of expression cell lines

To generate different MR-expressing and appropriate control HEK293 cells, HEK293-Flp-In cells (Invitrogen) were transfected with pcDNA5/FRT-MR, pcDNA5/FRT-myc-MR (provided by Dr. Horst Irlbacher) or pcDNA5/FRT-empty, each together with a Flp recombinase expression vector (pOG44). This *Saccharomyces cerevisiae*-derived DNA recombination system allows the stable insertion of pcDNA5/FRT containing the gene of interest into the genome of a host cell line carrying FRT site (100). 48 h post transfection recombinants were selected with hygromycin (100 µg/ml) for 15 days. Cell colonies were isolated under the microscope to obtain monoclonal cell clones and transferred to a 48-well plate. Clones were expanded and screened for MR activity by reporter gene transactivation assays. Clones that responded to physiological concentrations of aldosterone were further characterized by genotyping.

Mouse cortical collecting duct cells (M1) were purchased from ECACC (Health Protection Agency, Porton Down, UK). In order to generate MR-expressing M1 clones, cells were transfected with pcDNA3.1-rMR. M1 cells stably expressing rMR (referred to as M1-rMR$^+$ cells) were selected with hygromycin (150 µg/ml) for 15 days and subjected to cloning as described above. M1-rMR$^+$ cells stably overexpressing or repressing CNKSR3 were generated by infection with recombinant lentiviruses. Lentivirus production and infection of cells were carried out as described in sections 2.2.2.3 and 2.2.2.4. M1-rMR$^+$ cells stably overexpressing CNKSR3 or JRed as a control were selected with blasticidin (5 µg/ml) for 14 days. To assess whether the polyclonal cells express sufficient protein level cells were analyzed by Western blot or immunefluorescence using a fluorescence microscope (B2-8000K, Keyence, Osaka, Japan). In order to repress the expression of endogenous CNKSR3, M1-rMR$^+$ cells were infected with recombinant lentiviruses coding for shRNA3 or shRNA4 specific for cnksr3 or a non-target control shRNA, respectively. Cells were selected with puromycin (5 µg/ml) for 14 days. Individual clones were expanded and tested for relative cnksr3 knockdown efficiency by qPCR. For the maintenance of recombinant cells appropriate antibiotics were added to maintain selective pressure.

2.2.2.6. Luciferase reporter assays

Cells stably expressing MR were transfected with reporter plasmids containing the reporter gene Luciferase (Luc) under the control of a steroid hormone responsive promoter

element using Lipofectamine (Invitrogen) according to manufacturers' instructions. 20,000-30,000 cells per well were seeded in 96-well plates in assay medium containing 3% charcoal-treated serum. Starving cells were cultured for 24 h before addition of hormones. To determine the aldosterone response, cells were incubated with increasing aldosterone concentrations in presence or absence of RU486 or RU26752 and luciferase activity was determined after 6 h. Luciferase activity was measured with the Dual-Luciferase® reporter assay system (Promega) according to the manufacturers' instructions using a PHERAstar plate reader (BMG Labtech, Offenburg, Germany).

2.2.2.7. Electrophysiological measurements (Ussing chamber)

For electrophysiological experiments M1-rMR$^+$ cells were seeded onto Millicell-HA filters (pore diameter 0.45 µm; Millipore, Schwalbach, Germany) and grown until they formed polarized confluent monolayers (4-5 days post seeding). Typically, these monolayers build up transepithelial resistances of ~300-600 Ω·cm^2. To determine the effects of aldosterone, cells were starved in assay medium with 3% charcoal-treated serum for 24 h and then treated for 24 h with 10 nM aldosterone alone or in presence of 1 µM RU486 or RU26752. For short-circuit current measurements, M1-rMR$^+$ monolayers were mounted into conventional Ussing-type chambers with an exposed area of 0.6 cm^2. The bathing solution consisted of: Na^+ 140; Cl^- 123.8; K^+ 5.4; Ca^{2+} 1.2; Mg^{2+} 1.2; HPO_4^{2-} 2.4; $H_2PO_4^-$ 0.6; HCO^{3-} 21; D(+)-glucose 10 (mM). The solution was equilibrated with 95% O_2 and 5% CO_2 at pH 7.4. Short-circuit current (I_{SC}, µA/cm^2) and transepithelial resistance (Ω·cm^2) were recorded using a 8-channel computer-controlled voltage clamp device (CVC 8, Fiebig, Berlin, Germany). At the end of the measurement, amiloride (10^{-5} M, Sigma-Aldrich) was added to the apical site. At this concentration, amiloride blocks ENaC but not the Na^+/H^+ antiporter NHE3. The drop in I_{SC} after addition of amiloride, ΔI_{SC} (µA/cm^2), was assigned to ENaC-mediated Na^+ absorption (101).

2.2.2.8. Determination of EC_{50} and IC_{50} values

The EC_{50} is defined as the concentration of an agonist or stimulator resulting in 50% of a compound's maximal effect. The antagonistic potency of a compound is described by its IC_{50} value, which equals the concentration of the compound that results in 50% inhibition of the maximal inhibitory activity. Dose response curves and the derived parameters EC_{50} and IC_{50} were determined as follows: all replicate values measured in one experiment were

averaged by taking the means. Mean values were transferred into the SigmaPlot software for fitting a dose response curve using Chapman four parametric curve fit. Four parameters y_0, a, b and c are determined by that iterative approach. The Chapman equation is: $y = y_0 + a (1-e^{-bx})^c$. The maximum value of the sigmoidal curve is $Response_{Max}$ and the minimum value is $Response_{Min}$. EC_{50}/IC_{50} values were calculated as follows: $y_{1/2} = Response_{Max}-[(Response_{Max}-Response_{Min})/2]$. The corresponding concentration ($x_{1/2} = EC_{50}/IC_{50}$) was calculated by converting the Chapman equation with respect to x.

The relative efficacy is the maximal activation by a given compound (cpd) ($Rmax_{cpd}$) divided by the maximal activity of the reference (ref) compound ($Rmax_{ref}$) multiplied by 100 and expressed in percent (%).

2.2.3. Microdissection of renal tubules

Microdissection experiments were done in cooperation with Drs. Frederic Jassier and Nicolette Farmann, ISERM Paris, France. Mice were sacrificed by cervical dislocation and the left kidney was injected, using a fine needle, with 1-2 ml filtered (pore diameter 0.2 µm) collagenase solution: DMEM/HamF12 culture medium, collagenase A (1 mg/ml, Roche Diagnostics, Mannheim, Germany) and fetal bovine serum (2%). The kidney was excised, cut into small slices that were incubated at 37°C for 45 min in the collagenase solution. Microdissection was performed under sterile conditions under a binocular microscope as described (102), allowing collection of the proximal tubule (convoluted portion, PCT, and straight portion, PR), the distal convoluted tubule (DCT), the connecting tubule (CNT), and the cortical collecting duct (CCD). Pools of tubules of each category (about 10 mm in length) were transferred to 100 µl lysis buffer mix (RA1 Buffer, Macherey-Nagel) with 1% β-mercaptoethanol, and stored at -80°C. One, two or three pools of tubules of each category were collected from the same mouse kidney.

2.2.4. Statistical analysis

If not stated otherwise data are expressed as means ± standard error of the mean (SEM). Statistical analysis was performed using Student's two-tailed t-test and, if appropriate, Bonferroni–Holm correction for multiple testing. Significance was assumed at $p < 0.05$.

3. Results

3.1. Identification of early aldosterone-regulated genes

3.1.1. Generation of HEK293 cells stably expressing the human MR

Human embryonic kidney cells (HEK293) are devoid of functional MR while maintaining the expression of functional endogenous GR (103, 104). To determine MR specific gene regulation, HEK293-Flp-In cells were stably transfected with the pcDNA5/FRT/hMR expression plasmid as described in section 2.2.2.5. Several cell clones were screened for MR activity by reporter gene transactivation assays. To this end, cells were transiently transfected with a luciferase expression construct driven by a mouse mammary tumor virus (MMTV)-promoter (referred to as pMMTV-Luc reporter) and analyzed for aldosterone-mediated luciferase response. The measured luciferase activity was normalized to the respective vehicle control. Figure 3.1A shows the transactivation response to 10 nM aldosterone of various clones. Four HEK293-hMR expressing clones, #2, #3, #7 and #10, were further characterized by aldosterone dose-response transactivation assays (Fig. 3.1B). All clones responded to physiological concentrations of aldosterone in a dose-dependent manner with an EC_{50} of ~0.1 nM.

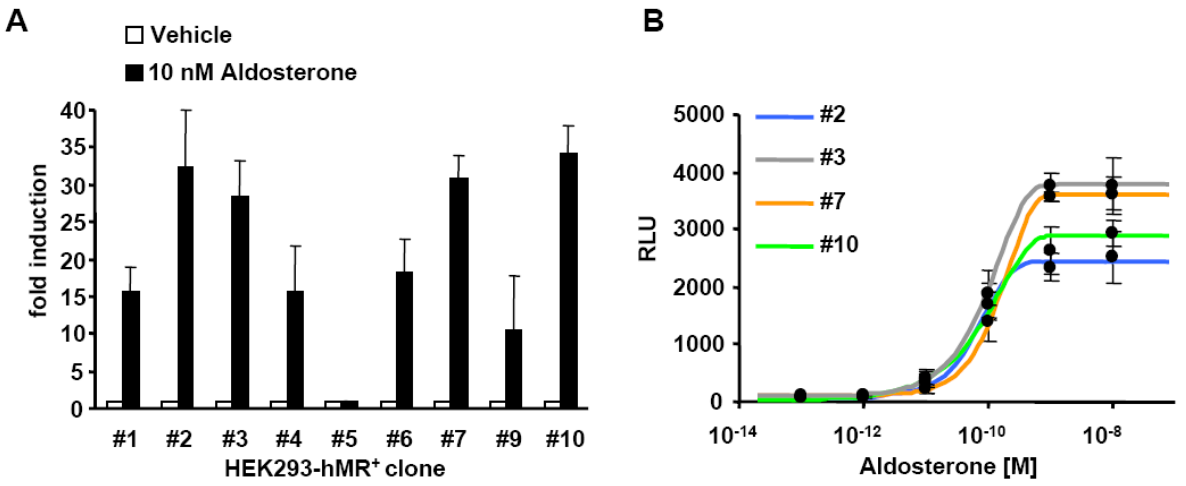

Fig. 3.1: Selection of HEK293 clones stably expressing the mineralocorticoid receptor
A: Aldosterone-mediated reporter gene activation of selected HEK293 hMR clones transiently transfected with pMMTV-Luc. Response is expressed as fold induction (vehicle control = 1). **B**: Dose-response curves of aldosterone-dependent reporter gene activation of 4 selected clones from A. All clones show a comparable EC_{50} of ~0.1 nM. Reponse is expressed as relative luciferase units (RLU).

The MR expression plasmid was integrated into the genome via Flp recombinase-mediated DNA recombination at the flp recombination target (FRT) site in the genome of the engineered HEK293-Flp-In cells (100). Every integration event of a pcDNA5/FRT expression plasmid into a FRT site brings an additional FRT site that is contained in the integration plasmid. Hence, this method does not exclude multiple integration events. The selected clones were further characterized by genotyping to identify potential multiple integration events. The integration of several MR open reading frames, each driven by a cytomegalovirus (CMV) promoter, would probably cause unphysiological high MR expression level. A PCR strategy was chosen for the genotyping. Figure 3.2A shows a schematic depiction of possible integration events via FRT sites. Specific PCR primers were designed that allowed a characterization of the Flp-In locus in the genome of the four selected clones (see Fig. 3.1) using genomic DNA as PCR template. Figure 3.2B shows exemplarily the genotyping results for the HEK293 hMR expression clones #3 and #10. As controls a HEK293 clone stably transfected with the empty pcDNA5/FRT vector alone and polyclonal HEK293-hMR$^+$ cells were analyzed. Parent HEK293-Flp-In cells and the pcDNA5/FRT/hMR expression plasmid were used as negative and/ or positive controls, respectively.

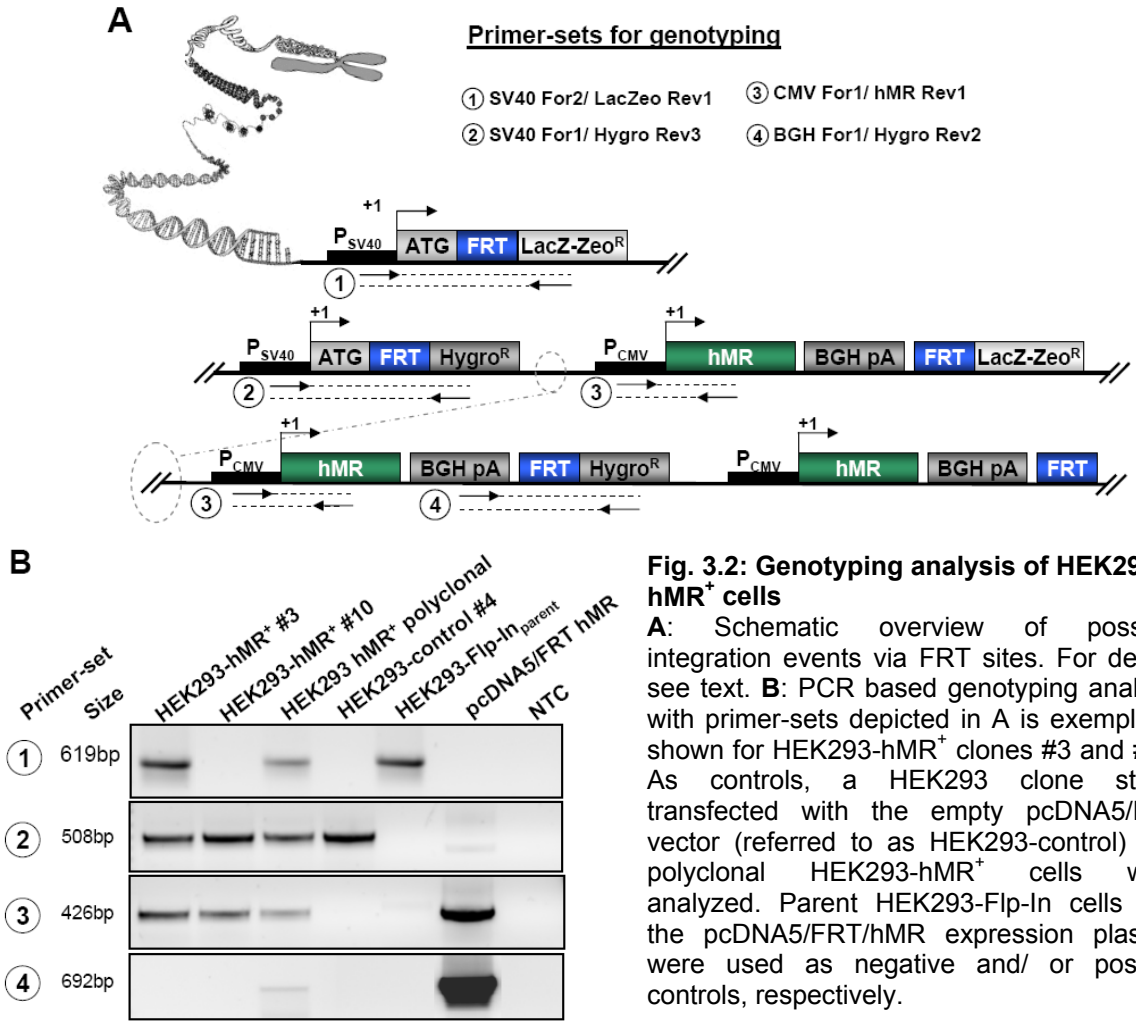

Fig. 3.2: Genotyping analysis of HEK293-hMR$^+$ cells
A: Schematic overview of possible integration events via FRT sites. For details see text. **B**: PCR based genotyping analysis with primer-sets depicted in A is exemplarily shown for HEK293-hMR$^+$ clones #3 and #10. As controls, a HEK293 clone stably transfected with the empty pcDNA5/FRT vector (referred to as HEK293-control) and polyclonal HEK293-hMR$^+$ cells were analyzed. Parent HEK293-Flp-In cells and the pcDNA5/FRT/hMR expression plasmid were used as negative and/ or positive controls, respectively.

Primer-set 1 detects the initial genomic situation found in parent HEK293-Flp-In cells with no integration at the FRT-site. By using primer-sets 2 and 4 it was possible to differentiate between single and multiple integrations events. Primer-set 3 detects the presence of the hMR CDS driven by a CMV promoter and was used to distinguish hMR expressing cells from parent and control cells. PCR analysis for the cells referred to as HEK293-hMR$^+$ clone #3 revealed that some cells failed the integration of the hMR expression plasmid. This indicates that these cells are not derived from a single clone. A heterogeneous cell population would probably drift in its composition and thus change its characteristics during maintenance. In contrast, for the HEK293-hMR$^+$ clone #10 cells no PCR products were obtained with primer-sets detecting a failed integration or multiple integration events, indicating monoclonality. Thus HEK293-hMR$^+$ clone #10 fulfilled all required quality criteria and was chosen for further experiments. The clone is further referred to as HEK293-hMR$^+$ cells. HEK293–control cells stably transfected with the empty pcDNA5/FRT vector exhibited the same integration pattern as described for the HEK293-hMR$^+$ cells and were used in further experiments as control cells.

3.1.2. Characterization of HEK293-hMR$^+$ cells

The expression of MR protein was determined by Western blot analysis in HEK293-hMR$^+$ and HEK293-control cells. As expected MR was only detected in HEK293-hMR$^+$ cells (Fig. 3.3A). Since supraphysiological concentrations of aldosterone can also activate the GR (28, 29), GR protein expression analysis was included. HEK293-hMR$^+$ and HEK293-control cells exhibited a profound expression of endogenous GR (Fig. 3.3A).

To determine the number of MR molecules expressed per cell, binding assays with tritium labeled aldosterone (^{3}H-aldosterone) were performed. HEK293-hMR$^+$ cells showed specific aldosterone binding which was not blockable by the GR antagonist RU486 (Fig. 3.3B). A small fraction of aldosterone binding was blockable by RU486, indicating binding of aldosterone to GR (Fig. 3.3B). In contrast, HEK293-control cells exclusively showed RU486-blockable aldosterone binding (Fig. 3.3B). Specific binding of aldosterone to MR was defined as the difference between the radioactivities measured for ^{3}H-aldosterone binding in presence of unlabeled RU486 and displaceable binding by unlabeled aldosterone. By applying the equation described in section 2.2.1.16, the number of MR molecules expressed per cell was calculated to 11,000. This was in good accordance with the physiological MR expression range in principal cells of the cortical collecting duct (CCD)

(102, 105). In contrast, for the HEK293-control cells no MR binding was determined, which supported the results obtained by Western blot analysis.

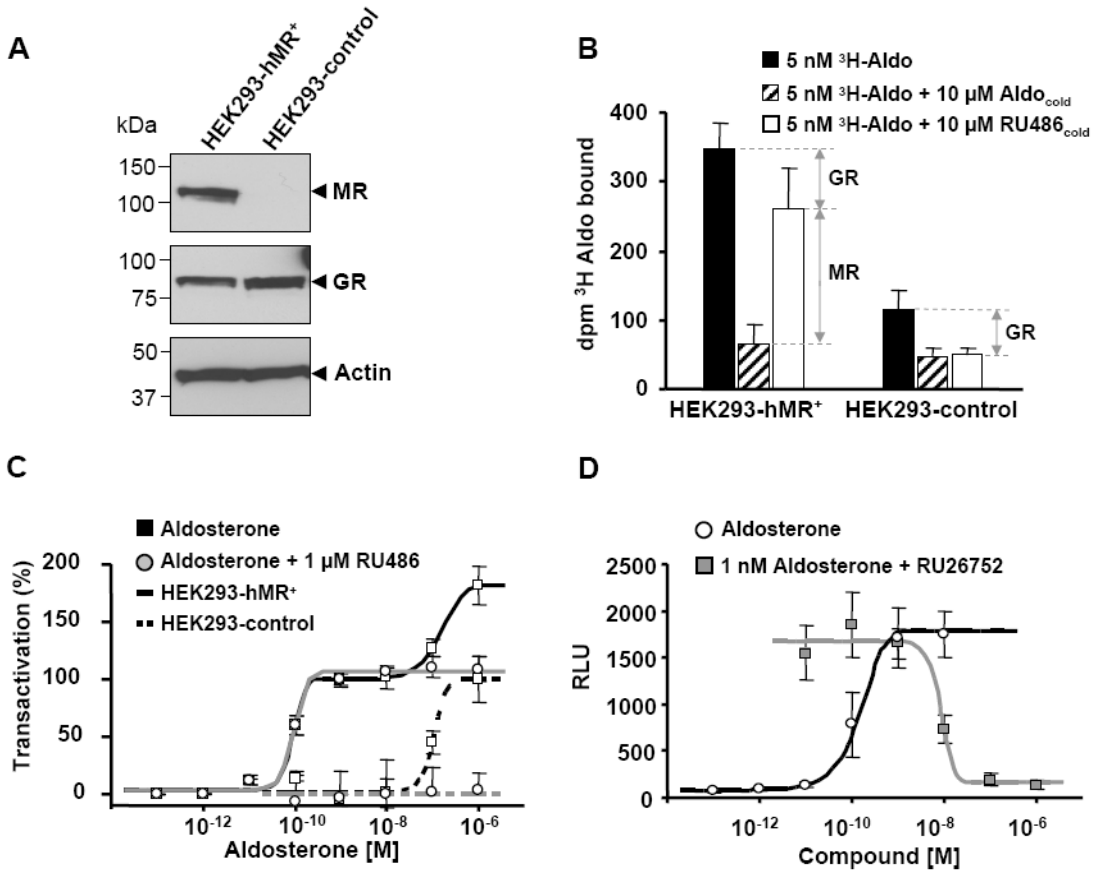

Fig. 3.3: Characterization of HEK293-hMR$^+$ and HEK293-control cells
A: Western blot analysis of MR (107 kDa) and GR (90 kDa) expression. Beta-Actin (42 kDa) was used as a loading control. **B**: Determination of aldosterone binding sites. Cells were incubated with 5 nM ^{3}H-aldosterone in the absence (black bars) or presence of unlabeled aldosterone (hatched bars) or the GR antagonist RU486 (white bars). Only HEK293-MR$^+$ cells show specific binding of aldosterone to MR in presence of RU486 (white bars). The difference between total aldosterone binding (black bars) and binding to MR (white bars) is indicative of binding to GR, which is comparable in both cell clones. **C**: Aldosterone-mediated transactivation response in presence or absence of RU486. Aldosterone concentrations above 10 nM activated endogenous GR, which was selectively blocked by the GR antagonist RU486. Transactivation response is given in % relative to the maximal response at 1 nM aldosterone. **D**: Aldosterone-induced transactivation signals were completely blocked by the MR antagonist RU26752 (grey curve) in dose-dependent manner. Transactivation response is given in relative luciferase units (RLU).

HEK293-hMR$^+$ and HEK293-control cells were further characterized by extended reporter gene transactivation assays. Cells were transiently transfected with a pMMTV-Luc reporter and analyzed for aldosterone-mediated luciferase response. HEK293-hMR$^+$ cells responded to physiological concentrations of aldosterone, whereas HEK293-control cells only responded to supraphysiological aldosterone doses (> 0.1 µM). A second increase in transactivation signal on top of the MR-mediated response at high aldosterone doses was observed for the HEK293-hMR$^+$ cells (Fig. 3.3C). High dose aldosterone responses were selectively blocked with 1 µM RU486 in HEK293-hMR$^+$ and HEK293-control cells

(Fig. 3.3C), suggesting that this response was mediated through the endogenous GR and not MR. In contrast, aldosterone at low concentrations (0.01-10 nM) induced transactivation signals that were completely blocked by the MR antagonist RU26752. Figure 3.3D shows exemplarily the dose-dependent transactivation blockade by RU26752 for HEK293-hMR$^+$ cells simulated with 1 nM aldosterone. These data indicate that concentrations of 0.1-10 nM aldosterone primarily activate MR.

In summary, HEK293 cells are devoid of MR but maintain expression of functional endogenous GR as assessed by Western blot analysis, binding studies and reporter gene assays. Importantly, the HEK293-hMR$^+$ cells express functional MR in a physiological range and allow the clear separation of MR- vs. GR-mediated effects.

3.1.3. The genome-wide aldosterone gene regulation pattern

To test whether overexpressed MR in HEK293-hMR$^+$ cells was able to regulate endogenous target genes (e.g. sgk1 and gilz) quantitative real time polymerase chain reaction (qPCR) experiments were carried out. To minimize activation of co-present GR (see Fig. 3.3A), HEK293-hMR$^+$ cells were stimulated with 10 nM aldosterone. At this concentration HEK293-MR$^+$ cells showed full transactivation activity, while the HEK293-control cells, devoid of MR, did not respond (see Fig. 3.3C). As expected mRNA levels of sgk1 and gilz, two well known MR target genes (68, 80, 106), were markedly increased in HEK293-hMR$^+$ cells but not in HEK293-control cells (data not shown). Thus HEK293-hMR$^+$ cells were considered as an appropriate cell system for the determination of MR responsive genes. To explore the aldosterone-activated MR regulation pattern on a genome-wide level an Affymetrix microarray gene expression study was carried out.

In order to identify early MR-regulated genes, a time course experiment was performed. Therefore HEK293-MR$^+$ cells were incubated with 10 nM aldosterone for 0, 1, 2, 4 and 8 h. As a vehicle control HEK293-hMR$^+$ cells were treated with appropriate amounts of DMSO [0.01% (v/v)] for all indicated time points. For every time point three parallel experiments were carried out. This experimental set-up required a total of 30 microarrays.

In order to identify aldosterone-regulated genes the two parameters, fold change and level of statistical significance were arranged in a volcano plot (Fig. 3.4). Genes with a fold change of 1.5-fold or higher at any time point and a p-value > 10^{-5} were considered as aldosterone-regulated as described in section 2.2.1.15.

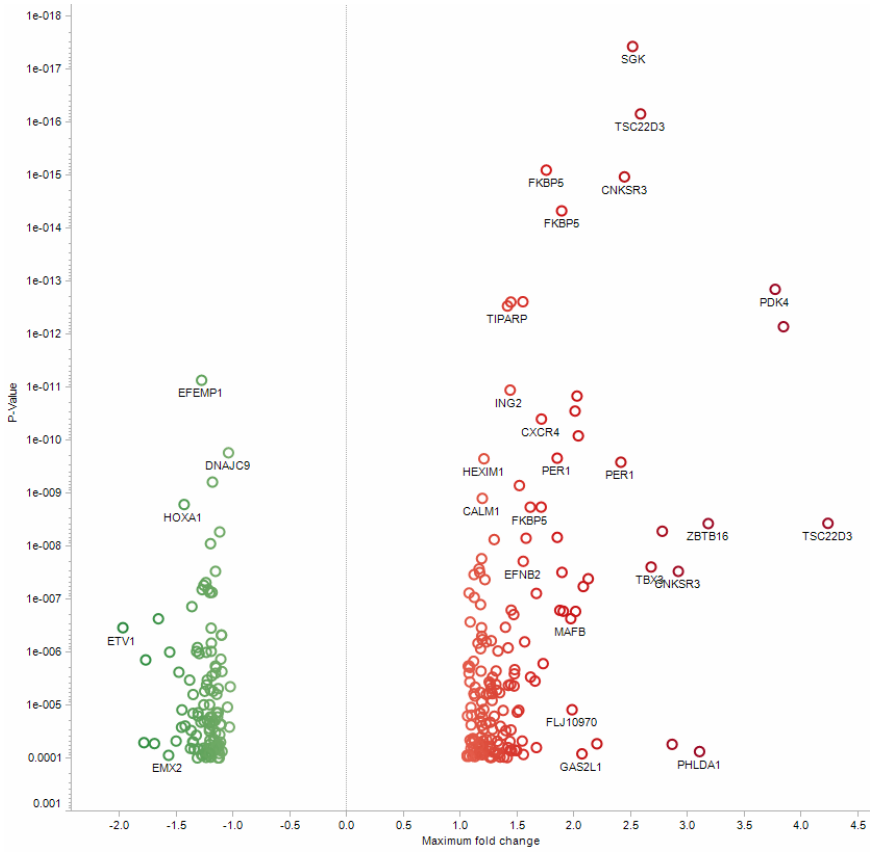

Fig. 3.4: Volcano plot of identified genes.
Genes with a fold change of 1.5 or higher at any time point and a significance level > 10^{-5} (corresponding to a false discovery rate of 0.018) were considered as aldosterone-regulated.

Previously described MR-regulated genes such as per1, plzf (also known as zbtb16), gilz or sgk1 (68, 80, 82, 107, 108) were among the most up-regulated genes (see Fig. 3.4), supporting the validity of the study. In addition, a number of genes not previously described as mineralocorticoid-regulated were identified, among them e.g. cnksr3, pdk4, or calm1 (Fig. 3.4 and Fig. 3.5).

Overall 36 transcripts were identified to be regulated by aldosterone, of which 31 transcripts were up-regulated and 5 were down-regulated (Fig. 3.5). Out of the 36 aldosterone-regulated genes 26 were verified by individual qPCR analysis with mRNAs derived from separate experiments. Gene symbols of qPCR verified transcripts are depicted in bold letters (Fig. 3.5). Interestingly, the majority of identified genes showed its maximum fold change in regulation after 4 h of aldosterone stimulation (Fig. 3.5).

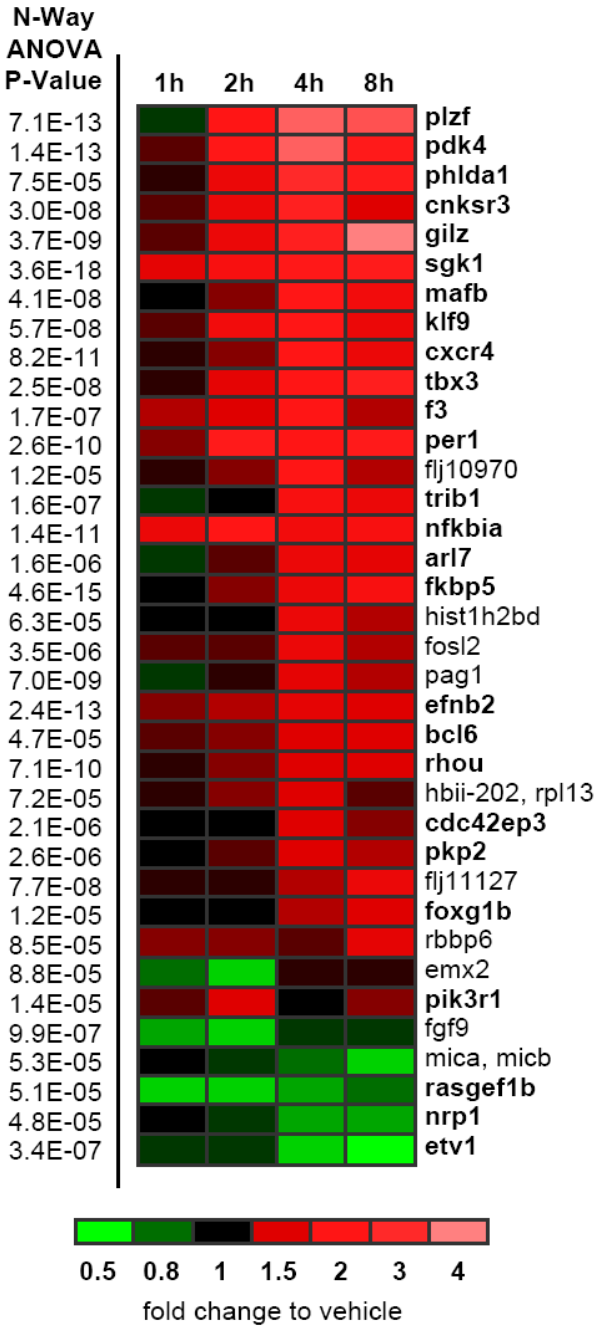

Fig 3.5: Identification of aldosterone-responsive genes
Colorimetric representation of aldosterone-regulated genes in HEK293-MR$^+$ cells; the color intensity reflects the relative fold change in gene expression in response to 10 nM aldosterone vs. the vehicle control; the time course spans 1, 2, 4, and 8 h; only genes were considered that showed a higher than 1.5-fold change in regulation; gene symbols depicted in bold were retested and confirmed by qPCR analysis using mRNA of independent experiments. Induced transcripts (red) or repressed transcripts (green). The left row represents p-values of an N-Way ANOVA analysis across all different time points.

Aldosterone-regulated genes were classified by their biological functions according to data obtained from the gene ontology (GO) platform and the human protein reference database (HPRD) (Table 3.1). Consistent with the physiological role of aldosterone as a modulator of cell communication and signal transduction the broad range of genes identified were associated with these processes.

12 aldosterone-responsive genes code for transcription factors, among them per1, plzf, and klf9 which have previously been shown as aldosterone-responsive (108-111). These genes are considered to be involved in the late phase of aldosterone response (12).

Furthermore, 15 genes responded to aldosterone stimulation that code for proteins that are presumably involved in signal transduction. Among them sgk1 and gilz, which have been demonstrated to mediate the early phase of the aldosterone response in renal transepithelial Na^+ transport by modulating the trafficking of the epithelial sodium channel (ENaC) (54).

Table 3.1: Summary of gene ontology categories

Gene	Biological Process	Molecular Function
pkp2	cell adhesion	unknown
calm1*	cell comunication, signal transduction	calcium ion binding
cdc42ep3		GTPase activity
cnksr3		predicted scaffold function
cxcr4		g-protein coupled receptor activity
efnb2		receptor binding
fgf9		growth factor activity
pik3r1		receptor signaling compex scaffold activity
rasgef1b		guanyl-nucleotide exchange factor
rhou		GTPase activity
trib1		protein serin/threonine kinase activity
nrp1	Immune response	receptor activity
fkbp5		protein folding and trafficking activity
gilz	sodium ion transport, immunoregulation	
sgk1	sodium ion transport, response to stress	protein serin/threonine kinase activity
scnn1a*	sodium and potassium ion transport	ion channel activity
hist1h2bd	chromosomal organisation	DNA binding
pdk4	glucose metabolism	catalytic activity
mica, micb	immune response	MHC class I receptor activity
arl7	not determined	unknown
flj10970		
flj11127		
f3	protein metabolism	co-factor binding
rbbp6		ubiquitin-specific protease activity
rpl13		RNA binding
phlda1		transcription factor activity, apoptosis
bcl6	regulation of nucleobase, nucleoside,	transcription factor activity
emx2	nucleotide and nucleic acid metabolism	
etv1		
fosl2		
foxg1b		
klf9		
mafb		
nfkbia		
pag1		
per1		
plzf		
tbx3		

*Not detected by microarray experiments; Gene symbols depicted in bold were validated by qPCR experiments

3.2. Identification of primary mineralocorticoid receptor target genes

The early phase of aldosterone action is traditionally considered to be exclusively mediated through primary effects on gene expression (12). These mechanisms classically include direct binding of activated MR to HREs in the promoter of target genes (5, 12, 112).

3.2.1. Generation of HEK293 cells stably expressing a myc-tagged hMR for ChIP analysis

Chromatin-immunoprecipitation (ChIP) followed by DNA microarray experiments (chip), known as (ChIP-chip) is an efficient technique for the identification of DNA transcription factor binding sites on a genome-wide level in cells (113). This approach requires antibodies that are suitable for ChIP. To date there is no ChIP-grade MR antibody available. For this reason the CDS encoding MR was fused to an N-terminal 9-fold myc-tag in order to make the MR immunoreactive to a ChIP-grade anti-myc antibody. The pcDNA5/FRT N-terminal 9-fold myc-tagged human MR expression plasmid was stably transfected to HEK293-Flp-In cells. The selection of an appropriate clone was carried out according to the procedure described for HEK293-hMR$^+$ cells (see section 3.1.1). HEK293 cells stably expressing the myc-MR are referred to as HEK293-myc-MR. By this approach it was possible to integrate both MR versions into the same genomic context minimizing clonal differences.

HEK293-hMR$^+$ and HEK293-myc-MR$^+$ cells exhibited comparable expression level of the MR protein while the parental cell line was devoid of functional MR as assessed by Western blot analysis (Fig. 3.6A). The myc-tagged MR was detectable with a MR-specific antibody as well as with an anti-myc antibody at 120 kDa, which corresponds to the predicted 107 kDa of the MR plus 13 kDa of the 9-fold myc-tag. As expected the untagged MR was only detected with the MR-specific antibody at 107 kDa (Fig 3.6A).

The myc-MR copy number was assessed by binding assays as described in section 3.1.2 and calculated to ~13000 molecules per cell for the HEK293-myc-MR$^+$ cells (data not shown), which is slightly above the level in HEK293-MR$^+$ cells (see section 3.1.2). To assure the functionality of myc-MR reporter gene transactivation experiments were carried out. To this end, HEK293-myc-MR$^+$ and HEK293-hMR$^+$ cells were transiently transfected with pMMTV-Luc. Transactivation signals were near maximal at 1 nM aldosterone and both cell clones exhibited comparable EC_{50} values of ~0.1 nM (Fig. 3.6B). This indicates that the 9-fold myc tag does not compromise the function of the MR.

To further elaborate on the uncompromised function, it was analyzed whether myc-MR was able to regulate MR target genes, e.g. sgk1 and gilz. To this end, HEK293-myc-MR$^+$ and

HEK293-hMR$^+$ cells as a control were stimulated with 10 nM aldosterone or 0.001% (v/v) DMSO as a vehicle control for 4 h. The aldosterone-induced alteration of target gene expression was determined by qPCR and normalized to the expression level in the vehicle group. Both cell clones showed comparable aldosterone-induced up-regulation of sgk1 and gilz mRNA level (Fig 3.6C). These data indicate that the N-terminal MR myc-tag did not constrain MR activity.

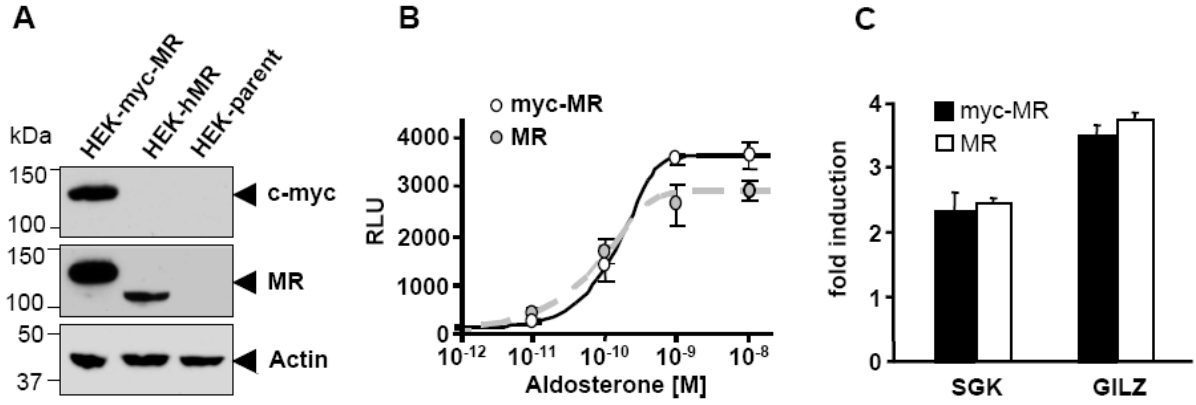

Fig. 3.6: Characterization of HEK293-myc-MR$^+$ cells
A: Expression levels of MR and myc-MR compared to the parental HEK293 cell line by Western blot. Molecular weight of MR: 107 kDa. Calculated molecular weight of myc-tagged MR: 120 kDa. **B:** HEK293-MR$^+$ and HEK293-myc-MR$^+$ cells show comparable affinity for aldosterone. EC_{50} values were ~0.1 nM for both cell clones in a transactivation assay using the pMMTV-Luc reporter plasmid. Full transactivation activity was observed at 1 nM. **C:** Expression of aldosterone target genes. HEK293-myc-MR$^+$ (black bars) and HEK293-hMR$^+$ cells (white bars) exhibited comparable aldosterone-mediated up-regulation of sgk1 and gilz. mRNA levels were determined after 4 h of incubation with 10 nM aldosterone and normalized to a time-matched vehicle control.

Taken together, it was shown that the HEK293-myc-MR$^+$ cells do not significantly differ from HEK293-hMR$^+$ cells in respect to MR copy number, affinity for aldosterone, and the ability to induce target gene expression. Therefore the HEK293-myc-MR$^+$ cells were considered to be suitable to perform ChIP-experiments.

3.2.2. Identification of functional MR binding sites

In order to identify novel MR binding regions (MBRs) on a genome-wide level, chromatin immunoprecipitation of myc-MR followed by microarray hybridization (ChIP-chip) experiments were performed (114). These experiments were carried out by Dr. Horst Irlbacher. The results from the ChIP-chip study and from the above described Affymetrix microarray gene expression study (see section 3.1.3) were compared, in order to identify aldosterone-regulated genes in which the MR is part of the transcriptional regulatory complex.

14 of 36 aldosterone-regulated genes had at least 1 MBR at a distance of less than 10 kb of the transcription start site (TSS). Already known binding sites for MR and/or GR in the promoter of e.g. sgk1, gilz, or scnn1a (39, 115, 116) were confirmed and thus supporting the validity of the ChIP-chip data. Importantly, novel MBRs were identified for e.g. cnksr3, klf9 or pik3r1. Surprisingly, other genes e.g. rhob, mgc21644, and mbln1 exhibited strong MR binding to regions upstream of their respective TSS even though these genes were less than 1.5-fold regulated by aldosterone in HEK293-hMR$^+$ cells (data not shown).

11 of 14 identified MBRs were verified by manual ChIP-qPCR experiments (Fig. 3.7) using the established HEK293-myc-MR$^+$ cell clone (see section 3.2.1). Fold enrichment of myc-MR was calculated as the ratio of PCR product in the aldosterone vs. vehicle group normalized for input DNA (see section 2.2.1.14). Most notably, the region 4 kb upstream of the TSS of cnksr3 exhibited a more than 40-fold MR enrichment. For this gene a second locus -500 bp relative to the TSS was also found to be highly occupied by aldosterone-activated MR (Fig. 3.7). For other genes e.g. pik3r1 or klf9 MR was also enriched higher than 15-fold at the indicated loci close to their respective TSS.

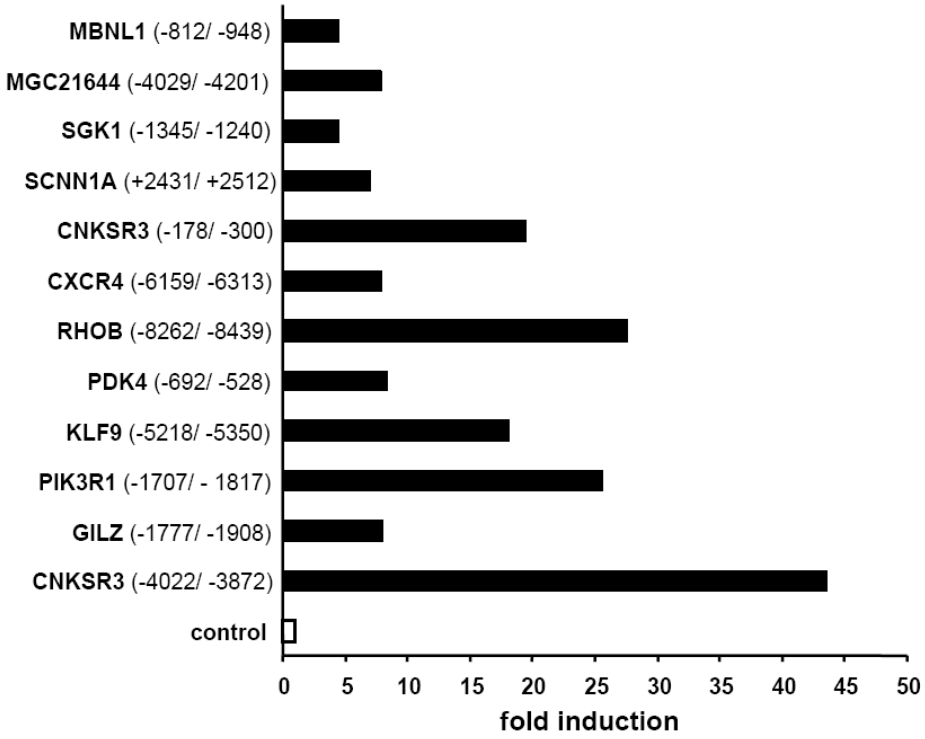

Fig. 3.7: Aldosterone-induced MR occupancy in the promoter of aldosterone-responsive genes
ChIP-qPCR experiments performed in HEK293-myc-MR$^+$ cells at indicated promoter loci of aldosterone-regulated genes. Fold enrichment was calculated as the ratio of PCR product in the aldosterone vs. vehicle group normalized for input DNA. Data are representative for at least three independent experiments.

A weaker, less than 10-fold MR enrichment was detected at previously described GR binding sites for sgk1,gilz and scnn1a (39, 116) (Fig 3.7). Interestingly, several MBRs were found in unexpected regions the latter genes such as in intronic region of e.g. scnn1a. This region had also been discovered recently in a ChIP-chip study for genomic binding sites of glucocorticoid-activated GR.

To examine whether the identified MBRs are active sites in terms of MR-mediated transcriptional activity reporter gene assays were performed. As a proof of concept the MBR of the gilz promoter was analyzed for MR responsiveness. This promoter region has been shown to contain at least two functional GR responsive elements (GREs) (116). A 500 bp promoter fragment of the gilz promoter, containing the ChIP-confirmed MBR was amplified by PCR from human genomic DNA and inserted into a pGL4.23-Luc reporter plasmid, referred to as pGL4.23-GILZ-Luc (Fig. 3.8).

HEK293-hMR$^+$ cells were transiently transfected with pGL4.23-GILZ-Luc and treated with aldosterone alone or in presence of the GR antagonist RU486 or the MR antagonist RU26752. Treatment with aldosterone alone or in presence of RU486 did not abrogate transactivation, whereas RU26752 completely blocked the luciferase response (Fig. 3.8). This indicates that the observed effects at 10 nM aldosterone were specifically mediated through MR and not by co-present GR. These results further suggest that the identified GREs within the gilz promoter (116) are accessible for MR and confer to MR-mediated aldosterone responsiveness.

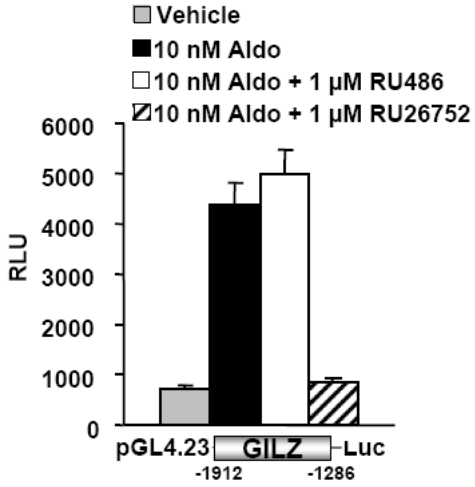

Fig. 3.8: MR-specific transactivation response
HEK293-hMR$^+$ cells were transiently transfected with pGL4.23-GILZ-Luc containing MR binding regions; transactivation response was specifically blocked by the MR antagonist RU26752 but not by the GR antagonist RU486; the response is given in relative luciferase units (RLU).

According to the procedure described above, 15 promoter fragments found to be occupied by MR close to aldosterone-responsive genes were cloned into pGL4 reporter plasmids (Fig. 3.9). The pGL4.10 vector was used for promoter fragments close to the TSS of a gene containing a TATA-box. The pGL4.23 vector contains a TATA-box promoter element.

This vector was used for fragments more than 600 bp from the TSS of a gene lacking a TATA-Box.

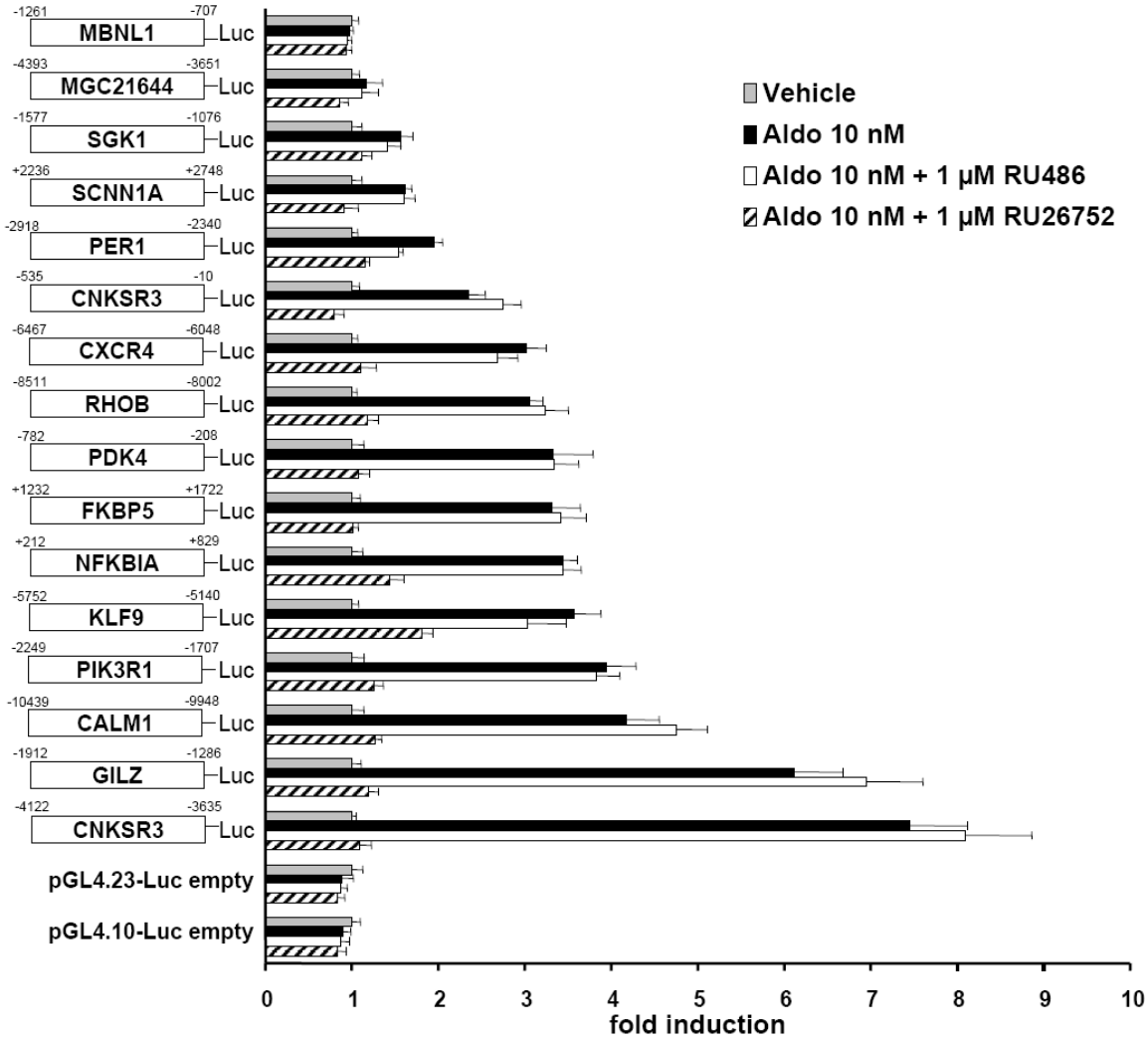

Fig. 3.9: Analysis of MR binding regions in the promoters of aldosterone-regulated genes
MBRs of aldosterone-regulated genes confer to MR responsiveness. HEK293-hMR$^+$ cells were transiently transfected with pGL4 reporter plasmids containing promoter fragments of ~500 bp length from indicated genes. Fold aldosterone-mediated induction (black bars) in presence of the MR antagonist RU26752 (hatched bars) and the GR antagonist RU486 (white bars) was normalized to the respective vehicle control (grey bars). Empty pGL4 reporter plasmids were used as control constructs.

All MBRs of aldosterone-responsive genes mediated transactivation between 1.5 and 8-fold compared to corresponding vehicle control (Fig. 3.9). Again, transactivation activities were MR- and not GR-mediated since the activity was blocked in presence of the MR-specific antagonist RU26752 but not with the GR antagonist RU486 (Fig. 3.8).

The previously described MR binding region of the sgk1 promoter was analyzed as a second control. As expected, this promoter fragment was confirmed as an active MR binding region. Importantly, by this approach it was possible to identify functional MBRs in the promoter of aldosterone-regulated genes e.g. pik3r1, pdk4, or cnksr3. Most notably ChIP

experiments revealed that the cnksr3 promoter exhibited strong MR occupancy 4 kb upstream of the TSS and another weaker MR binding region close to the TSS (see Fig. 3.7). Both MBRs did confer transactivation. Consistent with ChIP results, the distal cnksr3 promoter region showed stronger transactivation capabilities in comparison to the weaker proximal MBR.

Functional MBRs close to respective TSS of nfkb1a, fkbp5, per1, and calm1 were identified by direct evaluation of the ChIP-chip data and were not additionally verified by ChIP-qPCR experiments. Interestingly, two regions strongly bound by the MR, close to the genes mbln1 and mgc21644, were not active in the transactivation assays (Fig. 3.9). Congruent with this both genes did not alter mRNA expression level in response to aldosterone stimulation (data not shown). These results suggest that the identified MBRs within the promoter of aldosterone-regulated genes confer to their aldosterone responsiveness. Surprisingly, functional MBRs were identified in intronic regions of scnn1a, nfkia, and fkbp5.

In summary, ChIP experiments confirmed MR binding to different promoter segments of novel identified aldosterone-responsive genes, indicating that these are direct MR-regulated genes. The functionality of these binding sites was confirmed by reporter gene assays and thus reinforces mRNA expression data.

3.3. Cnksr3 is a direct MR target gene

Evidence that cnksr3 is an aldosterone target gene came from Affymetrix gene expression profiling experiments. ChIP experiments revealed that cnksr3 exhibited two loci of strong MR occupancy upstream of its TSS. Moreover, both identified MR binding regions responded to aldosterone-activated MR as demonstrated by reporter gene assays. These data strongly suggested that cnksr3 is a direct MR target gene. Hence, the mechanisms by which MR regulates cnksr3 expression were studied in extended detail.

3.3.1. Characterization of MR binding sites within the cnksr3 -4 kb promoter fragment

Since the cnksr3 -4 kb promoter fragment showed the strongest MR responsiveness, both in terms of MR binding and MR-mediated transcriptional activity, it was further characterized. To determine whether this promoter fragment is also responsive for GR transactivation assays were performed. To this end, Madin-Darby canine kidney (MDCK) cells, devoid of functional endogenous GR and MR, were transiently co-transfected either with pcDNA3.1-hMR or pcDNA3.1-hGR and the cnksr3 -4 kb reporter plasmid. 24 h post

transfection cells were treated with increasing concentrations of aldosterone, cortisol, or the GR-selective agonist RU28362 for 6 h. Figure 3.10A illustrates that the cnksr3 -4 kb promoter fragment is responsive to ligand-activated MR or GR in a dose-dependent manner. The cnksr3 -4 kb reporter construct was also dose-dependently activated by aldosterone and cortisol in HEK293-hMR$^+$ cells with comparable EC_{50} values (data not shown).

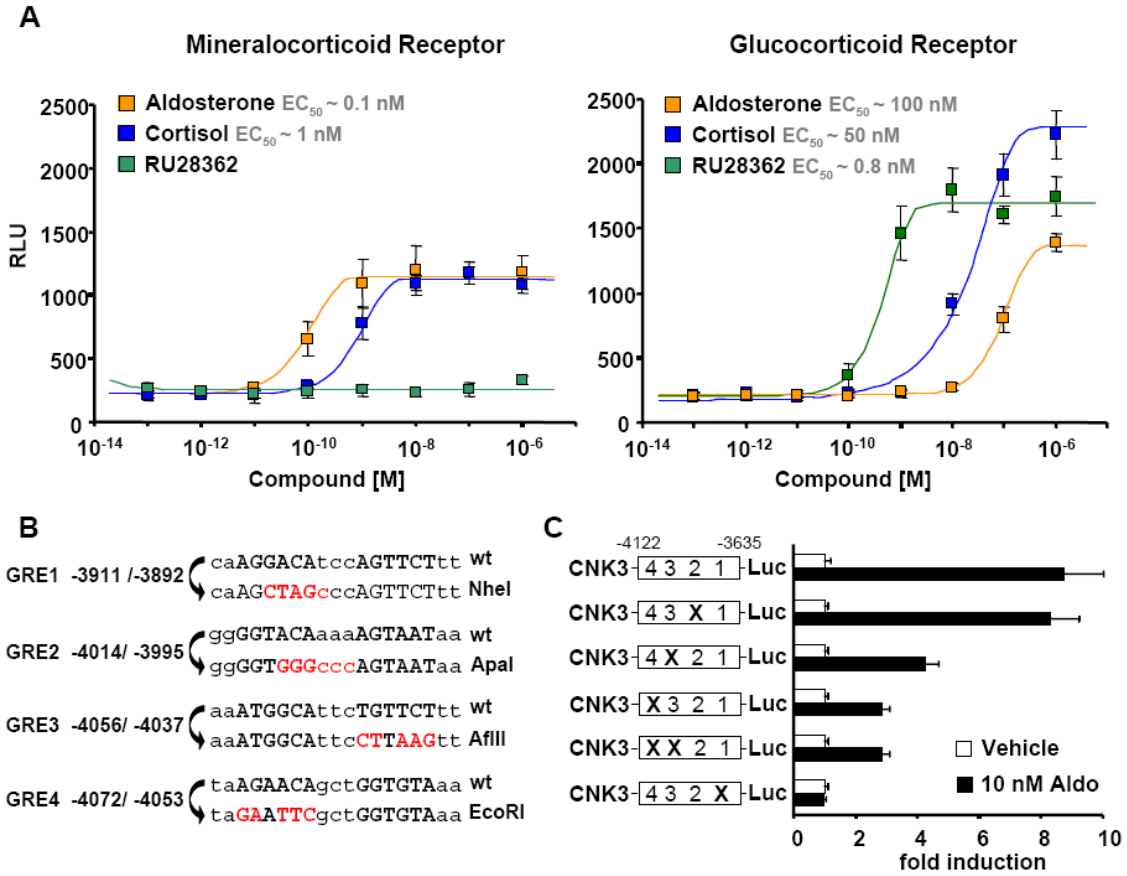

Fig. 3.10: Characterization of MR binding sites within the cnksr3 -4 kb promoter region
A: MDCK cells, devoid of functional MR or GR were transiently co-transfected with an MR or GR expression plasmid, respectively, and the cnksr3 -4 kb reporter plasmid. Cells were stimulated with increasing doses of aldosterone, cortisol, or the GR-selective agonist RU28362. The luciferase response of the cnksr3 -4 kb reporter construct was dose and ligand-dependet on MR and GR. **B**: Putative GREs (depicted in capitol letters) in the cnksr3 -4 kb promoter fragment were mutated by site-directed mutagenesis. **C**: GREs confer aldosterone responsiveness. Wild type (wt) and mutant reporters were transfected in HEK293-hMR$^+$ cells and luciferase activity was determined as described previously.

Putative MR binding sites were computationally predicted by using a core consensus sequence for glucocorticoid responsive element (GRE) family elements using experimentally verified data of AR, PR and GR response elements (117). The bioinformatically identified cluster of four putative GREs was further analyzed by site-directed mutagenesis. All predicted GREs contain at least six of eight conserved nucleotides of the consensus sequence (AGAACAnnnTGTTCT). A minimum of three conserved nucleotides of the more conserved half-site of each GRE were mutated. GREs were replaced by endonuclease restriction sites as

schematically depicted in figure 3.10B. Single and combinatorial mutations of GRE4 and GRE3 resulted in a decreased aldosterone response (Fig. 3.10C). The mutation of GRE2 had no effect on the aldosterone responsiveness. The mutation of GRE1, exhibiting the highest homology to the consensus sequence, caused a complete loss of reporter gene activation, indicating that this GRE is essential for the MR-mediated transcription initiation.

3.3.2. The aldosterone-induced cnksr3 expression pattern

Microarray expression analysis indicated that the aldosterone-induced cnksr3 mRNA expression followed a time course. To study the cnksr3 mRNA expression profile in further detail, aldosterone dose-response and time-course experiments in HEK293-hMR$^+$ cells were performed. Cnksr3 mRNA expression was induced by aldosterone in a dose-dependent manner and peaked after 4 h (Fig. 3.11A). Importantly, the effects were near maximal at 1 nM of aldosterone. This was in accordance with the results obtained in transactivation assays for the cnksr3 -4 kb promoter reporter construct (see Fig. 3.10A left panel). To further assess the role of aldosterone-activated MR in the regulation of cnksr3 expression, HEK293-hMR$^+$ in comparison to HEK293-control cells, devoid of functional MR (see Fig. 3.3A), were analyzed by qPCR experiments. MR expressing cells showed a marked up-regulation of cnksr3 and sgk1 mRNA when treated with 10 nM aldosterone, whereas parent cell lines showed no regulation (Fig. 3.11B). These data further confirmed that the up-regulation is indeed mediated by MR and not GR.

Western blot experiments were carried out in order to verify expression data on protein level. Due to the fact that there was only one CNKSR3 specific antibody available by the time of the study, this antibody was characterized for epitope specificity. To this end, two CNKSR3 expression plasmids were cloned. To make CNKSR3 immunoreactive to an anti-V5 antibody one CDS coding for CNKSR3 was fused to a C-terminal V5 tag. A second coding for wt CNKSR3 was generated as a control (see section 2.2.1.11). Both expression plasmids were transiently transfected in HEK293 cells. 24 h post transfection cells were lysed and probed with a CNKSR3 specific and a V5 specific antibody. As expected, the V5-tagged CNKSR3 protein could only detected by the anti-V5 antibody at about 66 kDa, which corresponds to the predicted 62 kDa of the CNKSR3 protein plus the 3.9 kDa of the V5-tag (Fig. 3.11C). In both experiments the CNKSR3 specific antibody showed only a single band corresponding to the predicted protein sizes (Fig 3.11C). Thus, the CNKSR3 antibody was considered as suitable to study endogenous CNKSR3 protein expression.

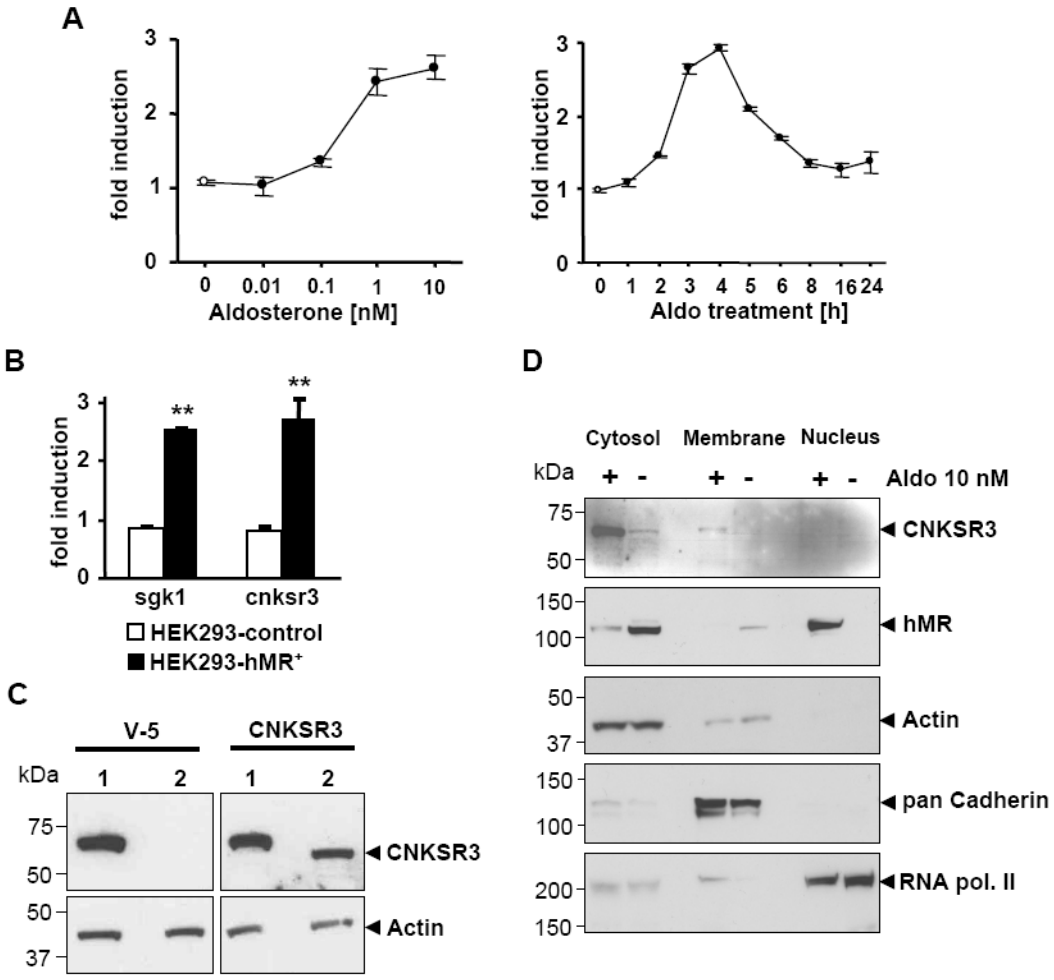

Fig. 3.11: Aldosterone-induced expression of CNKSR3
A: Cnksr3 mRNA transcription in response to increasing concentrations of aldosterone (left panel) and during a time course after 10 nM aldosterone treatment (right panel). Aldosterone regulation of cnksr3 mRNA expression in HEK293-hMR$^+$ cells was dose and time-dependent. **B**: mRNA up-regulation (10 nM, 4 h) of sgk1 and cnksr3 is dependent on MR expression. qPCR values measured for aldosterone-treated cells are time-matched to values obtained in vehicle-treated cells. (** $p < 0.01$) **C**: CNKSR3-antibody specificity: HEK293 cells were transiently transfected with expression plasmids coding for wt CNKSR3 or c-terminal V5-tagged CNKSR3, respectively. Cell lysates were probed with an anti-CNKSR3 and an anti-V5 antibody. Molecular weight of wt CNKSR3: 62 kDa. Calculated molecular weight of V5-tagged CNKSR3: 65.9 kDa. The CNKSR3 antibody recognizes specifically human CNKSR3 protein. **D:** CNKSR3 Western blot of different subcellular protein fractions derived from HEK293-hMR$^+$ cells treated with 10 nM aldosterone or vehicle for 8 h. Endogenous CNKSR3 protein was induced after aldosterone treatment and was detected predominantly in the cytosolic compartment. As expected, aldosterone treatment led to nuclear translocation of MR protein (107 kDa). Beta-Actin (42 kDa), pan-cadherin (135 kDa) and RNA polymerase II (217 kDa) were analyzed as compartment markers for the fractionation.

Cell fractionation experiments were performed followed by Western blot analysis (Fig. 3.11D) to examine whether endogenous CNKSR3 protein expression is induced by aldosterone and to further investigate where CNKSR3 protein is located in the cell. Increased expression of endogenous CNKSR3 protein was detected predominantly in the cytosolic compartment after 8 h of 10 nM aldosterone treatment. As expected, aldosterone treatment led

to nuclear translocation of MR protein. Beta-actin (42 kDa), pan-cadherin (135 kDa) and RNA polymerase II (217 kDa) were analyzed as compartment markers for the fractionation.

This experimental set-up revealed that cnksr3 mRNA expression was time and dose-dependent to aldosterone stimulation and required expression of MR. CNKSR3 protein expression was also strongly induced by aldosterone and was predominantly detected in the cytosol of the cell.

3.4. Functional characterization of CNKSR3

The results from the above experiments suggested that cnksr3 as an early and directly aldosterone-regulated gene might be an important mediator of aldosterone action.

3.4.1. Cnksr3 is expressed in the mouse aldosterone-sensitive distal nephron

In order to assess where cnksr3 is expressed *in vivo*, total RNA isolated from 10 different mouse tissues (purchased from Ambion) was analyzed by qPCR. Figure 3.12A shows the cnksr3 expression level in tissues examined relative to expression level obtained in mouse embryo. Highest cnksr3 expression was found in kidney, liver, heart and testicle. Interestingly, the highest cnksr3 expression level was found in the heart, which may be in part due to the fact that the cellular composition of the heart is rather uniform. In contrast the kidney is composed of different tissues and the epithelia involved in aldosterone-controlled Na^+ retention are restricted to a small part of the distal nephron called aldosterone-sensitive distal nephron (ASDN). Considering this and the fact that cnksr3 was identified as an aldosterone-induced gene in human embryonic kidney cells, the expression pattern of cnksr3 in the kidney was studied in further detail. To this end the cnksr3 mRNA expression pattern along different nephron segments microdissected from mice kidneys was analyzed by qPCR. These experiments were carried out in co-orporation with Dr. Frederic Jaisser, INSERM, Paris, France. QPCR analysis was performed in segments derived from the proximal tubule (PCT), the distal convoluted tubule (DCT), the connecting tubule (CNT), and in the cortical collecting duct (CCD). The cnksr3 expression level was low in the PCT and gradually increased along the ASDN, reaching a 7-fold difference between CCD and the PCT (Fig. 3.12B). This indicates that cnksr3, an aldosterone-modulated gene, is expressed *in vivo* in the renal aldosterone target tissues.

These results supported the view that CNKSR3 contributes to aldosterone-mediated transepithelial Na^+ transport in the kidney.

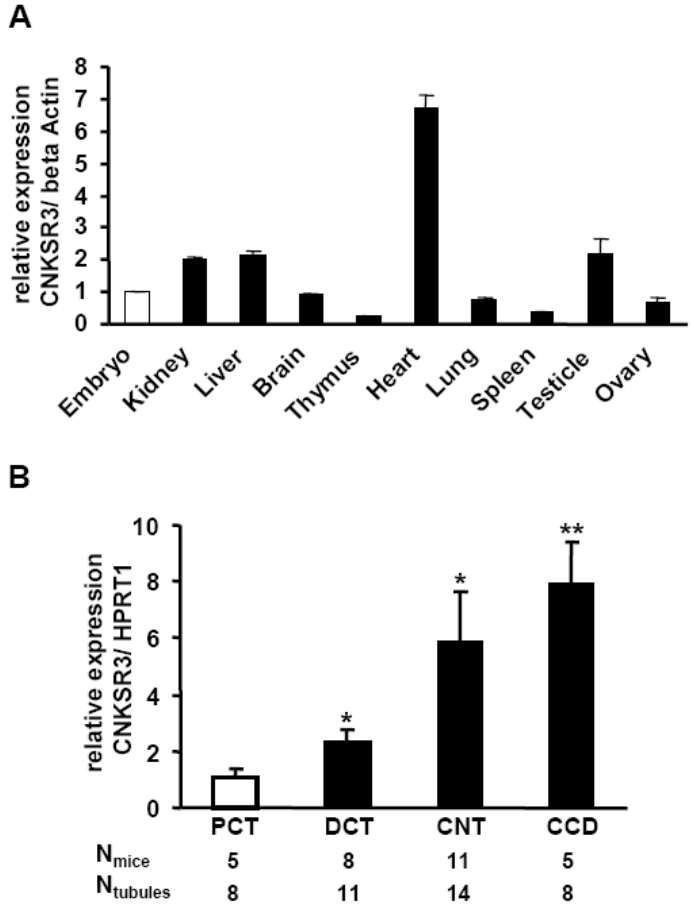

Fig. 3.12: *In vivo* expression pattern of cnksr3
A: cnksr3 expression in various mouse tissues was determined by qPCR. Expression levels in different organs were normalized to the expression level obtained in mouse embryo. Beta-Actin was used as a reference gene for normalization.
B: qPCR analysis of cnksr3 expression in microdissected nephrons segments from wt mice kidneys. Cnksr3 expression gradually increased along the ASDN.
proximal tubule (PCT), distal convoluted tubule (DCT), connecting tubule (CNT), and cortical collecting duct (CCD). Values are means ± SEM, n = 5-11 mice per group. (* $p < 0.05$, ** $p < 0.01$ versus PCT, Mann-Whitney test)

3.4.2. Generation and electrophysiological characterization of the MR stable M1 cell line

HEK293 cells do not develop a polarized electrically tight cell monolayer. Hence, to explore the functional role of CNKSR3 in the mechanism of transepithelial Na^+ transport , the mouse cortical collecting duct (CCD) cell line M1 was chosen as an *in vitro* model (118). However, M1 cells lack the expression of functional MR (119). To investigate the MR-regulated Na^+ transport, M1 cells were stably transfected with the rat MR. The cloning of the rat MR expression plasmid pcDNA3.1/rMR is described in section 2.2.1.11.

Over 50 clones were isolated and screened for aldosterone-induced MR activity in transactivation assays, as described in section 3.1.1. As a reference positive control for MR-mediated transactivation response the previous characterized HEK293-hMR^+ cells were used (see section 3.1.2). M1 rMR expression clone #35 was selected and is further referred to as M1-rMR^+. M1-rMR^+ cells exhibited an aldosterone-induced transactivation response at an EC_{50} of ~0.5 nM (Fig. 3.13A). Expression level of rMR protein level was verified by Western blot analysis (Fig. 3.13B). Additionally, the rMR expression number was determined in M1-

rMR$^+$ in comparison to parent M1 cells by ^{3}H-aldosterone binding assays as described in section 3.1.2. The range of rMR expression in M1-rMR$^+$ cells was determined to ~2500 molecules per cell, which was less the MR expression range in the CCD in vivo (102, 105). As expected, parent M1 cells did not exhibit measurable binding of ^{3}H-aldosterone.

To examine whether overexpressed MR are functional in regard to target gene regulation, qPCR experiments in M1-rMR$^+$ and parent M1 cells were carried out. Cnksr3 and sgk1 mRNA levels were determined after 4 h of incubation with 10 nM aldosterone and normalized to a respective vehicle control (Fig. 3.13C). Consistent with the results obtained for the HEK293-hMR$^+$ and HEK293-control cells (cf. Fig. 3.11B) M1-rMR$^+$ cells showed a substantial up-regulation of sgk1 and cnksr3 mRNA, whereas parent M1 cells showed no regulation (Fig. 3.13C).

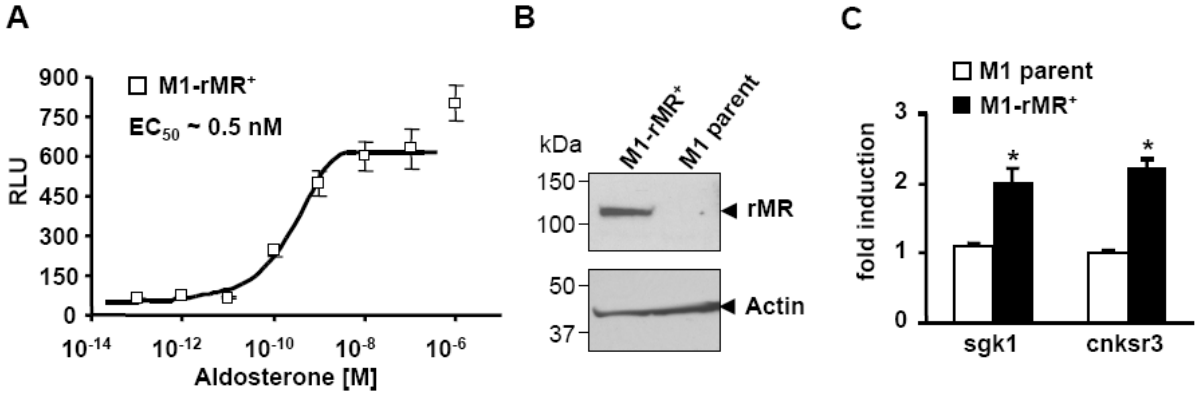

Fig. 3.13: The rat MR regulates endogenous target genes in M1 cells
A: M1-rMR$^+$ cells stably transfected with the rat MR were analyzed for MR activity by transient transactivation assays using the pMMTV-Luc reporter as described above. M1-rMR$^+$ cells exhibited an aldosterone dose-dependent transactivation response with an EC_{50} of ~0.5 nM. **B**: Western blot analysis of rMR (107 kDa) expression in M1-rMR$^+$ and parent M1 cells, which are devoid of MR expression. Beta-Actin (42 kDa) was used as a loading control. **C**: Aldosterone-dependent sgk1 and cnksr3 mRNA up-regulation after 4 h of 10 nM aldosterone treatment in M1-rMR$^+$ (black bars) in comparison to parent M1 cells (white bars). qPCR values measured for aldosterone-treated cells are time-matched to values obtained in vehicle-treated cells. (* $p < 0.05$)

To further elaborate whether the overexpressed MR was able to regulate ENaC-mediated transepithelial Na^+ transport (I_{SC}) M1-rMR$^+$ cells were electrophysiologically characterized in Ussing chamber experiments. The epithelial sodium channel (ENaC) can be blocked by application of 10^{-5} M amiloride. At these concentrations the diuretic amiloride does not block the Na^+/H^+ antiporter NHE3 (101). Thus the drop in I_{SC} after addition of amiloride, ΔI_{SC} ($\mu A/cm^2$), was assigned to ENaC-mediated Na^+ absorption. ΔI_{SC} increased within the first 6 h after 10 nM aldosterone stimulation until reaching a plateau, which was maintained up to 72 h (Fig. 3.14A, left panel). Increasing aldosterone concentrations from 0.1 to 10 nM activated the ENaC-controlled transepithelial Na^+ transport in a dose-dependent manner (Fig. 3.14A, right panel). At 1 nM aldosterone the effects were near maximal, which

is in accordance with the results obtained by transactivation assays using M1-rMR$^+$ cells (see Fig. 3.13A) or HEK-hMR$^+$ cells (see Fig. 3.3C). To assure that the ENaC-mediated Na^+ transport was induced via MR and not by co-present GR, M1-rMR$^+$ cells were treated with 10 nM aldosterone in the presence of 1 µM RU486 or 1 µM RU26752. Treatment with the MR antagonist RU26752 markedly inhibited the transepithelial Na^+ current, whereas the GR antagonist RU486 did not show a significant effect (Fig. 3.14B).

These results clearly indicate that this novel established M1-rMR$^+$ cell line is a well suited cell model to study the physiological effects of MR-mediated ENaC-controlled transepithelial Na^+ transport.

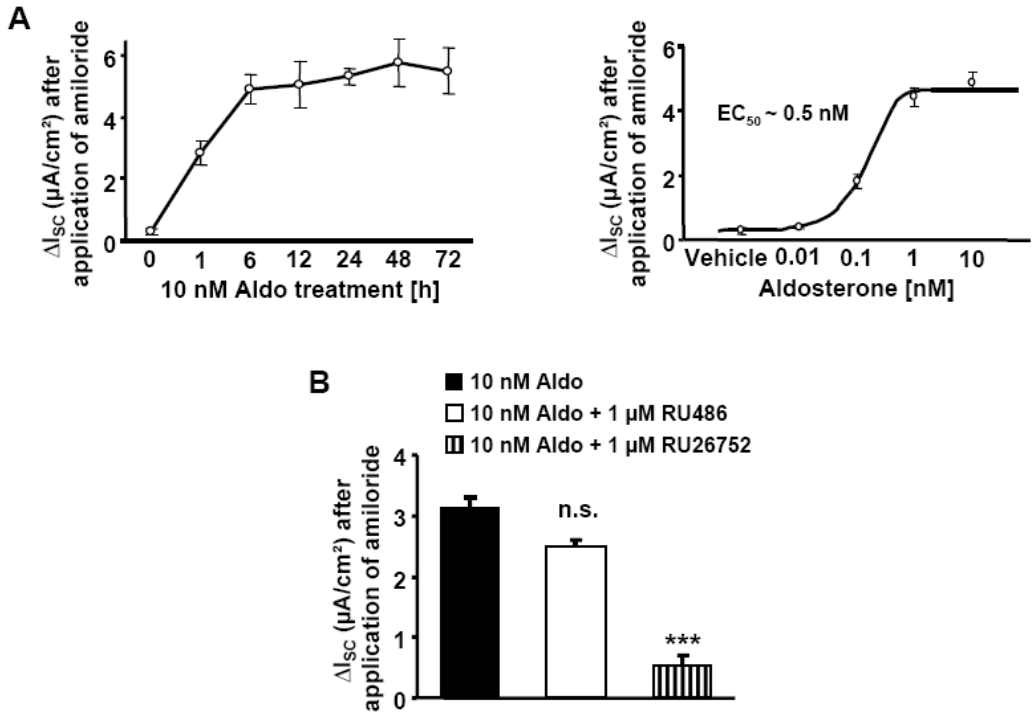

Fig. 3.14: Electrophysiological characterization of M1-rMR$^+$ cells in Ussing chamber experiments
A: Time-course in response to 10 nM aldosterone (left panel). Aldosterone dose-response curve analyzed 24 h after aldosterone stimulation (right panel). The amiloride-sensitive Na^+ current in M1-rMR$^+$ cells was time and dose-dependent. Values are means (n = 6) ± SEM. **B**: Transepithelial Na^+ flux in response to aldosterone alone (black bar) or presence of 1 µM RU486 (open bar) and 1 µM RU26752 (striped bar). MR blockade almost abolished aldosterone-mediated transepithelial Na^+ transport. Values are means ± SEM. (*** $p < 0.001$, n.s. = not significant ($p > 0.05$))

3.4.3. Generation of different M1-rMR$^+$ derived cell lines

Several M1-rMR$^+$-derived cell clones were generated that either stably overexpress mouse CNKSR3 or silence the expression by means of shRNA expression, in order to study the effects of CNKSR3 in the mechanism of transepithelial Na^+ transport by Ussing chamber experiments.

All these cell lines were generated by infection of M1-rMR$^+$ cells with recombinant lentiviruses as described in section 2.2.2.4. The CNKSR3 overexpressing cells and the control cells, stably overexpressing JRed as a non-pathway related protein, were oligoclonal. CNKSR3 expression levels in both cell pools were verified by qPCR and Western blot analysis (Fig. 3.15A/C). Additionally, the expression of JRed was analyzed by immunfluorecence microscopy (Fig. 3.15B).

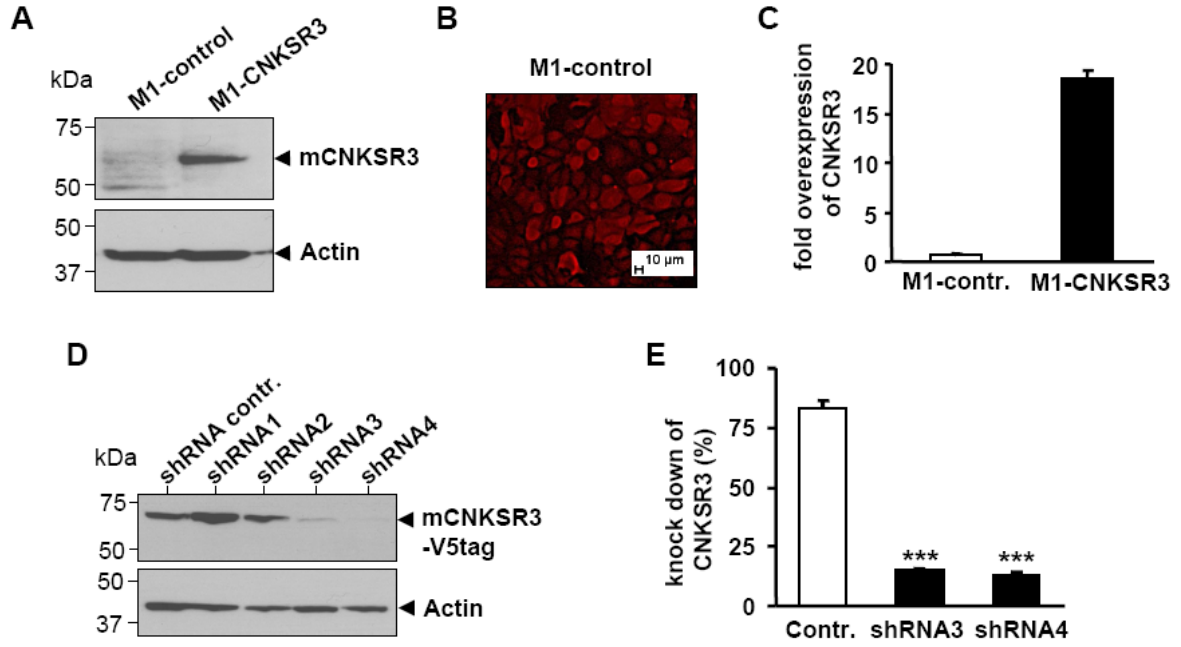

Fig. 3.15: Characterization of different M1-rMR$^+$ cell clones stably overexpressing or silencing CNKSR3
A: M1-rMR$^+$ cells stably overexpressing the murine CNKSR3 (62 kDa) as shown by Western blot **B**: Expression of JRed in M1- control cells verified by immunfluorecence microscopy **C**: Quantification of cnksr3 mRNA expression by qPCR. **D**: Characterization of different shRNAs (1-4) targeting cnksr3. A non-target shRNA (Qiagen) was used as a control. For further details see text. **E**: shRNA3 and shRNA4 were used for the generation of M1-rMR$^+$ cells stably silencing cnksr3. Knock down efficiency was verified by qPCR and is normalized to the endogenous cnksr3 expression in parent M1-rMR$^+$ cells. M1-rMR$^+$shRNA3 and M1-rMR$^+$shRNA4 displayed over 80% reduction of cnksr3 expression. M1-rMR$^+$ cells stably expressing a non-target shRNA were used as a control. (*** $p < 0.001$)

To ensure a sufficient knock down of endogenous CNKSR3 expression in M1-rMR$^+$ cells, different shRNAs (1-4) expression constructs were cloned as described in methods and characterized by transient co-transfection experiments. To this end, shRNA expression constructs pENTR/U6-shRNA #1-4 were co-transfected with pcDNA3.1-mCNKSR3-V5 into M1 parent cells. CNKSR3-V5 expression was analyzed by Western blot 36 h after transfection (Fig. 3.15D). A non-target shRNA (Qiagen) further referred to as shRNAcontrol was used as a control. The shRNAs 3 and 4 strongly suppressed mCNKSR3-V5 expression, whereas the non-target shRNA did not significantly reduce mCNKSR3-V5 protein level (Fig. 3.15D). Therefore shRNA3 and shRNA4 were chosen for the generation of M1-rMR$^+$-

derived cell clones that stably repress endogenous CNKSR3 expression. The shRNAcontrol was used for the generation of control cells. The cnksr3 knock down efficiency of several selected clones was verified by qPCR. For the cnksr3 knock down analysis two independent clones M1-rMR$^+$shRNA3 (#4) and M1-rMR$^+$shRNA4 (#8) were selected that were stably transduced with different shRNAs targeting cnksr3 mRNA. Both clones displayed over 80% reduction of cnksr3 expression as compared to parent M1-rMR$^+$ cells as assessed by qPCR analysis (Fig. 3.15E).

3.4.4. Impact of CNKSR3 on the aldosterone-induced ENaC-controlled Na^+ transport

The impact of CNKSR3 on MR-mediated ENaC-controlled transepithelial Na^+ transport was studied in different M1-rMR$^+$ derived cell clones stably overexpressing or silencing the cnksr3 gene (see section 3.4.3) in Ussing chamber experiments. As shown in Figure 3.16 overexpression of CNKSR3 resulted in a markedly increased aldosterone-dependent amiloride-blockable Na^+ transport (ΔI_{SC}). In contrast, both M1-rMR$^+$ cell clones stably silencing the cnksr3 gene exhibited a dramatically decreased ΔI_{SC}. Compared to parent M1-rMR$^+$ cells, ΔI_{SC} was unchanged in M1-rMR$^+$ cells stably over-expressing JRed as a non-pathway-related protein control as well as in M1-rMR$^+$ cells expressing a non-target shRNA. These results strongly suggest that CNKSR3 is required for the maintenance of MR-mediated ENaC-controlled transepithelial Na^+ transport in M1 CCD cells.

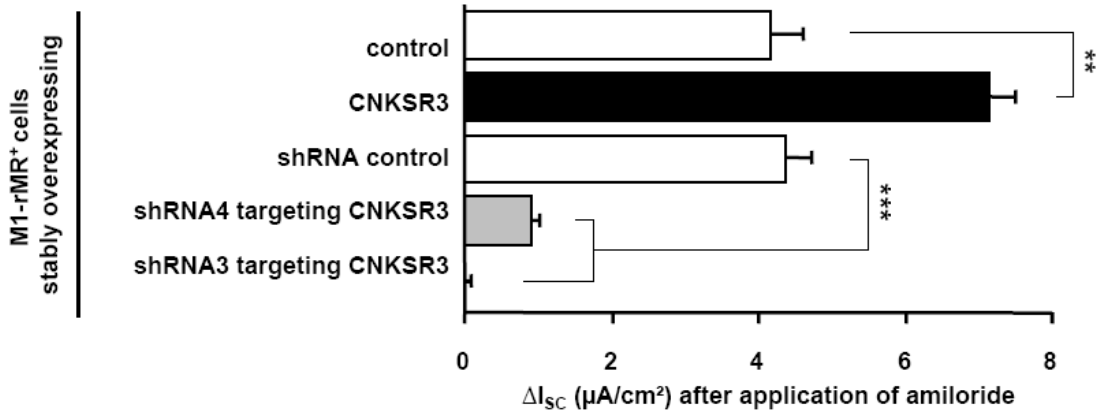

Fig. 3.16: Impact of CNKSR3 on MR-mediated ENaC-controlled Na^+ transport
ENaC-mediated transepithelial Na^+ absorption (ΔI_{SC}) in response to 10 nM aldosterone in M1-rMR$^+$-derived cell clones. Overexpression of CNKSR3 increased Na^+ transport (black bar), whereas silencing of the cnksr3 gene almost abrogated Na^+ transport (grey bars). ΔI_{SC} of appropriate control cell clones (open bars) was unchanged compared to M-1rMR$^+$ parent cells. Values were obtained after 24 h and are given as means (n = 6) ± SEM. (** $p < 0.01$, *** $p < 0.001$)

3.4.5. CNKSR3 suppresses phospho-MEK1/2 level

Previous studies suggested that the ERK pathway has a potent inhibitory effect on ENaC in CCD cells (76, 82, 120) and plays a role in aldosterone-controlled Na^+ regulation (82). As its name implies CNKSR3 is one of three members of the connector enhancer of kinase suppressor of RAS (CNK) family of proteins. CNK proteins have been shown to function as scaffolds in RHO/JNK and RAS/ERK signal transduction pathways (121-123). Due to the modular structure of CNKSR3 and its high homology to the C-terminal moiety of CNK1 and 2 the involvement of CNKSR3 in RAS/RAF signaling was studied. To this end the phosphorylation state of MEK1/2 and ERK1/2 was examined by Western blot analysis in M1-rMR$^+$ CNKSR3 overexpressing and silencing cells. M1-MR$^+$ cells in which CNKSR3 expression was inhibited by means of shRNA silencing showed a marked increase in MEK1/2 and ERK1/2 phosphorylation. On the other hand, overexpression of CNKSR3 slightly reduced phosphorylation of MEK1/2 and ERK1/2 (Fig. 3.17). In accordance with this the phosphorylation state of ERK1/2, a downstream target of MEK1/2, was altered in the same manner (Fig. 3.17), suggesting that CNKSR3 inhibits the RAS/ERK signaling cascade at the level of MEK1/2 or further upstream. These results indicate that the lack of CNKSR3 expression leads to a MEK/ERK pathway activation which has been correlated with decreased ENaC surface expression in previous studies (82). Preliminary results from Ussing chamber experiments revealed that ΔI_{SC} in M1-rMR$^+$ cells silencing the CNKSR3 gene can be markedly increased by U0126, a pharmacological inhibitor of MEK1/2.

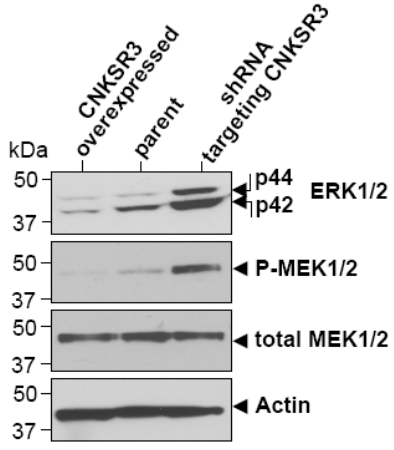

Fig. 3.17: CNKSR3 prevents phosphorylation of MEK1/2 and ERK1/2
Western blot analysis for phospho-MEK1/2 and phosho-ERK1/2 detection in M1-rMR$^+$ cells stably overexpressing or silencing the CNKSR3 gene. Parent M1-rMR$^+$ cells were used as a reference control. Total MEK and beta-Actin were monitored as loading controls.

In conclusion, these data show that cnksr3 is a novel direct aldosterone target gene and that its expression is critical for the maintenance of aldosterone-mediated transepithelial Na^+ transport in renal CCD cells. As a member of a scaffold protein family involved in RAS/ERK signaling, it was demonstrated that CNKSR3 expression is correlated with decreased MEK1/2 ERK1/2 phosphorylation.

4. Discussion

The present study examined the aldosterone-activated mineralocorticoid receptor-mediated gene regulation pattern on a genome-wide level by DNA microarray experiments. Chromatin immunoprecipitation (ChIP) in combination with reporter gene assays confirmed that several aldosterone-regulated genes are directly regulated by MR. This approach led to the identification of a so far unknown MR target gene, cnksr3. By using a renal cortical collecting duct cell model it was shown that cnksr3 is a crucial element in the mechanism of aldosterone-mediated ENaC-controlled transepithelial sodium transport. Moreover, it was shown that cnksr3 is highly expressed in the connecting tubule and the cortical collecting duct microdissected from mouse kidneys.

4.1. Early aldosterone target genes in HEK293 MR expressing cells

MR has a similar affinity for aldosterone and glucocorticoids (26, 27), and a number of MR target genes identified so far were initially found to be glucocorticoid-regulated, e.g. sgk and gilz (124, 125). In addition, supraphysiological concentrations of aldosterone also activate the GR (28-30). This overlap makes it experimentally difficult to attribute observed functional effects to either glucocorticoids or aldosterone, on the one hand, and to GR or MR activation, on the other (126). In the past a number of studies for aldosterone-regulated genes have been performed with supraphysiological concentrations of aldosterone ranging from 100 nM to 1 μM (80, 82, 109, 127). These studies face the disadvantage that the observed effects are not exclusively mediated by the MR since the GR is ubiquitously expressed (11, 128). For the present study HEK293-hMR$^+$ cells were established which stably express human MR in a physiological range, typical for cells of the CCD in the kidney. The HEK293-hMR$^+$ cells allow a clear separation of MR- vs. GR-mediated effects and were thus considered as an appropriate cell system to study the MR-mediated transcriptional response. Albeit the 293 cell line was derived by transformation of primary cultured human embryonic kidney (HEK) cells with sheared fragments of adenovirus 5 DNA (129), these cells exhibit some properties untypical for kidney epithelial cells. A recent study demonstrated that the constitutive expression pattern of HEK293 cells includes genes typically found in neurons (130). Since several genes identified as MR-regulated in kidney or kidney-derived cell lines, e.g. sgk1, gilz, k-ras, or scnn1a (68, 71, 82, 131), were induced by aldosterone in HEK293-hMR$^+$ cells in the same order of magnitude, HEK293-hMR$^+$ were considered as a suitable cell system for

the identification of further MR target genes by an Affymetrix microarray gene expression study.

The microarray study led to the identification of 36 aldosterone-regulated genes, including the well characterized aldosterone target genes sgk1 and gilz, whereas the majority of regulated genes had not been described as mineralocorticoid-responsive so far. A recent microarray study carried out with a cardiomyocyte-derived cell line stably expressing MR demonstrated that 48 genes were regulated by aldosterone (110) in a manner reminiscent of the regulation pattern obtained in HEK293-hMR$^+$ cells in terms of fold change and distribution of induced and repressed genes. However, the overlap of common regulated genes in both studies was restricted to sgk1, gilz, fkbp5, nfkbia, and klf9. This suggests that the MR has a tissue-specific gene expression profile and consequently modulates different pathways.

In HEK293-hMR$^+$ cells 12 genes were identified as being regulated by aldosterone, which code for transcription factors e.g. mafb, emx2, klf9, per1, or plzf. Recent studies showed that per1 and plzf are regulated by aldosterone in the kidney and demonstrated that these transcription factors modulate ENaC mRNA expression. PLZF overexpression in M1 CCD cells led to a reduced expression of the β and γ-ENaC mRNA and simultaneously reduced transepithelial sodium transport (108). In contrast, PER1 seems to have a stimulatory effect on α-ENaC mRNA expression. Silencing of per1 by means of siRNA in renal collecting duct cells markedly decreased α-ENaC mRNA level. In line with this per1 knockout mice excreted more sodium in comparison to their wt littermates (111). Also the krüppel-like transcription factor 9 (KLF9) modulates gene transcription by binding through its C-terminal C2H2 zinc finger motif to GC boxes in the promoter of many genes (132). As mentioned above KLF9 was found to be aldosterone-induced in rat cardiomyocytes. Bonett and colleagues (133) demonstrated that KLF9 is regulated by glucocorticoids in the *Xenopus leavis* brain where it promotes neuronal differentiation. The role of KLF9 in aldosterone-mediated signaling remains elusive at this time. As shown for PLZF and PER1 some aldosterone-induced transcription factors indirectly regulate transepithelial sodium transport by modulating the expression of components of the ion transport machinery. Although some genes code for transcription factors that were early or directly regulated by MR, this group of genes is assumed to be involved in the late phase of aldosterone-mediated regulatory effects. These factors can exert their regulatory function after a lag period needed for expression and translation before they can modulate the expression of other genes e.g. that code for the transporter themselves (12). The roles of the majority of identified aldosterone-responsive

transcription factors in MR signaling remains unclear. These factors may mediate the fine-tune regulation of sodium reabsorption during a long period of aldosterone exposure.

4.2. Direct MR target genes and their regulatory elements

The present study aimed at the identification of direct MR target genes. To this end short times of hormone exposure during a time-course experiment were chosen to identify early aldosterone-regulated genes, where the MR is probably the determinant of the transcription regulatory process. Early aldosterone-induced genes encoding regulatory factors have a great potential to mediate the acute and dynamic response of sodium reabsorption through modulation of ENaC activity e.g. sgk1 (68, 106) and gilz (82). It is generally assumed that the early phase of aldosterone action is mediated through direct effects on gene expression (12, 54). Direct regulatory mechanisms classically include binding of activated MR to DNA responsive elements in the promoter of target genes (12, 112). Evidence that several of the identified aldosterone responsive genes are directly regulated by MR came from a ChIP-chip study carried out in HEK293-myc-MR^{+} cells scanning 10 kb promoter fragments of approximately 25,500 promoters of the human genome for putative MR binding regions (MBR) (114).

Distribution of regulatory elements in the promoter of target genes

The comparison of microarray data from this study with the results obtained by the ChIP-chip analysis revealed that 12 out of 36 aldosterone-responsive genes (sgk1, gilz, scnn1a, per1, cxcr4, pdk4, fkbp5, nfkbia, klf9, pik3r1, calm1, and cnksr3) contain a least one MBR in the promoter region from 7.5 kb upstream through 2.5 kb downstream of the TSS.

MR binding to proximal promoter regions, i.e. within -800 bp to +200 bp from TSS, was only detected for cnksr3 and pdk4. All other identified MBRs in vicinity to aldosterone-responsive genes (including a second more distal MBR within the cnksr3 promoter) are located in promoter regions more distant from the TSS. This is in good accordance with binding studies for GR and the estrogen receptor (ER) in which less than 10% of all identified binding sites were mapped to the -800 bp to +200 bp proximal promoter region (39, 134). For the GR and the androgen receptor (AR) it has been demonstrated that approximately 30% of all glucocorticoid and androgen-regulated genes contain respective receptor binding sites within the 10 kb promoter region, whereas the majority of binding sites were found beyond 10 kb of TSS (39, 135). Thus it is likely that several aldosterone-regulated genes that do not have

a MR binding site within the 10 kb promoter region might be regulated by sites that have a larger distance to the TSS.

It is also conceivable that some of the aldosterone-responsive genes are regulated by a DNA element that does not contain a high-affinity binding site for the MR, rather MR recruitment is accomplished through stabilizing protein-protein interactions with other DNA-binding factors. This tethered binding mode has been described for GR and AR (136, 137). It is also possible that these genes are regulated by elements on different chromosomes (138). For instance, the expression of the promyelocytic leukemia zinc finger protein (PLZF) is described as regulated by androgens in the prostate (139) and was also found induced by aldosterone-activated MR by us and others (108). PLZF expression does not require *de novo* protein synthesis, suggesting a direct mechanism of action (108). However, no associated steroid receptor binding site in the 100 kb region surrounding the TSS of the PLZF gene has been identified so far.

Function of regulatory elements

All MR binding regions detected by the ChIP-chip approach could be verified by manual ChIP-qPCR experiments. As a proof of concept the already known functional MR binding site of the sgk1 promoter (115) was confirmed. The identified MBRs close to the TSS of gilz, scnn1a, and nfkbia overlap with functional binding regions previously identified for GR and AR (39, 116, 135). Reporter gene assays showed that all MBRs close to TSS of aldosterone-regulated genes are sufficient to mediate MR-dependent transcription. Hence it is likely that the identified MBRs confer to the aldosterone responsiveness of their associated genes. Computational analysis revealed that all these MBRs contain at least one core consensus sequence for glucocorticoid responsive element (GRE) family elements. For the distal cnksr3 promoter fragment a cluster of four putative GREs was identified. Mutation analysis revealed that three of four computationally predicted regulatory elements within the -4 kb MR binding region of the cnksr3 promoter contributed to aldosterone responsiveness. These experiments suggest that individual MR binding sites seem to be crucial for overall promoter activity and thus for target gene regulation.

Interestingly, MR binding as assessed by ChIP was not predictive for the degree of mRNA expression. As noted above the cnksr3 promoter exhibited two promoter regions with strong MR occupancy, whereas the sgk1 promoter contains only one MR binding site with moderate MR binding. However, aldosterone altered sgk1 and cnksr3 mRNA expression level in the same order of magnitude in HEK293-hMR$^+$ and M1-rMR$^+$ cells. Moreover, for

mgc21644 and rhob MR occupancy was detected close to their respective TSS, although both genes were unresponsive to aldosterone in HEK293-hMR$^+$ cells. This indicates that MR binding to bona fide DNA responsive elements is not necessarily the limiting factor in transcription initiation.

Another factor that might affect MR activity is the structure of the consensus DNA binding sequence itself. For the GR it has been reported that GREs vary around a core consensus sequence, but are highly conserved for a given sequence across species (39). Evidence that binding sites carry a regulatory code that affects the receptors function came from a recent study that demonstrated that consensus sequences differing in a single bp differentially affect GR conformation and its regulatory activity (40). This raises the possibility of distinct sets of MREs versus GREs for MR target genes. In this context it should be noted that the mgc21644-luciferase reporter construct had different transactivating capabilities with MR versus GR. Reporter gene transactivation assays revealed that aldosterone-activated MR in HEK-hMR$^+$ cells was unable to promote luciferase activity, whereas the cortisol-activated GR in HEK293-hGR$^+$ cells induced luciferase activity more than 3-fold (data not shown). It is interesting to speculate whether this promoter segment contains elements that force the MR in an inactive conformation or whether the vicinity to binding sites for inhibitory factors preclude interaction of MR with the transcription machinery.

4.3. The role of CNKSR3 in the mechanism of transepithelial sodium transport

Protein and mRNA expression data in combination with results obtained from ChIP analysis strongly indicate that cnksr3 is directly induced by the aldosterone-activated MR. Evidence that cnksr3 might be involved in the mechanism of sodium reabsorption came from qPCR expression analysis along different nephron segments microdissected from mice kidneys. Cnksr3 was found to be highly expressed in the connecting tubule (CNT) and the cortical collecting duct (CCD). The CNT and the CCD are the essential compartments whereby sodium reabsorption via ENaC is regulated by aldosterone (140). Murine CCD cells (e.g. M1) have been used as a surrogate *in vitro* model to elucidate the function of genes involved in transepithelial sodium transport, e.g. the recently identified MR target genes wnk1 (119) and plzf (108). Overexpression of murine CNKSR3 in M1-rMR$^+$ cells markedly increased ENaC activity, indicating that CNKSR3 is involved in the mechanism of aldosterone-controlled sodium transport. More important, M1-MR$^+$ cells that lack CNKSR3 gene expression by means of shRNA silencing showed almost abolished ENaC-mediated

sodium absorption. Apparently basic expression levels of CNKSR3 are required to maintain sodium reabsorption in the kidney.

CNKSR3 is one of three members of the 'connector enhancer of kinase suppressor of RAS' (CNK) family of proteins. The CNK family was first described in *Drosophila* (141) and homologues exist in vertebrates and *C. elegans* (142). CNK proteins have no catalytic motifes but contain several protein interaction domains: an N-terminal sterile alpha motif (SAM domain) followed by a conserved region in CNK proteins named the CRIC domain and a PDZ domain. CNK1 and -2 further contain a proline-rich SRC-homology-3 (SH3) and a pleckstrin homology (PH) domain (143). In contrast, CNKSR3 is much smaller, and is highly homologous to the N-terminal half of full-length CNK1 and -2 proteins. However, it lacks the part corresponding to the C-terminal half of CNK1 and -2. CNK proteins have been shown to function as scaffolds in RHO/JNK and RAS/ERK signal transduction where their C-terminal moiety associates with RAF (121, 122, 144, 145). CNK1 is ubiquitously expressed whereas CNK2 expression seems to be restricted to neurons (123). In contrast to CNK1, CNK2 fails to co-precipitate RAS, MEK, ERK or KSR1 (121), suggesting that CNK2 might scaffold RAF signaling complexes that do not interact with components of the MEK, ERK pathway (123).

It is conceivable that CNKSR3 shares scaffolding properties of CNK1 but fails to establish a fully active protein complex due to the lack of SH3 and PH domains. In effect, CNKSR3 would diminish the activity of the RAF/ERK signaling possibly by recruiting kinase suppressor of RAS (KSR) from the CNK1 signaling complex, which is required for MEK activation and thus for the maintainance of the phosphorylation cascade, suggesting that CNKSR3 might act as a dominant negative of CNK1 (Fig. 4.1). This model supports the view that CNKSR3, as an early aldosterone responsive gene, regulates ENaC-mediated sodium transport via inhibition of the RAF/ERK signaling cascade. Indeed, analysis of components of the RAS/ERK signaling cascade revealed that shRNA-mediated CNKSR3 silencing markedly increased MEK1/2 and ERK1/2 phosphorylation, while CNKSR3 overexpression had the opposite effects. There is increasing evidence that scaffold proteins dynamically modulate signal transduction by affecting assembly of individual components of signaling networks (123). Furthermore, the subcellular localization and differential utilization of scaffold proteins may represent a mechanism that ensures specific signal transduction through otherwise pleiotropic signaling cascades (146).

There are several lines of evidence that the RAS/RAF-1/MEK/ERK kinase pathway has a potent inhibitory effect on ENaC in CCD cells (76, 82, 120).

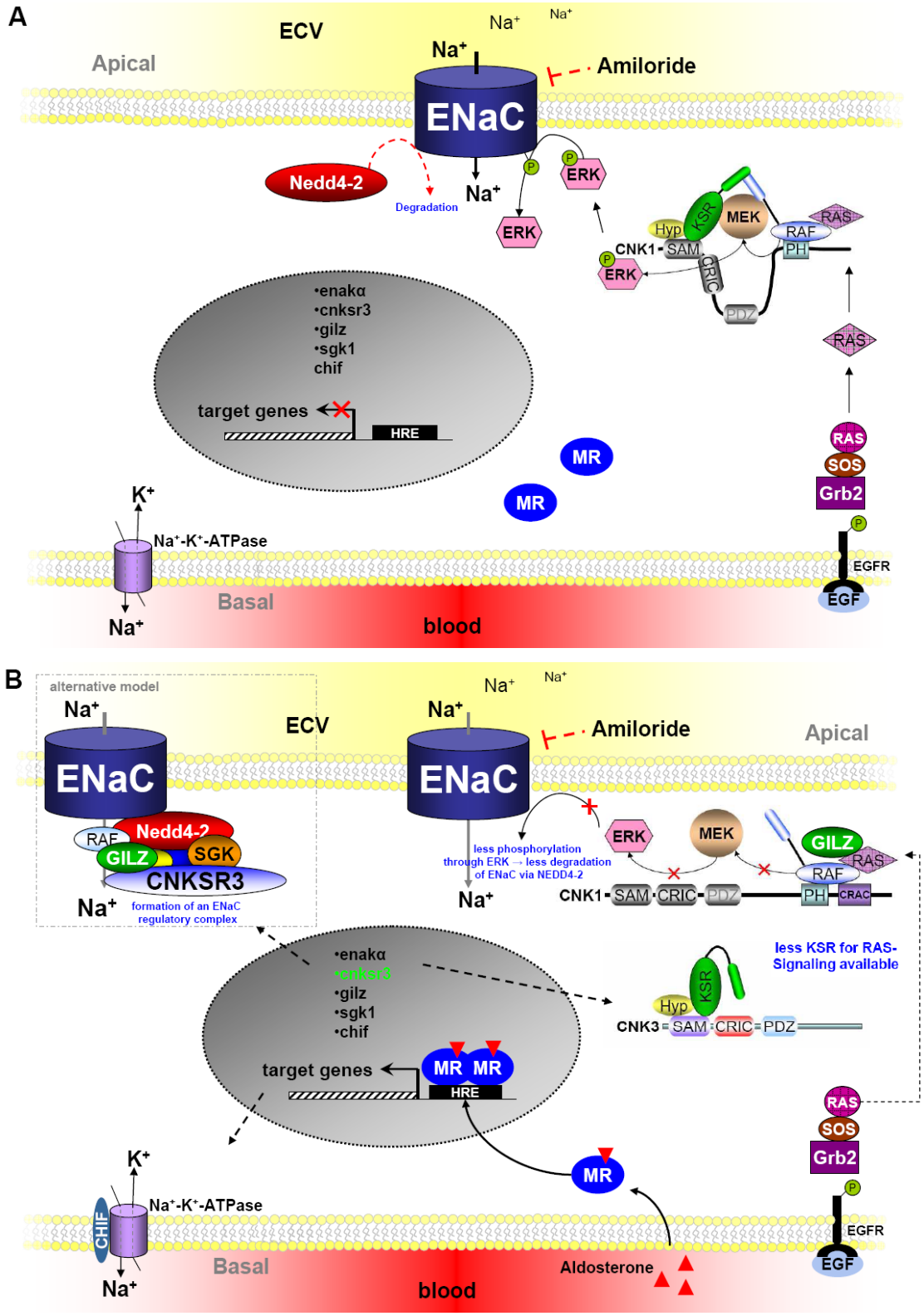

Fig. 4.1: The possible function of CNKSR3 in the mechanism of ENaC regulation
A: In the absense of aldosterone the expression of MR target genes including cnksr3 is relatively low. Nedd4-2 and ERK are fully active, which leads to ENaC degradation. CNK1 might function as molecular platform that allows the assembly of proteins required for the RAS/RAF/MEK/ERK phosphorylation cascade. **B**: In the presence of aldosterone CNKSR3 abundance increases and interferes with the CNK1 signaling complex, by recruiting components (e.g. KSR1) from the signaling complex and thus preventing ENaC from degradation, which leads to an interuption of the phosphorylation cascade. *An alternative model* is depicted in B upper left: CNKSR3 is part of a regulatory complex that protects ENaC from degradation. This complex contains SGK1, GILZ, RAF-1 Nedd4-2 and the α- and β-ENaC subunits. See text for details and references.

It appears that activated ERK phosphorylates ENaC and thereby facilitates interaction between Nedd4 proteins and ENaC, which triggers degradation of the channel and thus decreases ENaC surface expression (82). The best characterized modulator that stimulates ENaC activity by interfering with the ERK pathway is GILZ1. This protein is rapidly and robustly induced by aldosterone in the native collecting duct (131), as well as in cultured $mpkCCD_{C14}$ cells (80). Overexpression of GILZ1 stimulates ENaC activity and inhibits formation of phospho-ERK in progesterone-treated *Xenopus laevis* oocytes (82). Moreover it has been demonstrated that GILZ1 stimulates transepithelial sodium transport and concurrently inhibits ERK phosphorylation in $mpkCCD_{C14}$ cells. GILZ1 directly interacts with RAF-1 whereby it possibly interrupts the RAS/RAF/MEK/ERK signaling cascade by displacing RAS from the ras-binding domain of RAF-1 (81). In effect, CNKSR3 stimulates ENaC activity by a similar route as reported for GILZ proteins.

It is also conceivable that CNKSR3 acts as a scaffold by coordinating the assembly of ENaC regulatory proteins in a complex and thereby promoting proper signal transduction (Fig. 4.1B). A recent study from the Pearce laboratory demonstrated that RAF-1, SGK1, Nedd4-2, and the α and β-ENaC subunits are assembled in a multi-protein complex (83). Nevertheless, further studies will be needed, esspecially co-immunoprecipitation experiments, to elucidate the specific role of CNKSR3 in the context of ENaC regulation. Moreover, it would be interesting to study the role of CNKSR3 in other non-epithelial tissues particularly in the heart where the pathological actions of MR are as yet poorly understood.

4.4. Conclusion

The present study provides new insights into the genome-wide gene regulation pattern of aldosterone-activated MR. The identification of several functional MR DNA-binding sites in the proximity to aldosterone-regulated genes is an important step studying DNA sequence binding preferences and other functional properties by which the MR controls transcription. Furthermore functional studies revealed that cnksr3, a novel identified direct MR target gene, plays a key role in the regulation of ENaC-mediated sodium transport. CNKSR3 inhibits RAS/MEK/ERK signaling and thereby stimulates ENaC activity. As a scaffold protein CNKSR3 most probably interferes with the assembly of components of the RAS/MEK/ERK pathway to a fully functional complex. The dynamic regulation of a scaffold protein appears to be an effective mechanism to modulate ENaC activity. This mechanism of CNKSR3, and GILZ, to affect ENaC activity describes a novel route how MR mediates its effects to regulate sodium transport.

5. References

1. Hanke, C. J., and Bauer-Dantoin, A. C. (2006) Teaching aldosterone regulation and basic scientific principles using a classic paper by Dr. James O. Davis and colleagues. *Adv Physiol Educ* 30, 141-144
2. Young, D. B. (1985) Analysis of long-term potassium regulation. *Endocr Rev* 6, 24-44
3. Berger, S., Bleich, M., Schmid, W., Cole, T. J., Peters, J., Watanabe, H., Kriz, W., Warth, R., Greger, R., and Schutz, G. (1998) Mineralocorticoid receptor knockout mice: pathophysiology of Na+ metabolism. *Proc Natl Acad Sci U S A* 95, 9424-9429
4. Berger, S., Bleich, M., Schmid, W., Greger, R., and Schutz, G. (2000) Mineralocorticoid receptor knockout mice: lessons on Na+ metabolism. *Kidney Int* 57, 1295-1298
5. Beato, M., Herrlich, P., and Schutz, G. (1995) Steroid hormone receptors: many actors in search of a plot. *Cell* 83, 851-857
6. Lifton, R. P., Gharavi, A. G., and Geller, D. S. (2001) Molecular mechanisms of human hypertension. *Cell* 104, 545-556
7. Zennaro, M. C., Farman, N., Bonvalet, J. P., and Lombes, M. (1997) Tissue-specific expression of alpha and beta messenger ribonucleic acid isoforms of the human mineralocorticoid receptor in normal and pathological states. *J Clin Endocrinol Metab* 82, 1345-1352
8. Pascual-Le Tallec, L., and Lombes, M. (2005) The mineralocorticoid receptor: a journey exploring its diversity and specificity of action. *Mol Endocrinol* 19, 2211-2221
9. Black, B. E., Holaska, J. M., Rastinejad, F., and Paschal, B. M. (2001) DNA binding domains in diverse nuclear receptors function as nuclear export signals. *Curr Biol* 11, 1749-1758
10. Williams, S. P., and Sigler, P. B. (1998) Atomic structure of progesterone complexed with its receptor. *Nature* 393, 392-396
11. Farman, N., and Rafestin-Oblin, M. E. (2001) Multiple aspects of mineralocorticoid selectivity. *Am J Physiol Renal Physiol* 280, F181-192
12. Stockand, J. D. (2002) New ideas about aldosterone signaling in epithelia. *Am J Physiol Renal Physiol* 282, F559-576
13. Geller, D. S., Farhi, A., Pinkerton, N., Fradley, M., Moritz, M., Spitzer, A., Meinke, G., Tsai, F. T., Sigler, P. B., and Lifton, R. P. (2000) Activating mineralocorticoid receptor mutation in hypertension exacerbated by pregnancy. *Science* 289, 119-123
14. Rafestin-Oblin, M. E., Souque, A., Bocchi, B., Pinon, G., Fagart, J., and Vandewalle, A. (2003) The severe form of hypertension caused by the activating S810L mutation in the mineralocorticoid receptor is cortisone related. *Endocrinology* 144, 528-533
15. McEwen, B. S., and Wallach, G. (1973) Corticosterone binding to hippocampus: nuclear and cytosol binding in vitro. *Brain Res* 57, 373-386
16. Funder, J. W., Pearce, P. T., Smith, R., and Smith, A. I. (1988) Mineralocorticoid action: target tissue specificity is enzyme, not receptor, mediated. *Science* 242, 583-585
17. Caprio, M., Feve, B., Claes, A., Viengchareun, S., Lombes, M., and Zennaro, M. C. (2007) Pivotal role of the mineralocorticoid receptor in corticosteroid-induced adipogenesis. *Faseb J* 21, 2185-2194
18. Lim, H. Y., Muller, N., Herold, M. J., van den Brandt, J., and Reichardt, H. M. (2007) Glucocorticoids exert opposing effects on macrophage function dependent on their concentration. *Immunology* 122, 47-53

19. Pitt, B., Zannad, F., Remme, W. J., Cody, R., Castaigne, A., Perez, A., Palensky, J., and Wittes, J. (1999) The effect of spironolactone on morbidity and mortality in patients with severe heart failure. Randomized Aldactone Evaluation Study Investigators. *N Engl J Med* 341, 709-717
20. Pitt, B., Remme, W., Zannad, F., Neaton, J., Martinez, F., Roniker, B., Bittman, R., Hurley, S., Kleiman, J., and Gatlin, M. (2003) Eplerenone, a selective aldosterone blocker, in patients with left ventricular dysfunction after myocardial infarction. *N Engl J Med* 348, 1309-1321
21. Rickard, A. J., and Young, M. J. (2009) Corticosteroid receptors, macrophages and cardiovascular disease. *J Mol Endocrinol* 42, 449-459
22. Berger, S., Wolfer, D. P., Selbach, O., Alter, H., Erdmann, G., Reichardt, H. M., Chepkova, A. N., Welzl, H., Haas, H. L., Lipp, H. P., and Schutz, G. (2006) Loss of the limbic mineralocorticoid receptor impairs behavioral plasticity. *Proc Natl Acad Sci U S A* 103, 195-200
23. Fuller, P. J., Lim-Tio, S. S., and Brennan, F. E. (2000) Specificity in mineralocorticoid versus glucocorticoid action. *Kidney Int* 57, 1256-1264
24. Funder, J. W. (1997) Glucocorticoid and mineralocorticoid receptors: biology and clinical relevance. *Annu Rev Med* 48, 231-240
25. Arriza, J. L., Weinberger, C., Cerelli, G., Glaser, T. M., Handelin, B. L., Housman, D. E., and Evans, R. M. (1987) Cloning of human mineralocorticoid receptor complementary DNA: structural and functional kinship with the glucocorticoid receptor. *Science* 237, 268-275
26. Krozowski, Z. S., and Funder, J. W. (1983) Renal mineralocorticoid receptors and hippocampal corticosterone-binding species have identical intrinsic steroid specificity. *Proc Natl Acad Sci U S A* 80, 6056-6060
27. Rupprecht, R., Reul, J. M., van Steensel, B., Spengler, D., Soder, M., Berning, B., Holsboer, F., and Damm, K. (1993) Pharmacological and functional characterization of human mineralocorticoid and glucocorticoid receptor ligands. *Eur J Pharmacol* 247, 145-154
28. Claire, M., Machard, B., Lombes, M., Oblin, M. E., Bonvalet, J. P., and Farman, N. (1989) Aldosterone receptors in A6 cells: physicochemical characterization and autoradiographic study. *Am J Physiol* 257, C665-677
29. Schmidt, T. J., Husted, R. F., and Stokes, J. B. (1993) Steroid hormone stimulation of Na+ transport in A6 cells is mediated via glucocorticoid receptors. *Am J Physiol* 264, C875-884
30. Ziera, T., Irlbacher, H., Fromm, A., Latouche, C., Krug, S. M., Fromm, M., Jaisser, F., and Borden, S. A. (2009) Cnksr3 is a direct mineralocorticoid receptor target gene and plays a key role in the regulation of the epithelial sodium channel. *Faseb J*
31. Edwards, C. R., Stewart, P. M., Burt, D., Brett, L., McIntyre, M. A., Sutanto, W. S., de Kloet, E. R., and Monder, C. (1988) Localisation of 11 beta-hydroxysteroid dehydrogenase--tissue specific protector of the mineralocorticoid receptor. *Lancet* 2, 986-989
32. Stewart, P. M., Corrie, J. E., Shackleton, C. H., and Edwards, C. R. (1988) Syndrome of apparent mineralocorticoid excess. A defect in the cortisol-cortisone shuttle. *J Clin Invest* 82, 340-349
33. Mune, T., Rogerson, F. M., Nikkila, H., Agarwal, A. K., and White, P. C. (1995) Human hypertension caused by mutations in the kidney isozyme of 11 beta-hydroxysteroid dehydrogenase. *Nat Genet* 10, 394-399
34. Albiston, A. L., Obeyesekere, V. R., Smith, R. E., and Krozowski, Z. S. (1994) Cloning and tissue distribution of the human 11 beta-hydroxysteroid dehydrogenase type 2 enzyme. *Mol Cell Endocrinol* 105, R11-17

35. Funder, J. W. (2009) Reconsidering the roles of the mineralocorticoid receptor. *Hypertension* 53, 286-290
36. Hellal-Levy, C., Fagart, J., Souque, A., and Rafestin-Oblin, M. E. (2000) Mechanistic aspects of mineralocorticoid receptor activation. *Kidney Int* 57, 1250-1255
37. Rupprecht, R., Arriza, J. L., Spengler, D., Reul, J. M., Evans, R. M., Holsboer, F., and Damm, K. (1993) Transactivation and synergistic properties of the mineralocorticoid receptor: relationship to the glucocorticoid receptor. *Mol Endocrinol* 7, 597-603
38. Rogerson, F. M., and Fuller, P. J. (2003) Interdomain interactions in the mineralocorticoid receptor. *Mol Cell Endocrinol* 200, 45-55
39. So, A. Y., Chaivorapol, C., Bolton, E. C., Li, H., and Yamamoto, K. R. (2007) Determinants of cell- and gene-specific transcriptional regulation by the glucocorticoid receptor. *PLoS Genet* 3, e94
40. Meijsing, S. H., Pufall, M. A., So, A. Y., Bates, D. L., Chen, L., and Yamamoto, K. R. (2009) DNA binding site sequence directs glucocorticoid receptor structure and activity. *Science* 324, 407-410
41. Viengchareun, S., Le Menuet, D., Martinerie, L., Munier, M., Pascual-Le Tallec, L., and Lombes, M. (2007) The mineralocorticoid receptor: insights into its molecular and (patho)physiological biology. *Nucl Recept Signal* 5, e012
42. Hermanson, O., Glass, C. K., and Rosenfeld, M. G. (2002) Nuclear receptor coregulators: multiple modes of modification. *Trends Endocrinol Metab* 13, 55-60
43. O'Malley, B. W. (2007) Coregulators: from whence came these "master genes". *Mol Endocrinol* 21, 1009-1013
44. Fuse, H., Kitagawa, H., and Kato, S. (2000) Characterization of transactivational property and coactivator mediation of rat mineralocorticoid receptor activation function-1 (AF-1). *Mol Endocrinol* 14, 889-899
45. Zennaro, M. C., Souque, A., Viengchareun, S., Poisson, E., and Lombes, M. (2001) A new human MR splice variant is a ligand-independent transactivator modulating corticosteroid action. *Mol Endocrinol* 15, 1586-1598
46. Hultman, M. L., Krasnoperova, N. V., Li, S., Du, S., Xia, C., Dietz, J. D., Lala, D. S., Welsch, D. J., and Hu, X. (2005) The ligand-dependent interaction of mineralocorticoid receptor with coactivator and corepressor peptides suggests multiple activation mechanisms. *Mol Endocrinol* 19, 1460-1473
47. Kitagawa, H., Yanagisawa, J., Fuse, H., Ogawa, S., Yogiashi, Y., Okuno, A., Nagasawa, H., Nakajima, T., Matsumoto, T., and Kato, S. (2002) Ligand-selective potentiation of rat mineralocorticoid receptor activation function 1 by a CBP-containing histone acetyltransferase complex. *Mol Cell Biol* 22, 3698-3706
48. Tallec, L. P., Kirsh, O., Lecomte, M. C., Viengchareun, S., Zennaro, M. C., Dejean, A., and Lombes, M. (2003) Protein inhibitor of activated signal transducer and activator of transcription 1 interacts with the N-terminal domain of mineralocorticoid receptor and represses its transcriptional activity: implication of small ubiquitin-related modifier 1 modification. *Mol Endocrinol* 17, 2529-2542
49. Obradovic, D., Tirard, M., Nemethy, Z., Hirsch, O., Gronemeyer, H., and Almeida, O. F. (2004) DAXX, FLASH, and FAF-1 modulate mineralocorticoid and glucocorticoid receptor-mediated transcription in hippocampal cells--toward a basis for the opposite actions elicited by two nuclear receptors? *Mol Pharmacol* 65, 761-769
50. Pascual-Le Tallec, L., Simone, F., Viengchareun, S., Meduri, G., Thirman, M. J., and Lombes, M. (2005) The elongation factor ELL (eleven-nineteen lysine-rich leukemia) is a selective coregulator for steroid receptor functions. *Mol Endocrinol* 19, 1158-1169
51. Hu, X., and Funder, J. W. (2006) The evolution of mineralocorticoid receptors. *Mol Endocrinol* 20, 1471-1478

52. Verrey, F., Fakitsas, P., Adam, G., and Staub, O. (2008) Early transcriptional control of ENaC (de)ubiquitylation by aldosterone. *Kidney Int* 73, 691-696
53. Pearce, D., Bhargava, A., and Cole, T. J. (2003) Aldosterone: its receptor, target genes, and actions. *Vitam Horm* 66, 29-76
54. Bhalla, V., Soundararajan, R., Pao, A. C., Li, H., and Pearce, D. (2006) Disinhibitory pathways for control of sodium transport: regulation of ENaC by SGK1 and GILZ. *Am J Physiol Renal Physiol* 291, F714-721
55. Hummler, E., Barker, P., Gatzy, J., Beermann, F., Verdumo, C., Schmidt, A., Boucher, R., and Rossier, B. C. (1996) Early death due to defective neonatal lung liquid clearance in alpha-ENaC-deficient mice. *Nat Genet* 12, 325-328
56. McDonald, F. J., Yang, B., Hrstka, R. F., Drummond, H. A., Tarr, D. E., McCray, P. B., Jr., Stokes, J. B., Welsh, M. J., and Williamson, R. A. (1999) Disruption of the beta subunit of the epithelial Na+ channel in mice: hyperkalemia and neonatal death associated with a pseudohypoaldosteronism phenotype. *Proc Natl Acad Sci U S A* 96, 1727-1731
57. Barker, P. M., Nguyen, M. S., Gatzy, J. T., Grubb, B., Norman, H., Hummler, E., Rossier, B., Boucher, R. C., and Koller, B. (1998) Role of gammaENaC subunit in lung liquid clearance and electrolyte balance in newborn mice. Insights into perinatal adaptation and pseudohypoaldosteronism. *J Clin Invest* 102, 1634-1640
58. Bens, M., Vallet, V., Cluzeaud, F., Pascual-Letallec, L., Kahn, A., Rafestin-Oblin, M. E., Rossier, B. C., and Vandewalle, A. (1999) Corticosteroid-dependent sodium transport in a novel immortalized mouse collecting duct principal cell line. *J Am Soc Nephrol* 10, 923-934
59. Garty, H., and Palmer, L. G. (1997) Epithelial sodium channels: function, structure, and regulation. *Physiol Rev* 77, 359-396
60. Renard, S., Voilley, N., Bassilana, F., Lazdunski, M., and Barbry, P. (1995) Localization and regulation by steroids of the alpha, beta and gamma subunits of the amiloride-sensitive Na+ channel in colon, lung and kidney. *Pflugers Arch* 430, 299-307
61. Snyder, P. M. (2005) Minireview: regulation of epithelial Na+ channel trafficking. *Endocrinology* 146, 5079-5085
62. Geering, K. (2006) FXYD proteins: new regulators of Na-K-ATPase. *Am J Physiol Renal Physiol* 290, F241-250
63. Horisberger, J. D. (2004) Recent insights into the structure and mechanism of the sodium pump. *Physiology (Bethesda)* 19, 377-387
64. Lingrel, J. B., Van Huysse, J., O'Brien, W., Jewell-Motz, E., and Schultheis, P. (1994) Na,K-ATPase: structure-function studies. *Ren Physiol Biochem* 17, 198-200
65. Whorwood, C. B., and Stewart, P. M. (1995) Transcriptional regulation of Na/K-ATPase by corticosteroids, glycyrrhetinic acid and second messenger pathways in rat kidney epithelial cells. *J Mol Endocrinol* 15, 93-103
66. Kolla, V., and Litwack, G. (2000) Transcriptional regulation of the human Na/K ATPase via the human mineralocorticoid receptor. *Mol Cell Biochem* 204, 35-40
67. Staub, O., and Verrey, F. (2005) Impact of Nedd4 proteins and serum and glucocorticoid-induced kinases on epithelial Na+ transport in the distal nephron. *J Am Soc Nephrol* 16, 3167-3174
68. Naray-Fejes-Toth, A., Canessa, C., Cleaveland, E. S., Aldrich, G., and Fejes-Toth, G. (1999) sgk is an aldosterone-induced kinase in the renal collecting duct. Effects on epithelial na+ channels. *J Biol Chem* 274, 16973-16978
69. Naray-Fejes-Toth, A., and Fejes-Toth, G. (2000) The sgk, an aldosterone-induced gene in mineralocorticoid target cells, regulates the epithelial sodium channel. *Kidney Int* 57, 1290-1294

70. Wulff, P., Vallon, V., Huang, D. Y., Volkl, H., Yu, F., Richter, K., Jansen, M., Schlunz, M., Klingel, K., Loffing, J., Kauselmann, G., Bosl, M. R., Lang, F., and Kuhl, D. (2002) Impaired renal Na(+) retention in the sgk1-knockout mouse. *J Clin Invest* 110, 1263-1268
71. Brennan, F. E., and Fuller, P. J. (2006) Mammalian K-ras2 is a corticosteroid-induced gene in vivo. *Endocrinology* 147, 2809-2816
72. Foschi, M., Chari, S., Dunn, M. J., and Sorokin, A. (1997) Biphasic activation of p21ras by endothelin-1 sequentially activates the ERK cascade and phosphatidylinositol 3-kinase. *Embo J* 16, 6439-6451
73. Ichimura, T., Yamamura, H., Sasamoto, K., Tominaga, Y., Taoka, M., Kakiuchi, K., Shinkawa, T., Takahashi, N., Shimada, S., and Isobe, T. (2005) 14-3-3 proteins modulate the expression of epithelial Na+ channels by phosphorylation-dependent interaction with Nedd4-2 ubiquitin ligase. *J Biol Chem* 280, 13187-13194
74. Bhalla, V., Daidie, D., Li, H., Pao, A. C., LaGrange, L. P., Wang, J., Vandewalle, A., Stockand, J. D., Staub, O., and Pearce, D. (2005) Serum- and glucocorticoid-regulated kinase 1 regulates ubiquitin ligase neural precursor cell-expressed, developmentally down-regulated protein 4-2 by inducing interaction with 14-3-3. *Mol Endocrinol* 19, 3073-3084
75. Liang, X., Peters, K. W., Butterworth, M. B., and Frizzell, R. A. (2006) 14-3-3 isoforms are induced by aldosterone and participate in its regulation of epithelial sodium channels. *J Biol Chem* 281, 16323-16332
76. Shi, H., Asher, C., Chigaev, A., Yung, Y., Reuveny, E., Seger, R., and Garty, H. (2002) Interactions of beta and gamma ENaC with Nedd4 can be facilitated by an ERK-mediated phosphorylation. *J Biol Chem* 277, 13539-13547
77. Spindler, B., Mastroberardino, L., Custer, M., and Verrey, F. (1997) Characterization of early aldosterone-induced RNAs identified in A6 kidney epithelia. *Pflugers Arch* 434, 323-331
78. Boulkroun, S., Fay, M., Zennaro, M. C., Escoubet, B., Jaisser, F., Blot-Chabaud, M., Farman, N., and Courtois-Coutry, N. (2002) Characterization of rat NDRG2 (N-Myc downstream regulated gene 2), a novel early mineralocorticoid-specific induced gene. *J Biol Chem* 277, 31506-31515
79. Wielputz, M. O., Lee, I. H., Dinudom, A., Boulkroun, S., Farman, N., Cook, D. I., Korbmacher, C., and Rauh, R. (2007) (NDRG2) stimulates amiloride-sensitive Na+ currents in Xenopus laevis oocytes and fisher rat thyroid cells. *J Biol Chem* 282, 28264-28273
80. Robert-Nicoud, M., Flahaut, M., Elalouf, J. M., Nicod, M., Salinas, M., Bens, M., Doucet, A., Wincker, P., Artiguenave, F., Horisberger, J. D., Vandewalle, A., Rossier, B. C., and Firsov, D. (2001) Transcriptome of a mouse kidney cortical collecting duct cell line: effects of aldosterone and vasopressin. *Proc Natl Acad Sci U S A* 98, 2712-2716
81. Ayroldi, E., Zollo, O., Macchiarulo, A., Di Marco, B., Marchetti, C., and Riccardi, C. (2002) Glucocorticoid-induced leucine zipper inhibits the Raf-extracellular signal-regulated kinase pathway by binding to Raf-1. *Mol Cell Biol* 22, 7929-7941
82. Soundararajan, R., Zhang, T. T., Wang, J., Vandewalle, A., and Pearce, D. (2005) A novel role for glucocorticoid-induced leucine zipper protein in epithelial sodium channel-mediated sodium transport. *J Biol Chem* 280, 39970-39981
83. Soundararajan, R., Melters, D., Shih, I. C., Wang, J., and Pearce, D. (2009) Epithelial sodium channel regulated by differential composition of a signaling complex. *Proc Natl Acad Sci U S A*

84. Beguin, P., Crambert, G., Guennoun, S., Garty, H., Horisberger, J. D., and Geering, K. (2001) CHIF, a member of the FXYD protein family, is a regulator of Na,K-ATPase distinct from the gamma-subunit. *Embo J* 20, 3993-4002
85. Brennan, F. E., and Fuller, P. J. (1999) Acute regulation by corticosteroids of channel-inducing factor gene messenger ribonucleic acid in the distal colon. *Endocrinology* 140, 1213-1218
86. Capurro, C., Coutry, N., Bonvalet, J. P., Escoubet, B., Garty, H., and Farman, N. (1996) Cellular localization and regulation of CHIF in kidney and colon. *Am J Physiol* 271, C753-762
87. Wald, H., Goldstein, O., Asher, C., Yagil, Y., and Garty, H. (1996) Aldosterone induction and epithelial distribution of CHIF. *Am J Physiol* 271, F322-329
88. Gomez-Sanchez, C. E., de Rodriguez, A. F., Romero, D. G., Estess, J., Warden, M. P., Gomez-Sanchez, M. T., and Gomez-Sanchez, E. P. (2006) Development of a panel of monoclonal antibodies against the mineralocorticoid receptor. *Endocrinology* 147, 1343-1348
89. Livak, K. J., and Schmittgen, T. D. (2001) Analysis of relative gene expression data using real-time quantitative PCR and the 2(-Delta Delta C(T)) Method. *Methods* 25, 402-408
90. Pfaffl, M. W. (2001) A new mathematical model for relative quantification in real-time RT-PCR. *Nucleic Acids Res* 29, e45
91. Ouvrard-Pascaud, A., Sainte-Marie, Y., Benitah, J. P., Perrier, R., Soukaseum, C., Cat, A. N., Royer, A., Le Quang, K., Charpentier, F., Demolombe, S., Mechta-Grigoriou, F., Beggah, A. T., Maison-Blanche, P., Oblin, M. E., Delcayre, C., Fishman, G. I., Farman, N., Escoubet, B., and Jaisser, F. (2005) Conditional mineralocorticoid receptor expression in the heart leads to life-threatening arrhythmias. *Circulation* 111, 3025-3033
92. Technologies, L. GATEWAY Cloning Technology Instruction Manual Version 1
93. Invitrogen (2003) Gateway® LR Clonase™ Enzyme Mix; Catalog no. 11791-019
94. Invitrogen (2008) RNAi Designer Online Platform *https://rnaidesigner.invitrogen.com/rnaiexpress/setOption.do?designOption=shrna*
95. Invitrogen (2007) BLOCK-iT™U6 RNAi Entry Vector Kit Catalog nos. K4944-00 and K4945-00.
96. Nelson, J. D., Denisenko, O., and Bomsztyk, K. (2006) Protocol for the fast chromatin immunoprecipitation (ChIP) method. *Nat Protoc* 1, 179-185
97. Benjamini, Y., Drai, D., Elmer, G., Kafkafi, N., and Golani, I. (2001) Controlling the false discovery rate in behavior genetics research. *Behav Brain Res* 125, 279-284
98. Fuhrmann, U., Slater, E. P., and Fritzemeier, K. H. (1995) Characterization of the novel progestin gestodene by receptor binding studies and transactivation assays. *Contraception* 51, 45-52
99. Invitrogen (2006) ViraPower™ Lentiviral Expression Systems.
100. Invitrogen (2002) Flp-In™ System For Generating Stable Mammalian Expression Cell Lines by Flp Recombinase-Mediated Integration; Catalog nos. K6010-01, K6010-02.
101. Fromm, M., Schulzke, J. D., and Hegel, U. (1993) Control of electrogenic Na+ absorption in rat late distal colon by nanomolar aldosterone added in vitro. *Am J Physiol* 264, E68-73
102. Farman, N., Vandewalle, A., and Bonvalet, J. P. (1983) Autoradiographic determination of dexamethasone binding sites along the rabbit nephron. *Am J Physiol* 244, F325-334
103. Tian, L., Hammond, M. S., Florance, H., Antoni, F. A., and Shipston, M. J. (2001) Alternative splicing determines sensitivity of murine calcium-activated potassium channels to glucocorticoids. *J Physiol* 537, 57-68

104. Oakley, R. H., Webster, J. C., Sar, M., Parker, C. R., Jr., and Cidlowski, J. A. (1997) Expression and subcellular distribution of the beta-isoform of the human glucocorticoid receptor. *Endocrinology* 138, 5028-5038
105. Naray-Fejes-Toth, A., Rusvai, E., and Fejes-Toth, G. (1994) Minealocorticoid receptors and 11 beta-steroid dehydrogenase activity in renal principal and intercalated cells. *Am J Physiol* 266, F76-80
106. Chen, S. Y., Bhargava, A., Mastroberardino, L., Meijer, O. C., Wang, J., Buse, P., Firestone, G. L., Verrey, F., and Pearce, D. (1999) Epithelial sodium channel regulated by aldosterone-induced protein sgk. *Proc Natl Acad Sci U S A* 96, 2514-2519
107. Tanaka, K., Ashizawa, N., Kawano, H., Sato, O., Seto, S., Nishihara, E., Terazono, H., Isomoto, S., Shinohara, K., and Yano, K. (2007) Aldosterone induces circadian gene expression of clock genes in H9c2 cardiomyoblasts. *Heart Vessels* 22, 254-260
108. Naray-Fejes-Toth, A., Boyd, C., and Fejes-Toth, G. (2008) Regulation of epithelial sodium transport by promyelocytic leukemia zinc finger protein. *Am J Physiol Renal Physiol* 295, F18-26
109. Gumz, M. L., Popp, M. P., Wingo, C. S., and Cain, B. D. (2003) Early transcriptional effects of aldosterone in a mouse inner medullary collecting duct cell line. *Am J Physiol Renal Physiol* 285, F664-673
110. Fejes-Toth, G., and Naray-Fejes-Toth, A. (2007) Early aldosterone-regulated genes in cardiomyocytes: clues to cardiac remodeling? *Endocrinology* 148, 1502-1510
111. Gumz, M. L., Stow, L. R., Lynch, I. J., Greenlee, M. M., Rudin, A., Cain, B. D., Weaver, D. R., and Wingo, C. S. (2009) The circadian clock protein Period 1 regulates expression of the renal epithelial sodium channel in mice. *J Clin Invest* 119, 2423-2434
112. Fuller, P. J., and Young, M. J. (2005) Mechanisms of mineralocorticoid action. *Hypertension* 46, 1227-1235
113. Hanlon, S. E., and Lieb, J. D. (2004) Progress and challenges in profiling the dynamics of chromatin and transcription factor binding with DNA microarrays. *Curr Opin Genet Dev* 14, 697-705
114. Irlbacher, H., Ziera, T., Sommer, A., Weiss, B., and Borden, S. A. (2009) Genome-wide promoter localization of the mineralocorticoid receptor. *manuscript in preparation*
115. Itani, O. A., Liu, K. Z., Cornish, K. L., Campbell, J. R., and Thomas, C. P. (2002) Glucocorticoids stimulate human sgk1 gene expression by activation of a GRE in its 5'-flanking region. *Am J Physiol Endocrinol Metab* 283, E971-979
116. Wang, J. C., Derynck, M. K., Nonaka, D. F., Khodabakhsh, D. B., Haqq, C., and Yamamoto, K. R. (2004) Chromatin immunoprecipitation (ChIP) scanning identifies primary glucocorticoid receptor target genes. *Proc Natl Acad Sci U S A* 101, 15603-15608
117. Genomatix Software GmBH Munich, G. (2008) www.genomatix.de.
118. Nakhoul, N. L., Hering-Smith, K. S., Gambala, C. T., and Hamm, L. L. (1998) Regulation of sodium transport in M-1 cells. *Am J Physiol* 275, F998-F1007
119. Naray-Fejes-Toth, A., Snyder, P. M., and Fejes-Toth, G. (2004) The kidney-specific WNK1 isoform is induced by aldosterone and stimulates epithelial sodium channel-mediated Na+ transport. *Proc Natl Acad Sci U S A* 101, 17434-17439
120. Zentner, M. D., Lin, H. H., Wen, X., Kim, K. J., and Ann, D. K. (1998) The amiloride-sensitive epithelial sodium channel alpha-subunit is transcriptionally down-regulated in rat parotid cells by the extracellular signal-regulated protein kinase pathway. *J Biol Chem* 273, 30770-30776

121. Lanigan, T. M., Liu, A., Huang, Y. Z., Mei, L., Margolis, B., and Guan, K. L. (2003) Human homologue of Drosophila CNK interacts with Ras effector proteins Raf and Rlf. *Faseb J* 17, 2048-2060
122. Jaffe, A. B., Aspenstrom, P., and Hall, A. (2004) Human CNK1 acts as a scaffold protein, linking Rho and Ras signal transduction pathways. *Mol Cell Biol* 24, 1736-1746
123. Kolch, W. (2005) Coordinating ERK/MAPK signalling through scaffolds and inhibitors. *Nat Rev Mol Cell Biol* 6, 827-837
124. Webster, M. K., Goya, L., Ge, Y., Maiyar, A. C., and Firestone, G. L. (1993) Characterization of sgk, a novel member of the serine/threonine protein kinase gene family which is transcriptionally induced by glucocorticoids and serum. *Mol Cell Biol* 13, 2031-2040
125. D'Adamio, F., Zollo, O., Moraca, R., Ayroldi, E., Bruscoli, S., Bartoli, A., Cannarile, L., Migliorati, G., and Riccardi, C. (1997) A new dexamethasone-induced gene of the leucine zipper family protects T lymphocytes from TCR/CD3-activated cell death. *Immunity* 7, 803-812
126. Muller, O., Pradervand, S., Berger, S., Centeno, G., Milet, A., Nicod, P., Pedrazzini, T., Tronche, F., Schutz, G., Chien, K., Rossier, B. C., and Firsov, D. (2007) Identification of corticosteroid-regulated genes in cardiomyocytes by serial analysis of gene expression. *Genomics* 89, 370-377
127. Kellner, M., Peiter, A., Hafner, M., Feuring, M., Christ, M., Wehling, M., Falkenstein, E., and Losel, R. (2003) Early aldosterone up-regulated genes: new pathways for renal disease? *Kidney Int* 64, 1199-1207
128. Gross, K. L., and Cidlowski, J. A. (2008) Tissue-specific glucocorticoid action: a family affair. *Trends Endocrinol Metab* 19, 331-339
129. Graham, F. L., Smiley, J., Russell, W. C., and Nairn, R. (1977) Characteristics of a human cell line transformed by DNA from human adenovirus type 5. *J Gen Virol* 36, 59-74
130. Shaw, G., Morse, S., Ararat, M., and Graham, F. L. (2002) Preferential transformation of human neuronal cells by human adenoviruses and the origin of HEK 293 cells. *Faseb J* 16, 869-871
131. Muller, O. G., Parnova, R. G., Centeno, G., Rossier, B. C., Firsov, D., and Horisberger, J. D. (2003) Mineralocorticoid effects in the kidney: correlation between alphaENaC, GILZ, and Sgk-1 mRNA expression and urinary excretion of Na+ and K+. *J Am Soc Nephrol* 14, 1107-1115
132. Kobayashi, A., Sogawa, K., Imataka, H., and Fujii-Kuriyama, Y. (1995) Analysis of functional domains of a GC box-binding protein, BTEB. *J Biochem* 117, 91-95
133. Bonett, R. M., Hu, F., Bagamasbad, P., and Denver, R. J. (2009) Stressor and glucocorticoid-dependent induction of the immediate early gene kruppel-like factor 9: implications for neural development and plasticity. *Endocrinology* 150, 1757-1765
134. Carroll, J. S., Meyer, C. A., Song, J., Li, W., Geistlinger, T. R., Eeckhoute, J., Brodsky, A. S., Keeton, E. K., Fertuck, K. C., Hall, G. F., Wang, Q., Bekiranov, S., Sementchenko, V., Fox, E. A., Silver, P. A., Gingeras, T. R., Liu, X. S., and Brown, M. (2006) Genome-wide analysis of estrogen receptor binding sites. *Nat Genet* 38, 1289-1297
135. Bolton, E. C., So, A. Y., Chaivorapol, C., Haqq, C. M., Li, H., and Yamamoto, K. R. (2007) Cell- and gene-specific regulation of primary target genes by the androgen receptor. *Genes Dev* 21, 2005-2017
136. Luecke, H. F., and Yamamoto, K. R. (2005) The glucocorticoid receptor blocks P-TEFb recruitment by NFkappaB to effect promoter-specific transcriptional repression. *Genes Dev* 19, 1116-1127

137. McDonnell, D. (2009) Gene Regulation by Androgen Receptor Coregulators. *ENDO 2009 Washington DC, USA* SYMPOSIUM SESSION: BASIC - On Again, Off Again: Coregulators & Gene Expression
138. Spilianakis, C. G., Lalioti, M. D., Town, T., Lee, G. R., and Flavell, R. A. (2005) Interchromosomal associations between alternatively expressed loci. *Nature* 435, 637-645
139. Jiang, F., and Wang, Z. (2004) Identification and characterization of PLZF as a prostatic androgen-responsive gene. *Prostate* 59, 426-435
140. Loffing, J., Zecevic, M., Feraille, E., Kaissling, B., Asher, C., Rossier, B. C., Firestone, G. L., Pearce, D., and Verrey, F. (2001) Aldosterone induces rapid apical translocation of ENaC in early portion of renal collecting system: possible role of SGK. *Am J Physiol Renal Physiol* 280, F675-682
141. Therrien, M., Wong, A. M., and Rubin, G. M. (1998) CNK, a RAF-binding multidomain protein required for RAS signaling. *Cell* 95, 343-353
142. Rocheleau, C. E., Ronnlund, A., Tuck, S., and Sundaram, M. V. (2005) Caenorhabditis elegans CNK-1 promotes Raf activation but is not essential for Ras/Raf signaling. *Proc Natl Acad Sci U S A* 102, 11757-11762
143. Claperon, A., and Therrien, M. (2007) KSR and CNK: two scaffolds regulating RAS-mediated RAF activation. *Oncogene* 26, 3143-3158
144. Ziogas, A., Moelling, K., and Radziwill, G. (2005) CNK1 is a scaffold protein that regulates Src-mediated Raf-1 activation. *J Biol Chem* 280, 24205-24211
145. Jaffe, A. B., Hall, A., and Schmidt, A. (2005) Association of CNK1 with Rho guanine nucleotide exchange factors controls signaling specificity downstream of Rho. *Curr Biol* 15, 405-412
146. Casar, B., Arozarena, I., Sanz-Moreno, V., Pinto, A., Agudo-Ibanez, L., Marais, R., Lewis, R. E., Berciano, M. T., and Crespo, P. (2009) Ras subcellular localization defines extracellular signal-regulated kinase 1 and 2 substrate specificity through distinct utilization of scaffold proteins. *Mol Cell Biol* 29, 1338-1353

6. Appendix

6.1. Experimental flow-chart

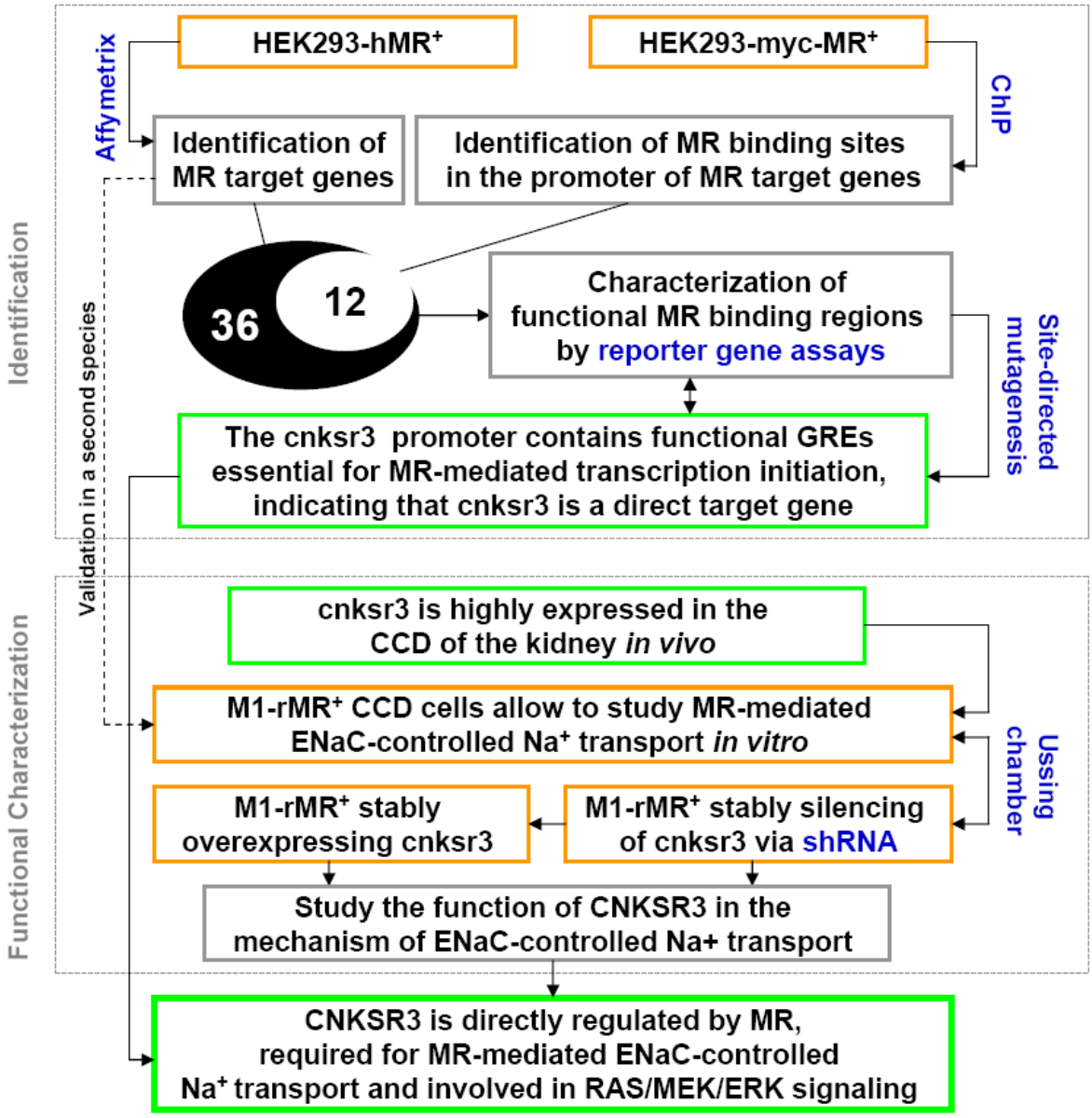

Experimental set-up for the identification of direct MR target genes and for the functional characterization of CNKSR3 in the mechanism of transepithelial sodium transport; Orange boxes indicate novel established cell clones; Grey boxes indicate the experimental purpose; applied experimental techniques are highlighted in blue; Results are framed in green

6.2. Abbreviations

11β-HSD2	11β-hydroxysteroid dehydrogenase type 2
A6	Xenopus leavis oocytes
AF	transactivating function
AR	androgen receptor
ASDN	aldosterone-sensitive distal nephron
ATP	adenosinetriphosphate
c	centi
CCD	cortical collecting duct
cDNA	copy DNA
CDS	coding sequence
CHIF	channel inducing factor
ChIP	chromatin immunoprecipitation
CNK	connector enhancer of KSR
CNKSR3	connector enhancer of kinase suppressor of Ras
CNT	connecting tubule
cRNA	copy RNA
°C	degree celcius
DBD	DNA binding domain
DCT	distal convoluted tubule
DNA	desoxyribonucleic acid
ENaC	epithelial sodium channel
ERK1/2	extracellular signal-regulated kinase
EtBr	ethidium bromide
EtOH	ethanol
FBS	fetal bovine serum
g	gram
GILZ	glucocorticoid-induced leucine zipper
GR	glucocorticoid receptor
GRE	glucocorticoid response element
h	hour
HEK293	human embryonic kidney cell line
HRE	hormone response element
KSR	kinase suppressor of Ras
l	liter
LBD	ligand binding domain
m	milli
M	molar (mol/l)
M-1	mouse CCD derived cell line
MDCK	madin-darby canine kidney cells
MEK1/2	mitogen-activated protein kinase kinase
min	minutes
MR	mineralocorticoid receptor
mRNA	messenger RNA
µ	micro

n	nano
Na-K-ATP	sodium potassium adenosinetriphosphatase
Nedd4	neural precursor cell expressed, developmentally down-regulated 4
NTD	N-terminal domain
p	plasmid
PBS	phosphate buffered saline
PCR	polymerase chain reaction
PCT	proximal convoluted tubule
PDK1	pyruvate dehydrogenase kinase, isozyme 1
PI3K	phosphatidylinositol 3-kinase
PIC	preinitiation complex
PLZF	promyolotic leucin zink finger
PR	progesterone receptor
qPCR	quantitative PCR
r	rat
RAF1	v-raf-1 murine leukemia viral oncogene homolog 1
RNA	ribonucleic acid
RNAi	RNA interference
RT	room temperature
RTPCR	reverse transcription PCR
SDS	sodium dodycyl sulfate
sec	seconds
SGK	serum and glucocorticoid-induced kinase
shRNA	short hairpin RNA
t	time
TAF	TBP associated factors
TBP	TATA-Box binding protein
TBS	tris buffered saline
TD-PCR	touch down PCR
TSS	transcription start site

6.3. List of Figures and Tables

6.4. Publications and Awards

Publications

Ziera, T., Irlbacher, H., Fromm, A., Latouche, C., Krug, S. M., Fromm, M., Jaisser, F., and Borden, S. A. (2009) Cnksr3 is a direct mineralocorticoid receptor target gene and plays a key role in the regulation of the epithelial sodium channel. *The FASEB Journal*

Irlbacher, H.*, **Ziera, T.***, Sommer, A., Weiss, B., and Borden, S. A. (2009) Genome-wide promoter localization of the mineralocorticoid receptor. *Manuscript in preparation*

*shared first-authorship

Poster presentations

Tim Ziera, Horst Irlbacher, Steffen Borden (2008) Specific Gene Regulation by the Mineralocorticoid Receptor, 34th Annual Meeting of the International Aldosterone Conference, 2008, San Francisco, USA

Tim Ziera, Horst Irlbacher, Steffen Borden (2008) Specific Gene Regulation by the Mineralocorticoid Receptor, 90th ENDO Annual Meeting, 2008, San Francisco, USA

Tim Ziera, Horst Irlbacher, Michael Fromm, Steffen Borden, (2008) The aldosterone signature: Identification and functional characterization of a novel mineralocorticoid receptor target gene, Bayer Schering Pharma Young Scientist Postersession, 2008, Berlin, Germany

Horst Irlbacher, **Tim Ziera**, Bertram Weiss, Anette Sommer, Steffen Borden (2008) Genome-wide promoter localization of the Mineralocorticoid Receptor, 90th ENDO Annual Meeting, 2008, San Francisco, USA

Horst Irlbacher, **Tim Ziera**, Bertram Weiss, Anette Sommer, Steffen Borden (2008) Genome-wide promoter localization of the Mineralocorticoid Receptor, Keystone Conference Steroid Sisters, 2008, Whistler, Canada

Sebastian Mendyk, **Tim Ziera***, Steffen Borden (2008) Generation of a Mineralocorticoid Receptor Screening Cell Line, Bayer Schering Pharma Young Scientist Postersession, 2008, Berlin, Germany

Awards

Bayer Schering Pharma Young Scientist Competition, 2008, Berlin, Germany

First place winner of the Young Investigator Competition at the 35th Annual Meeting of the International Aldosterone Conference, 2009, Washington DC, USA – Oral presentation

6.5. Acknowledgements

Diese Arbeit wurde in der Bayer Schering Pharma AG in der Arbeitsgruppe von Dr. Steffen Borden in der Zeit von April 2006 bis August 2009 angefertigt. Mein Dank gilt Prof. Dr. Ursula Habenicht und Dr. Karl-Heinrich Fritzemeier die mir das Anfertigen dieser Arbeit in der Abteilung Women's Health ermöglicht haben, sowie die Teilnahme an internationalen Konferenzen unterstützt haben.

Meinen Gutachtern Prof. Dr. Roland Lauster, PD Dr. Katja Prelle und Prof. Dr. L.-A. Garbe danke ich für ihre Hilfsbereitschaft sowie für die stets freundliche und angenehme Gesprächsatmosphäre.

Mein ganz besonderer Dank gilt Dr. Steffen Borden für die zahlreichen Diskussionen, das "challenging Feedback", den Support über all die Jahre und vor allem für die freundschaftliche Arbeitsatmosphäre. Es hat einfach Spaß gemacht!

Meinem Laborkollegen Dr. Horst Irlbacher danke ich die vielen Diskussionen die gute und produktive Zusammenarbeit, sowie für die freundschaftliche Stimmung im Labor.

Den Studenten Sebastian Mendyk und besonders Hans-Hermann Wessels danke ich für ihre Unterstützung und Vitalität im Labor.

Dr. Dr. Florian Prinz danke ich für die gute Zusammenarbeit und den Support mit lentiviralen Konstrukten.

Dr. Florian Sohler danke ich für die statistische Auswertung der Microarrayergebnisse sowie für seine stete Hilfsbereitschaft.

Den Kooperationspartnern Prof. Dr. Michael Fromm und Dr. Frederic Jaisser sowie ihren Arbeitsgruppen möchte ich für die sehr gute Zusammenarbeit und hilfreichen Diskussionen danken.

Anja Fromm danke ich für zahlreiche elektrophysiologische Messungen.

Für kritische Anmerkungen und Feedback danke ich Dr. Peter Muhn.

Weiter möchte ich mich bei allen Mitarbeitern und Mitarbeiterinnen der Abteilung Women's Health bedanken, die auf die eine oder andere Art zum Gelingen dieser Arbeit beigetragen haben, ohne dass ich alle persönlich nennen kann.

Meiner Familie danke ich ganz besonders für die stete Unterstützung und das in mich gesetzte Vertrauen und natürlich nicht nur dafür…

6.6. Curriculum vitae

Persönliche Daten

Name	Tim Ziera
Geburtsdatum	28.04.1976
Geburtsort	Hamburg

Dissertation

03/ 2006 – 10/ 2009	Bayer Schering Pharma AG, Berlin, Therapeutic Research Women's Health, AG Dr. Steffen Borden

Hochschulausbildung

02/ 2006	Diplom-Ingenieur - Schwerpunkt Medizinische Biotechnologie
WS 1998/ 1999	Biotechnologie an der Technischen Universität Berlin
WS 1997 – SS 1998	Wirtschaftsingenieurwesen an der Universität Bremen

Schulausbildung

06/ 1997	Abitur
1986 – 1997	Gymnasium in Jaderberg
1983 – 1986	Grundschule in Oldenburg